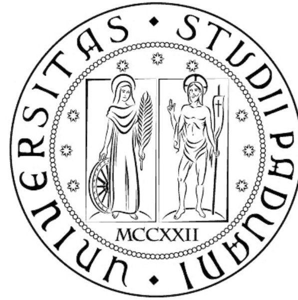

UNIVERSITÁ DEGLI STUDI DI PADOVA

FACOLTÁ DI INGEGNERIA

DIPARTIMENTO DI PROCESSI CHIMICI DELL'INGEGNERIA

CORSO DI LAUREA MAGISTRALE IN INGEGNERIA DEI MATERIALI

TESI DI LAUREA

Role of supply chain logistics and manufacturing process on the reliability of electronic devices

Relatore: Prof. Guglielmi Massimo

Laureando: Riccardo Rizzo

Matr. n. 622325

Anno Accademico 2011/2012

Acknowledgements

First and foremost I would like to thank my two main supervisors Dr. Rajan Ambat from the Technical University of Denmark and Prof. Massimo Guglielmi from the University of Padova, Italy.

Dr. Rajan Ambat has always given me advice and guidance throughout the whole project, constantly providing me with positive and encouraging feedback. He has always showed interest and enthusiasm in my work and has always been available for discussion and advisory. It has been a pleasure for me working under his supervision. I have never learned so much.

Prof. Massimo Guglielmi has been my reference for the Italian University and the T.I.M.E. project I took part in. Although we have not met for more than two years, he has always supported my work and my studies in Denmark, besides helping me solving bureaucratic issueswhich would have complicated my study career. I am sincerely grateful for this.

Special thanks to Senior Scientist Morten S. Jellensen for all the technicalhelp and encouragements he gave me.

Special acknowledgments go to Ph.D. studentVadimas Verdingovas for his patience and accuracy in following me during this project. He has always been available for advising me regarding the experimental setups employed in this work. He has given me invaluable help in understanding and clarifying the results of this project, besides being a good lab-fellow.

Special thanks go to PhD students Chakravarthy Gudla, Fredrico Fernandes, Rameez Kang and Svava Davíðsdóttir for making me laugh and keeping me company during the countless breaks I took during this project. I wish you all the best.

I am in debt with my friends, Rasmus and Guille, for motivating me and pushing me through this project. Denmark would have been different without you.

Last but not the least, I want to say huge thanks to my family who suffered and fought with me,allowing me to overcome every obstacle I had on my way to Denmark. Thanks for being there when I had the most need…. I finally made it…believe me...it was worth it.

I cannot help but thank another special person. Thanks Tj, I would have not been here without you and I would have not gone so far.

Abstract

The climatic reliability of electronic circuits has become a relevant issue for the electronic industry. Due to factor like miniaturization, the electric field applied on the system and contamination, the corrosion and climatic effects related failures in electronics have become topics of intense research. The spread of electronic products and their complexity has dramatically increased, and they surround everyday life, as well as advanced applications and products. The propensity of electronic devices to fail is greatly dependent on the environmental conditions wherein they are operating and the type and levels of contamination present. The process related solder flux residues is an issue of great concern due to their hygroscopic behavior which attracts humidity creating a conductive moisture layer on the PCB surface. "No-clean" flux types are commonly employed as their residues should totally decompose during soldering requiring no post-cleaning processes. It occurs however that, due to trapping between components or different thermal profiled, that flux residues remain on the PCB, thus compromising the reliability.

Weak organic acids are commonly employed as activators in solder flux systems. These acids are capable of reacting with the oxide layers on the PCB, removing it from the metals surfaces, easing the solder process. Adipic, malic, succinic and glutaric acid are the most frequent activators in "No-clean" flux types. They should be able to vaporize as a result of thermal exposure during soldering, minimizing the presence of residues.

This study investigates the effects of the foretold weak organic acids on the climatic reliability of PCBAs. Polarization curves on tin with different concentrations of the four WOAs are followed by reliability studies in terms of leakage currents and electrochemical migration. These effects have been studied under condensing, near-condensing and full condensing conditions. In addition to this, a number of seven flux systems containing one of the four WOAs as activator has been tested regarding the possibility of electrochemical migration. The results were then interpreted in terms of physical and chemical properties of the four WOAs. The concentrations used have been selected in regards to 1.56 NaCl $\mu g/cm^2$ stated in IPC J-STD-001D standard.

The results of this study showed the importance of knowing the kind and the concentration of the weak organic acid which is the activator in a solder flux system. The WOAs have different chemical and

physical properties, thus their effects on the climatic reliability of PCBAs will vary. Some of these acids resulted to be more aggressive than others, affecting to a greater extent the functioning of the electronic components tested in this work.

Abbreviations

ECM	Electrochemical Migration
ENIG	Electroless Nickel Immersion Gold
IC	Ion Chromatography
LC	Leakage Current
LRTD	Localized Surface Insulation Detection (system)
LOM	Light Optical Microscopy
PCB	Printed Circuit Board
PCBA	Printed Circuit Board Assembly
PWB	Printed Wiring Board
RH	Relative Humidity
SCEM	Single Component Electrochemical Migration
SEM/EDX	Scanning Electron Microscope/Energy Dispersive using X-ray (analysis)
SIR	Surface Insulation Resistance
SMC	Surface Mounted Component
TBBA	Tetrabromobisphenol A
WOA	Weak Organic Acid

Contents

Acknowledgements 2

Abstract 3

Abbreviations 5

1 Introduction 10

1.1 Major reasons for corrosion reliability issues in electronics 10

1.2 Cost of corrosion 11

1.3 Factors affecting the climatic reliability of electronics 13

1.4 Aim of the present project 14

2 An outline of PCBA manufacturing process 16

2.1 Electronic components and materials 17

2.1.1 Passive components 17

2.1.2 Active components 18

2.2 Component mounting 19

2.2.1 Through hole technology 19

2.2.2 Surface mount technology 20

2.3 Soldering process 20

2.3.1 Solder flux 20

2.3.2 How fluxes work 21

2.3.3 Rosin based fluxes 22

2.3.4 Water soluble fluxes 22

2.3.5 "No-clean" fluxes 22

2.4 Soldering techniques 23

2.4.1 Reflow soldering 23

2.4.2 Wave soldering 24

3 Major corrosion failure mechanisms in electronics 25

3.1 Wet corrosion 25

3.2 Leakage currents 26

3.2.1 Factors which influence the leakage currents 27

3.3 Cathodic corrosion 28

3.4 Galvanic corrosion 29

3.4.1 Series of standard potentials 30
3.5 Anodic corrosion and electrochemical migration 31
3.5.1 Factors influencing ECM 32
4 Critical factors for the reliability of electronic devices 34
4.1 Environmental factors 34
4.1.1 Temperature and humidity 34
4.2 Sources of contamination 35
4.2.1 Process related contamination 36
4.2.2 Service related contamination 37
5 Materials and theory behind experimental methods 39
5.1 Weak Organic Acids 39
5.2 Tin 39
5.3 Solder Flux Systems 39
5.4 Single Component Electrochemical Migration Setup 39
5.5 Test PCB setup 40
5.6 RTD Sensors 42
5.7 Climatic conditions for investigations 44
5.7.1 Climatic chamber 45
5.7.2 Peltier stage set up for cooling 46
5.8 Double Pt electrode set up for leakage current measurements 47
5.9 Potentiostat 49
5.10 Conductivity measurement setup 49
5.11 Reference Electrode 50
5.12 Techniques 51
5.12.1 Leakage Current and Conductivity 51
5.12.2 Conductivity measurements 52
5.12.3 Polarization Curves 53
5.13 Electrolyte preparation 55
5.13.1 Sodium chloride and WOAs 56
5.13.2 Solder Flux residues 57
6 Physical and chemical properties of the investigated WOAs 58

6.1 Chemical Structure 58
6.2 Physical Properties 59
7 Results and discussion 61
7.1 Electrochemical studies on pure Tin in WOA 62
7.1.1 Effect of different concentrations of WOAs on the polarization curves 62
7.1.2 Comparisons 64
7.1.3 Comparision between acids (behaviour at 100 μg/cm^2) 65
7.1.4 Chemical structure and physical properties 66
7.1.5 Conclusions 67
7.2 Measurements for finding equivalent concentrations of WOAs to provide equivalent conducitivity to NaCl 68
7.2.1 Conductivity measurements 68
7.2.2 Determination of the equivalent concentration 69
7.2.3 Strong electrolytes vs. weak electrolytes 70
7.2.4 Discussion 71
7.2.5 Aggressiveness of the WOA solutions: the pK$_a$ value 71
7.2.6 Leakage current measurements 72
7.2.7 Determination of the LC 73
7.2.8 Discussion 74
7.2.9 Different behavior in AC and DC voltage 75
7.2.10 Conclusions 76
7.3 Effect of WOAs and flux types on Electrolytic migration 77
7.3.1 Results and discussion 78
7.3.2 Possible implications on PCBA manufacturing 90
7.3.3 Conclusion 91
7.4 Effect of WOAs residues on SIR pattern under non-condensing conditions 92
7.4.1 Results and discussion 92
7.4.2 Hydrophilic behavior of the various WOA residues 96
7.4.3 Possible implications in PCBA manufacturing 97
7.4.4 Conclusions 97
7.5 Effect of contamination on corrosion under condensing conditions 99

7.5.1 PCB level tests using Peltier stage for continuous cooling 99
7.5.2 Experiments under condensing conditions using WOAs residues 103
7.5.3 Comparison of leakage current for various contaminations and condensing conditions 107
7.5.4 Possible implication in PCBA manufacturing 108
7.5.5 Conclusions 108
8 Conclusions 109
9 Future perspectives 111
10 List of references 112
Appendix I: Materials and design used for electronic components 116
Appendix II: current leaking from capacitors 116
NaCl 116
Adipic acid 117
Glutaric acid 117
Malic acid 118
Succinic acid 118
Appendix III: Product datasheet for Solder Flux Systems 119
Appendix IV: CELCORR test PCB 125
Appendix IV: Mollier Diagram 125

1 Introduction

During the past couple of decades, use of electronic devices has increased in gigantic proportions. Clear examples of this trend are mobile phones: devices must integrate more and more complex functions, such as camera, GPS and several wireless communication technologies. The device is expected to be both cheap and as much as possible reliable. Climatic reliability aspects are often underestimated during the design of these electronics systems. Climatic reliability issues of electronics leading to corrosion can introduce intermittent malfunctions and permanent failures, which cause severe economic loss.

Plating baths, etching, cleaning and soldering are processes which tend to introduce contamination during PCB manufacturing. Solder Flux Systems, although necessary from the production point of view, often leave residues which are able to absorb humidity. The synergistic effect of these contaminants and humidity leads to formation of corrosion cells resulting in reliability issues. The interaction between contamination and atmospheric conditions is worth to be investigated as it affects to a great extent the climatic reliability of electronic components.

This chapter aims at giving a brief introduction concerning the importance of investigating the corrosion in electronics devices. Additionally, by analysing the cost consequences of electronic reliability and the factors affecting it, the aim of this project will be defined.

1.1 Major reasons for corrosion reliability issues in electronics

Electronic devices have been rapidly developed during the past few years. These can be found in normal daily life devices as well as high tech applications where they have to withstand severe conditions that were never thought off few years back. Electronics is increasingly used as integrated into various machines and also in outdoor conditions where corrosivity is greater[1]. The knowledge of the electronic corrosion process and the know-how to prevent it, have become topics of great interests in order to ensure product reliability.

Before describing the main reasons for corrosion failure, it is worth to emphasize that, in this field, size really matters. The size of the ICs has been decreased by a factor of 10 reducing the spacing between the IC components to around 200nm. On a PCB, the spacing is now around 5 µm, while in mid-90's was around 100 µm. This increased packaging density of electronics has become so great in all major product areas (Figure 1) that makes the electronics sensitive to the corroding and contamination effects of the

environment also in relatively mild conditions. A material loss of the order of picograms (10^{-12}) is, indeed, sufficient to generate a fault in the conducting path of a PCB[2].

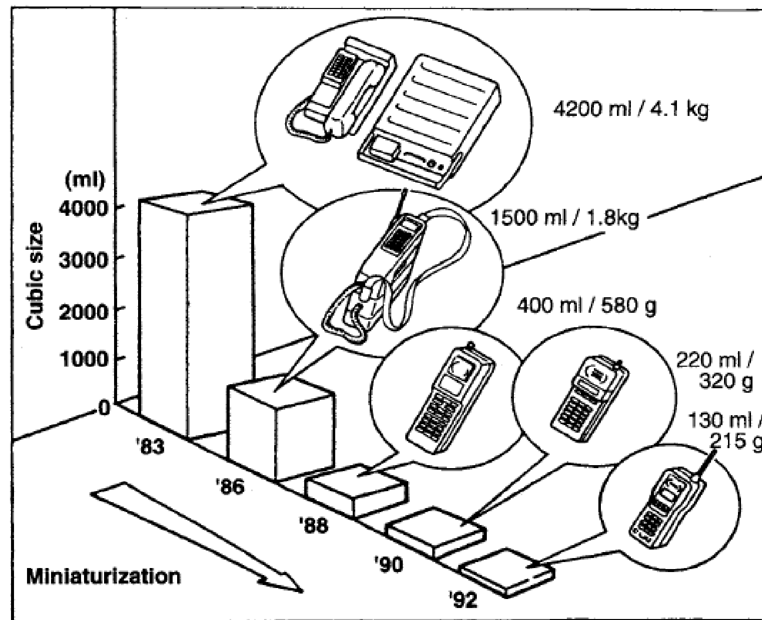

Figure 1 Reduction in the volume of communication system with time [3]

The average size of dew droplet formation on a surface at different temperatures varies from 20 – 50 μm at about 50% RH. Hence smaller distance on the PCBs makes it easy for the local electrochemical cell to form.

1.2 Cost of corrosion

The cost of corrosion in industrialized countries has been estimated to be about 3-4% of the gross national product. The direct and indirect costs of corrosion can be generally summarized in:

- efforts to give structures an attractive appearance
- replacement and maintenance of components
- economic loss due to production interruptions
- extra cost of using expensive materials and other measures for the prevention of corrosion
- loss or destruction of products.

Besides the financial cost, a good deal of attention should be paid to safety risks and the pollution of the environment due to corrosion[4].

The corrosion process and failure in electronic component is subtle and insidious as it cannot be readily detected. Most of the time the corrosion failure is dismissed as just a failure and the component is replaced when it breaks down or malfunctions. This makes the cost of corrosion difficult to estimate[5]. However, in industries like the defense and automotive, where significant investments and efforts in durable equipment has been done, there is a tendency to keep the equipment for longer periods of time and corrosion has become a relevant issue[6].
An important voice in the consequences of electronic equipment corrosion is the cost of downtime. In manufacturing facilities, corrosion of electronic control equipment can lead to shutdown of the production processes with a consequent lost of production time[4]. In services and other industries, the breakdown of electronic components like servers and database, leads to data center down time, stopping transactions, communications, logistical operations and the like. Figure 2 shows some of the foretold costs for some specific manufacturing and services industries.
Recent studies in the U.S have summarized the cost of the total cost of electronic corrosion to be in the order of 0.5-0.7% of the GDP, meaning around 90 billion US dollars.

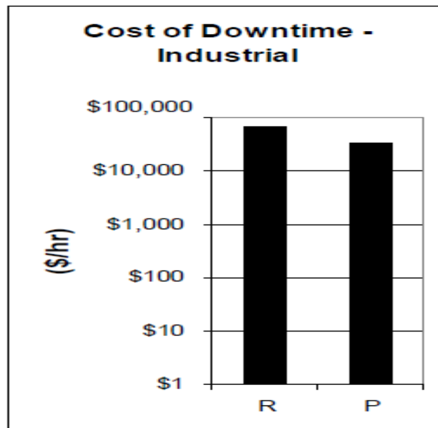

Figure 2 — Cost of Industrial Downtime[4,5,6,(1)]
R = Refinery;
P = Pulp and Paper Mill

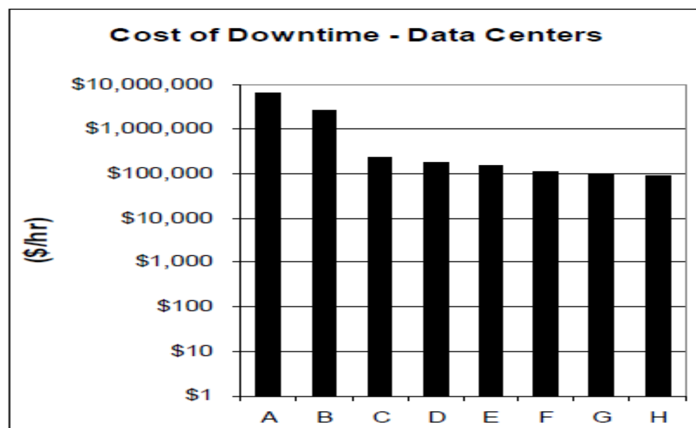

Figure 3 — Cost of Data Center Downtime[7]
A = Brokerage operations; E = Package shipping services;
B = Credit card authorization; F = Home shopping channel;
C = Ebay; G = Catalog sales center;
D = Amazon.com; H = Airline reservation center

Figure 2 Cost of industrial and data center downtime[5]

1.3 Factors affecting the climatic reliability of electronics

There are two inherent factors on the PCBA, which are essential for corrosion are the presence of various metals/alloys and the potential bias. This together with other factors such as humidity forming water layer results in the formation of corrosion cell. Apart from the metals and alloys, the four main factors affecting the climatic corrosion reliability of electronic devices are temperature, bias, humidity and contamination (Figure 3). When these four factors perform together simultaneously, the likelihood of failure on the PCB component is much higher[1][7].

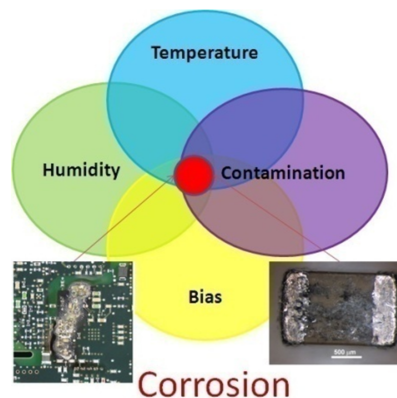

Figure 3 Factors influencing electronic corrosion

The main factor affecting climatic corrosion is perhaps temperature through humidity, since it affects the prevailing humidity conditions. According to the Arrhenius equation, an increase of temperature has an accelerating effect of the chemical reactions involved in the process. Corrosion caused by humidity can progress quickly even at 0-30°C temperature[1]. A change of temperature influences also the relative humidity. If the temperature drops, the relative humidity will at some point exceed 100% RH leading to the formation of a layer of water on the surface. This water layer accelerates corrosion rate to several thousand times faster than at the starting point. When the temperature rises again, the water evaporates and corrosion nearly stops.

Contamination plays also a significant role concerning the reliability of electronic devices. Two main sources of contaminants are the process related contamination resulting from the manufacturing process and service related contamination enters into the device during service [2]. The former concerns about chemical residues from the production process, which could be solder flux residues, human

handling and remnants from the plating baths. The latter regards the environment wherein the electronic device is operating. These can be aggressive ions like chlorides, SO_2, NO_2 and dust[8][2]. These contaminants can be themselves corrosive or can attract humidity from the air to form a condensed phase at humidity levels below 100%.

However, pure water layer on a clean PCBA surface only has limited conductivity to introduce any significant leak current or corrosion effects. However, PCBA surface is seldom clean due to the process related residues which dissolves into the water layer. Water layer with dissolved ionic residues are more conducting, which cause first level corrosion effect such as the increased levels of leak current causing functionality problems.

In addition to this, the applied potential between the components on the biased PCB accelerates corrosion failures. The closer spacing increases the electric field (E=V/d) between points, which eases the corrosion cell formation during local condensation in humid environments[9].

All these factors contribute to make the corrosion in electronics a subtle process, difficult to forecast and to understand. Presently the knowledge on corrosion issues of electronics is very limited.

1.4 Aim of the present project

Presently soldering process in the electronic industry is carried out using the "No-Clean flux" Technology, which means no cleaning is required after the soldering process which uses the "no-clean flux system". The idea behind the no-clean flux system is that it leaves only negligible residues, which are benign. However, this is seldom the case on a actual PCBA irrespective of the board is wave, re-flow, selective, or hand soldered. . The ''No-clean" flux systems often contain weak organic acids (WOA) as activators with the purpose of removing oxides on the metal surface. Flux systems have been studied in detail[2], [10], [11] and residues have been found to be corrosion accelerating depending on the amount and composition. These solder flux residues, necessary for the production process have, a direct impact on the climatic reliability of electronic devices. Four main WOAs employed as activatos in the no-clean flux systems are adipic, succinic, malic and glutaric acid.

This project aims to understand the relative effects on these acids on the corrosion reliability under humid and condensing conditions as well the effect of some of the flux system using these acids. The behavior of these acids is compared to 1.56 $\mu g/cm^2$ of sodium chloride, which is referred in IPC standards as the upper limit of ionic contamination to be present on PCBAs. These acids are tested on the PCB with the aim of measuring two parameters from the board: (i) leakage current levels, and (ii)

corrosion especially electrochemical migration. These can directly be correlated to reliability as a function of flux residue under condensing, near-condensing and non-condensing conditions. Seven flux systems have been tested under condensing conditions as well. These results are then compared to physical properties and behaviors of the different WOAs.

The following will be the experimental part of the work:

- Polarization curves on tin with different concentration of WOAs
- Conductivity measurements of the different WOAs with the purpose of finding the concentrations which give the same conductivity as 1.56 $\mu g/cm^2$ of sodium chloride
- Single component electrochemical migration experiments on capacitors contaminated with WOAs and flux system at full-condensing conditions
- Climatic testing of PCBAs with different amounts of WOAa under non-condensing and near-condensing conditions using in-situ Peltier stage, and measurement of leakage current and electrochemical migration
- Analysis of corrosion morphology using optical microscope and scanning electron microscopy

Work in this thesis also focus on optimizing the test under condensation using the Peltier stage set up, which will be further explored in the future work. Finally the results obtained from the investigations are compared and analyzed.

2 An outline of PCBA manufacturing process

In this chapter the main technologies, together with the core materials and components, used to produce large volumes of PCBAs will be briefly introduced.

A printed circuit board (PCB),Figure 4, is the platform upon which microelectronic components such as semiconductor chips and capacitors are mounted. It guarantees the electrical interconnection between components and in all electronics products. PCB manufacturing is highly complicated, requiring large equipment investments and over 50 process steps[12]. A PCB is formed from a series of laminate, tracking and prepreg layers separated by insulating materials. Within the stack is often a series of drilled holes, forming vias between tracking or between surfaces. A Printed Circuit Board Assembly (PCBA) is a PCB where all the components have been assembled.

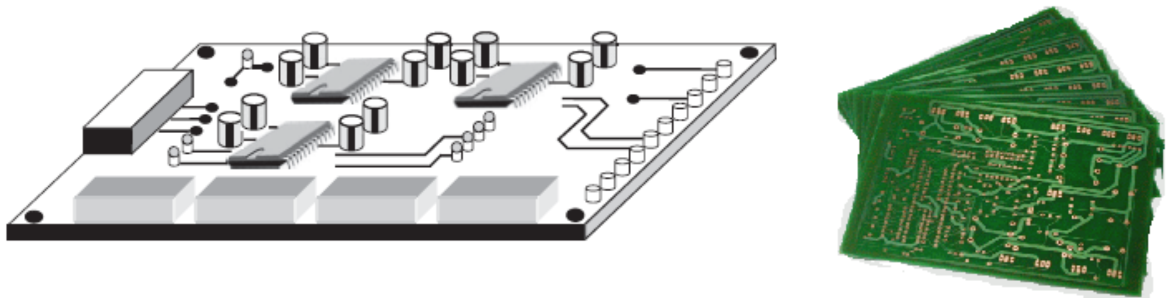

Figure 4 Graphical representation of an example PCB[13]

Copper conduction lines, embedded on a dielectric medium of epoxy resin reinforced with glass fibers ensure the electrical connections along the PCB[13].In order to increase the amount of components a PCB can consist of 2-6 layers. This number is increasing, leading to a higher complexity of the board[8]. A PCB can undergo different surface finishing, like ENIG, HASL and immersion tin or silver finish. ENIG stands for "Electroless Nickel Immersion Gold": an underlying layer of nickel is coated with a thin layer of gold over the top. The gold layer just act as a protective coating for the nickel to prevent it tarnishing before it is soldered. Hot Air Solder Levelling is the most common surface finish: PCBs are dipped in molten solder and then the excess is cleaned off using hot-air knives to leave behind the thinnest possible layer of solder. By mean of immersion tin finishing, alayer of tin is applied to the PCB by means of a special process, in which the copper atoms of the exposed conductors and contact areas are exchanged for tin atoms. With a similar process, silver can also be applied.

2.1 Electronic components and materials

In order to better understand the various types of corrosions that can occur on a PCBA, it is necessary to understand the materials involved and how they are connect with each other. A list of the main materials that can be found on a PCB can be seen in **Appendix I**. A detailed description of all the components and materials on a PCB will be a too broad range of investigation for this thesis, therefore only the most important ones will be described in this paragraph.

2.1.1 Passive components

A passive components is a device that either consume (but does not produce) energy[14]. There are several components on a PCBA namely resistors, capacitors, transducers, etc… In this paragraph an overview of capacitors and resistors will be introduced.

2.1.1.1 *Capacitors*

Capacitors, Figure 5, are bi-polar components on a PCBA consisting of two electrical conductors separated by a dielectric material (insulator). As the potential is applied to the electrodes, a static electric field develops across the dielectric, building up positive charge on one plate and negative charge on the other plate. Energy is thus stored in the electrostatic field. The capacitance of a capacitor is defined by the relation C=Q/V, where C is the capacitance (measured in Farads, F), Q is the charge and V is the applied potential[15].

Figure 5Capacitor[16]

Capacitors are used to store energy, as the charge that is built up on the electrodes can be released after the potential has been removed. On an electronic circuit, capacitors are used as filters for DC signals coming from an AC source and noise smoothers[8].

Capacitors are particularly vulnerable to the formation of condensed water layer due to their bi-polar nature[17]. This condensed water layer within the two electrodes ensures the electrolytic medium for

the formation of a tiny corrosion cell. Electrochemical migration is commonly found on capacitors, causing electric short of the component[8].

2.1.1.2 *Resistors*

A resistor is an electrical component that implements electrical resistance[8]. The direct proportion of the current flowing through the transistor and the applied voltage is represented by Ohm's law *I=V/R* More specifically, Ohm's law states that the *R* in this relation is constant, independent of the current. Resistors are common elements of electrical networks and electronic circuits and are ubiquitous in electronic equipment[18].

Figure 6Resistors[19]

Al_2O_3 is the main constituent of the ceramic body of a resistor, while the resistive element is made of metal oxides or ceramic/metallic composites (cermet)[20].

Although resistors are less susceptible to aqueous corrosion due to the generation of heat which dries the surface, electrochemical migration can happen in the same way as with the capacitors.

2.1.2 Active components

On the contrary, active components are the ones that give a gain to the current. Passive and active component are integrated with each other to function as one single component. Transistors, amplifiers and integrated circuits are all examples of active components that can be found in an electronic device[21].

2.1.2.1 *Integrated circuits*

An integrated Circuite (IC), Figure 7, is built up upon several components which are integrated into one single device. Most of the ICs components, like transistors and amplifiers, are made of a silicon mono-crystal and in some application of GaAs[18]. The lead frame is connected to the legs by mean of thin gold wire, while the external frame is made of Cu based materials, which provide electrical connection to the PCB, while dissipating the heat (7). Aluminum doped connector lines with few per cent of Cr, Ti or W reduces the risk of electromigration[22].

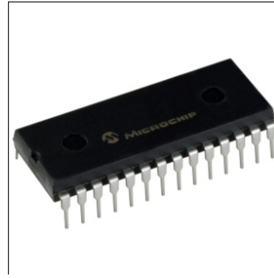

Figure 7 Integrated circuit[23]

2.2 Component mounting

In this paragraph the two main techniques, namely Through Hole and Surface Mount Technology, used for mounting the components to the PCB will be briefly introduced.

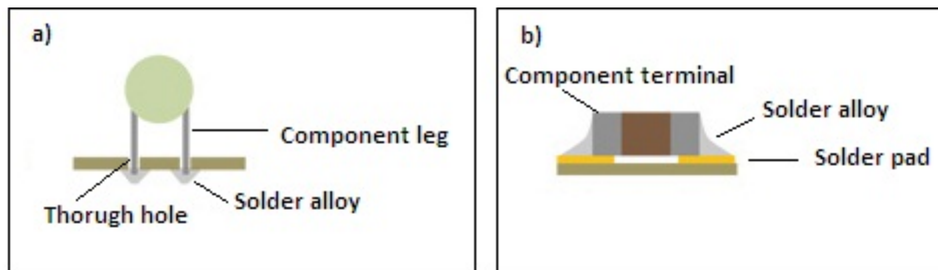

Figure 8 a) through hole technology b) surface mount technology

2.2.1 Through hole technology

In this technology (Figure 8 a)) the components are inserted into holes drilled in PCBs and then soldered with lead to pads on the opposite side [24]l. This can be done either manually or, most likely, by the use of automated insertion mount machines[25]. Traditional solder is an alloy of tin and lead (typically 60-40), which melts at a temperature of about 200 °C.

While through-hole mounting provides strong mechanical bonds when compared to Surface Mount Technology techniques, the board becomes more expensive to produce and physically larger due to the additional drilling.

Wave soldering process (Chapter 2.4.2) is the main technique used to solder Through Hole Components

2.2.2 Surface mount technology

An alternative to the through-hole technology is the surface mount technology, SMT(Figure 8 b))[26]. With this technology the connections for soldering the component to the PCB pads are on the same side of the PCB as the component itself, avoiding legs that are pushed through the board. In this way it is possible to mount physically smaller components onto smaller PCBs, with superior high frequency performance when compared to through-hole equivalent. The process is itself faster and more precise than the Through Hole technology[24]. It ensures better mechanical performance under shake and vibration conditions. However this manufacturing process requires a higher initial cost[8].

2.3 Soldering process

Through soldering metals items are joined by the process of melting and flowing a filler metal, namely the solder. This metal has of course a lower melting point than the workpiece.

The main alloy of choice in electronics assembly is the eutectic of 63% tin and 37% lead[24][27]. By using an eutectic composition it is possible to avoid the range of temperature where the two phases coexist, while achieving a single liquidus and solidus temperature. This guarantees a quicker wetting as the solder heats up, a quicker setup as the solder cools and the lowest melting point, minimizing heat stresses on during soldering.

Other mixtures of tin and lead with a range of melting temperature, amongst these the 60/40 and the 50/50 are the most common[27].

2.3.1 Solder flux

Fluxes are used in the first place to clean the metal surface to be soldered and then cover it to prevent further formation of contaminants[9]. Contaminants, like oxides, form a barrier between the pure metal and solder preventing a proper wetting of the surface by the solder.

Figure 9 shows a section of copper track of an assembly which shows three distinct layers of material. Most externally is an absorption layer in which water, gases and other residues are collected. Underneath there is a reaction layer of strongly bound and adherent materials such as oxides. Most internal is the metal part to be soldered i.e., pure metal copper. [27]

From outside in, therefore, flux must:

- Dissolve materials of the absorption layer
- Remove oxides, sulphides and carbonates and any other residues

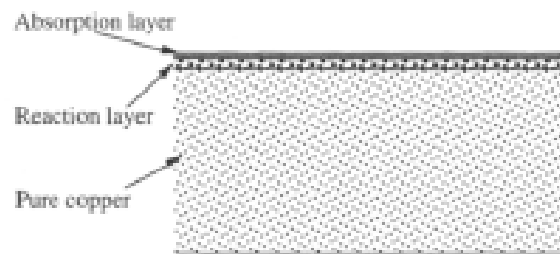

Figure 9 Three layers of a copper track[27]

On the other hand, besides this vital cleaning and covering function, fluxes must have several secondary characteristics[28][27]:

- They must be able to withstand the soldering temperature
- They must break down oxide layers formed on the surface of molten solder: this allows solder to flow and wet
- Ideally they should not attack and corrode either the metal of the joint or the surrounding materials
- They and their residues after the soldering process should be easily removable.

2.3.2 How fluxes work

In Figure 10 the effect of the flux on a component during soldering is displayed. First, as the metal sheet heats, it melts the flux which then becomes chemically active. By melting, it dissolves the oxides from the copper surface and prevents any further oxidization.

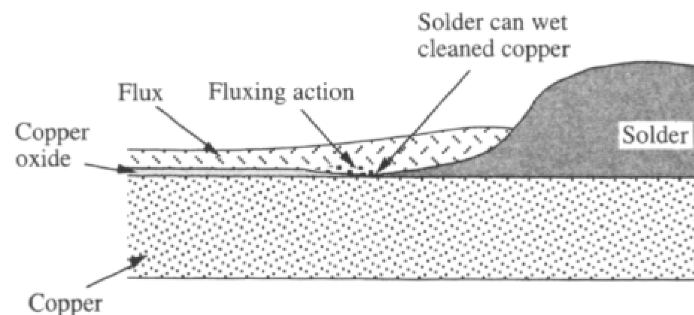

Figure 10 Wetting action of solder on a copper surface, aided by flux[27]

The cleaned solder wets the cleaned metal surface underneath the flux and starts to flow. As the solder flows, it pushes the flux (and its resultant fluxing action) ahead of it, moving the process forward. Thus

when heated up the flux becomes strongly reducing: by sealing out air it prevents the formation of metal oxides.

The activity of a flux is defined as its effectiveness in removing oxide and contaminants from the surface of metals. Fluxes vary in their chemical activity thus the type of flux to be used depends on the oxide layers of the surfaces to be soldered. The thicker the oxide layers is, the higher the requested activity is[28][24][27].

Flux activity is closely allied with the corrosivity of the residues remaining after soldering has taken place. A highly active flux often leaves corrosive residues which may corrode the solder itself; thus is essential to immediately clean the surfaces after soldering.

The main solder fluxes are divided into:

- Rosin based flux
- Water soluble flux
- No-clean flux

2.3.3 Rosin based fluxes

Rosin is a mixture of organic acids which become mildly reactive to metal oxides at molten state: it is able to dissolve thinner layers of surface oxides from copper without additives[8]. Rosin has two excellent properties which make its use as an electronic solder flux preferable to many others. First as a liquid at soldering temperature it is active and so provides good wetting capabilities for solder. Second, its residues after the soldering process are basically non reactive, and do not corrode the completed joint[27]. Due to its low activity, basic rosin flux is only useful for removing very thin oxides of metals.

2.3.4 Water soluble fluxes

These are a type of flux whose residues after soldering are often soluble in water rather than in cleaning solvent[29]. The activity of these fluxes is usually higher, making them more suitable to cope with high oxide amounts and replacing the less active rosin-based and resin-based fluxes. The higher activity often implies a higher corrosivity and these kinds of fluxes must be removed after soldering.

2.3.5 "No-clean" fluxes

This term relates to fluxes whose residues left is kept at minimum and, theoretically, does not need to be removed from the PCB as the active agent should decompose itself under the influence of heat. In these type of fluxes the main component of the activator is a weak organic acid: the most common are adipic, glutaric, malic or succinic acid[9]. Additionally, while Rosin based fluxes contain 15-35% solids,

the solids weight content of No-Clean fluxes is limited to 2%. These systems often contain carboxylic acid-or/and halogenide (activator) in order to ease the removal of the oxides on the surfaces. Resin in the system prevents the re-oxidation of the cleaned metal. The solvent, where the activator and the resin are dissolved, is typically isopropyl alcohol.

2.4 Soldering techniques

The manufacturing of a PCBA requires several soldering processes which can differ with each other. The numbers and the types of processes depend on the complexity of the architecture of the PCBA: therefore a reflow solder process can be followed by a wave solder process and then by a hand soldering for peculiar components whose joining cannot be automated[24].

The technology behind hand soldering is the simplest: a solder iron is used to melt the solder supplied in wire form. The flux is usually incorporated into the wire. Hand-soldering techniques require a great deal of skill to use on the finest pitch chip packages.

It is mainly used for prototyping and repairs and the amount of residues left by this process is higher than for the others.

2.4.1 Reflow soldering

Reflow soldering (Figure 11) is the most common method of attaching SM components to a PCB. Through the use of a mixture of powdered solder and flux (solder paste) and controlled heat, which melts the solder, the joints are permanently connected to the pads. Heat sources could be reflow ovens, infrared lamps or hot air pencils.

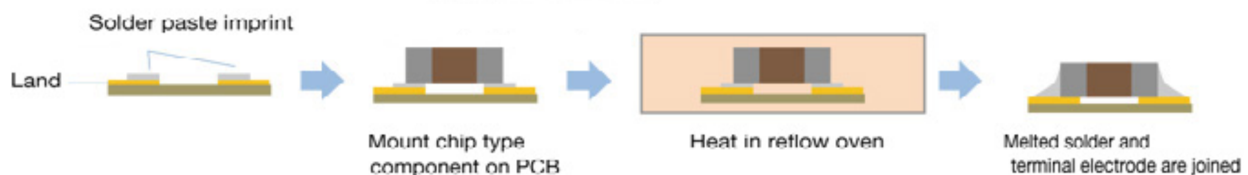

Figure 11 Reflow soldering process

The heat exposure is extremely important for the quality of the soldering[30]. A ramp-up stages where the temperature is slowly increased is followed by a stage where the temperature is kept constant in order to activate the flux and etch the surface oxide film away. The temperature is then rapidly increased above the melting point of the solder alloy (220-235°C)[31].

2.4.2 Wave soldering

Wave soldering (Figure 12) is one of the primary techniques used for PCBs mass production and it is still a widely utilized soldering process. The molten solder is hold into a tank and the components are inserted into or placed on the PCB. The whole PCB is then passed across a pumped wave of solder which wets the exposed metallic areas of the board, creating the connections. A solder mask is used to protect the connections from being bridged by the solder. In this way the connections have a high mechanical and electrical reliability[32].

The cleaning of the lead components and plated through-holes is performed by a fluxing process applied to the bottom side of the assembly in order to remove oxide layers and expose the pristine metal during heating and soldering.

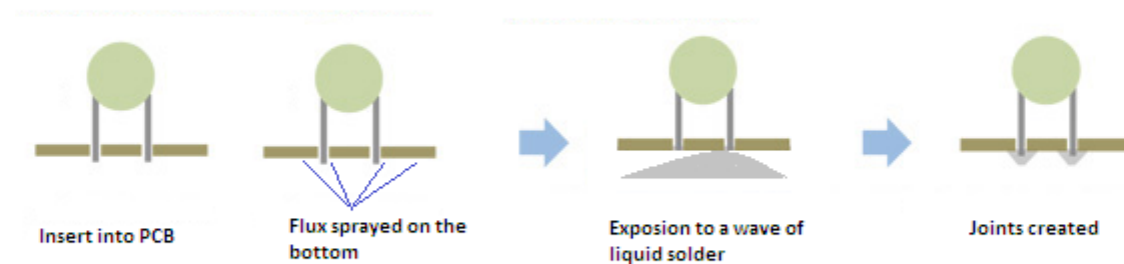

Figure 12 Wave soldering process

3 Major corrosion failure mechanisms in electronics

The corrosion induced failure on electronic devices is a very subtle process, due to the very low amount of corrosion that could create failures. . The influence of humidity, temperature and contaminants plays the main role on the formation of the thin moisture layer which initiates the corrosion failures. The main failure mechanism in electronic are presented in this chapter, together with the general theory which supports them.

3.1 Wet corrosion

The corrosion mechanism on electronic devices is in many ways similar to the atmospheric corrosion (Figure 13)[33]. Thus it is possible to describe the general process in terms of wet corrosion process. Under certain condition related to temperature and humidity, a moisture layer happens to condensate on the surface of an electronic component bridging two oppositely biased terminals. From the positively charged one, the anode, the metal is dissolved and transferred to the solution as ions M^{2+} (oxidation). The negatively charged terminal is called the cathode and it is where the reduction process occurs: the electrons released by the anodic reaction are conducted through the metal to the cathodic area where they are consumed in the cathodic reaction. This moisture layer is thus the necessary electrolyte which closes the electrical circuit allowing the ions to flow from the anodic area to the cathodic area where they are consumed. An electrical circuit has been created without any accumulation of charges[34].

This basic corrosion process can be described by the following reaction

$M \rightarrow M^{2+} + 2e^-$ anodic reaction Eq 1

$\frac{1}{2}O_2 + H_2O + 2e^- \rightarrow 2OH^-$ cathodic reaction Eq 2

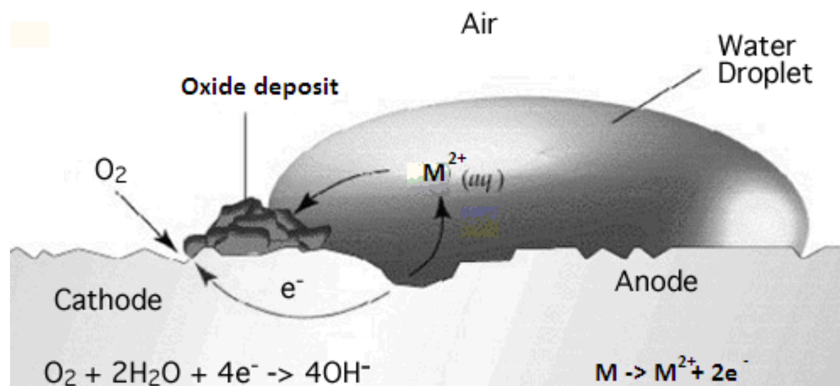

Figure 13 Atmospheric corrosion

It is worth to mention that the previous equations are a simplistic view of the phenomena. The presence of an applied biased, which often exceeds the equilibrium potentials of the metals, and the resulting high electric field between closely spaced conductors, makes indeed the previous situation more complicated and diverse[35]. The transfer of charges from the two electrodes through the electrolyte is measured as a leakage current, and its magnitude determines the aggressiveness and severity of the corrosion mechanism.

To briefly summarize the general corrosion process in electronic devices on can say that three are the factors which constitute the principle of the corrosion cell leading to the degradation of the metallic components on a PCB. These are[2][10][1]:

- A potential difference
- A bridging electrolyte
- Dissolved conductive species

The first one is the driving force which moves the charged species through the second one. The conductive species coming from contaminants will increase the ability of the electrolyte to carry the current. In order to avoid or limit the degradation of electronic circuits, these three factors have to be minimize. Amongst these the control of the contamination is the most feasible and effective.

3.2 Leakage currents

One of the main factors which is responsible for the majority of the failures arising in circuits and which greatly influences the mechanisms of electronic corrosion is the reduction of surface insulation resistance[36]. Surface insulation resistance is a property of the material and electrode system. It represents the electrical resistance between two electrical conductors separated by some dielectric material and it facilitates and enhances the conduction of leakage current, which is the current that flows either through the body or over the surface of an insulator[9]. Electrons are responsible for the conduction of the current in the metallic part of the insulator, whereas, as a consequence of a charge-transfer process at the electrode surface, the current is conducted by ions in the surrounding environment.

By looking at the general principles of the corrosion process, explained in the previous paragraph, the presence of a leakage current is one of the prerequisites for the mechanism to occur. The passage of a leakage current plays, indeed, a double role: on one side it maintain the charge balance, ensuring that

the process runs without any accumulation of charges; on the other side, by the motion of ions and electrons it sustains the detrimental corrosion reactions[37]. The aggressiveness of a medium could be determined by the measure of the current leaking from the solution and can be interpreted as the ability to sustain corrosion during services. Thus it is possible to say that the higher the leakage current is, the higher the activity of the anodic/cathodic reaction is.

3.2.1 Factors which influence the leakage currents

Many are the factors which lead to a decrease of surface insulation resistance (SIR) and, as a consequence, to an increase in leakage current (LC). Amongst these, the most important are[2], [37], [38]:

- Relative humidity and temperature
- Contamination
- Voltage

The relative humidity and its connection to the temperature determine the volume and thickness of the condensed water layer. This water layer, due to miniaturization of devices, may be sufficient to create a bridge between two connectors and form a path for the leakage current. In addition to this, the ability of water to dissolve ionic contamination can further increase the conductivity by orders of magnitude. Contamination has itself a double effect: on one hand ionic contamination left on the PCB easily dissolve in the condensed layer of water increasing the conductivity of the medium and thus its aggressiveness; on the other hand, in form of inorganic salts, it decreases the relative humidity of the surface due to their hygroscopic nature. The origin and the sources of contamination will be better explained in Chapter 4. The previous issues will result in malfunctioning of PCBAs and signal alteration, reducing the performances of the device. This can be permanent or disappear as the condensed water evaporates, making the phenomenon more problematic to identify. The voltage is the driving force for the ions to flow through the medium, and if sufficient high it can increase the leakage current by enhancing the anodic or cathodic dissolution of the metal.

To briefly summarize, the decrease of SIR and increase of LC while on one side it influences the performance of electronics devices by signal alterations, interruptions and so on, on the other side it is a prerequisites mechanism for typical electronic failures, which will be discussed in the following paragraph

3.3 Cathodic corrosion

Metals, like Al and Sn, which are thermodynamically unstable in alkaline environment, are sensitive to dissolution due to cathodic corrosion. As it is a cathodic mechanism it involves a reduction process occurring on the negatively charged electrode, thus the cathode, and, depending on the chemistry of the solution, it can consist of several chatodic reactions, namely oxygen (Eq.2) and solvent (water) reduction (Eq.3). The former one is supported by continuous dissociation of water[34]:

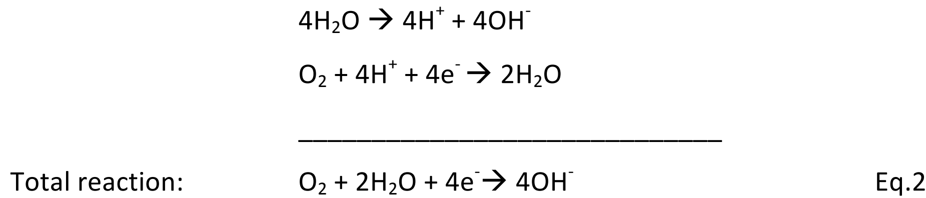

$$4H_2O \rightarrow 4H^+ + 4OH^-$$

$$O_2 + 4H^+ + 4e^- \rightarrow 2H_2O$$

Total reaction: $$O_2 + 2H_2O + 4e^- \rightarrow 4OH^- \qquad \text{Eq.2}$$

The latter one leads to an increase of hydrogen gas in the solution:

$$2H_2O + 2e^- \rightarrow 2OH^- + 2H_2 \qquad \text{Eq 3}$$

Both these cathodic reaction lead to formation of OH^- which increase s the pH of the solution, creating a highly alkaline environment near the cathode[2]. Depending on the stability of the metal/alloy in alkaline condition, the increase in pH can cause dissolution of the material constituting the cathode[35]. By looking at the Pourbaix diagrams for Al (Figure 14) it is possible to notice how this alkaline environment can dissolve the passivating Al_2O_3 layer on the aluminum, which can utterly dissolve as $Al(OH)_4^-$ which deposits on the component. Due to its higher resistance this can lead to overheating of the conductor, or it can result in an open circuit causing failure. Similar mechanism can involve tin which dissolves in hydroxides $Sn(OH)_6^-$[39].

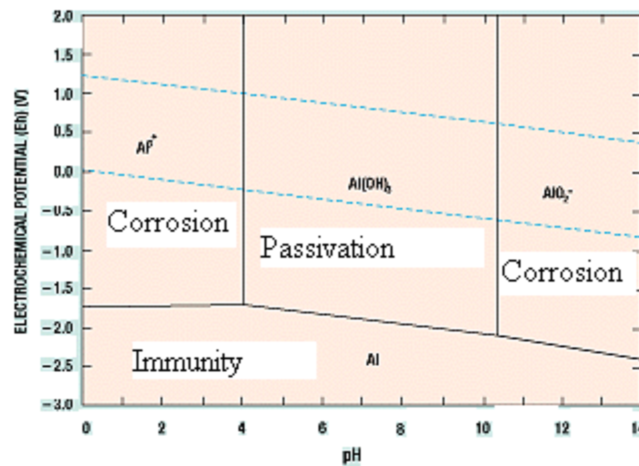

Figure 14 Pourbaix diagram for aluminum

3.4 Galvanic corrosion

Electronic devices are becoming more and more complex, both from the architectural point of view of the PCB and the materials used for the components. New materials are introduced and, overall, combinations of materials are selected in order to achieve the requested performances (Appendix I) [2] When dissimilar metallic materials are coupled together (Figure 15), electrochemical reactions, which bring to the dissolution of one of the metals, take place leading to the malfunctioning of the device. The driving force for this corrosion process is the different electrochemical equilibrium potentials between the two metals in contact with each other[34]. This equilibrium potential represents the tendency of one metal to form ions during electrochemical reactions: a low electrochemical potential means that a metal readily dissolves into ions. Stable metals are thus characterized by high potentials, and the higher the potential the higher the "nobility" of the metal. Due to frequent and large combination of dissimilar metallic materials to produce component for electronic devices, galvanic corrosion is, thus, one of the most common corrosion mechanisms in electronics[36].

Figure 15 Galvanic corrosion: metal A, less noble, acts as the anode; metal B, more noble, acts as a cathode

When a metallic contact is made between a more noble metal and a less noble one, the corrosion rate will increase on the latter and decrease on the former, resulting in the corrosion of the less noble one, which will act as the anode of the reaction. A necessary condition is that the circuit is closed by an electrolytic connection[2], [10], [34], [39].

3.4.1 Series of standard potentials

A general overview for the estimation of the risk of galvanic corrosion for different metals can be given by the series of standard reversible potential of the various metals. Table 1 lists the standard electrode potentials for various metals used in electronics at 25°C. The tendency for galvanic corrosion increases with the potential difference, thus metals close to each other (e.g. tin and lead) do not have a strong effect to one another, while metals like gold and copper have a higher driving force which will lead to the corrosion of the less noble one (Cu). It is worth to mention that the series of potential express only thermodynamic properties, which do not tell anything about the reaction rate (e.g. passivation tendencies are not taken into account)[34].

Another crucial factor for the galvanic corrosion is the area ratio between the metals in the galvanic couple, which play a significant role for the galvanic corrosion rate. If the cathodic area A_c is much larger than the anodic area A_a, meaning a large area ratio A_c/A_a, the corrosion rate of the less noble material may increase strongly, even with small differences between the corrosion potentials of the separate materials.

Table 1 Standard electrode potentials at 25 °C

Element	Chemical Reaction	Potential (V)
Gold	$Au \rightarrow Au^{3+} + 3e^-$	1.50
Silver	$Ag \rightarrow Ag^+ + e^-$	0.80
Copper	$Cu \rightarrow Cu^{2+} + 2^{e-}$	0.34
Lead	$Pb \rightarrow Pb^{2+} + 2^{e-}$	-0.13
Tin	$Sn \rightarrow Sn^{2+} + 2^{e-}$	-0.14
Nickel	$Ni \rightarrow Ni^{2+} + 2^{e-}$	-0.25
Iron	$Fe \rightarrow Fe^{2+} + 2^{e-}$	-0.44
Chromium	$Cr \rightarrow Cr^{3+} + 3e^-$	-0.74
Aluminum	$Al \rightarrow Al^{3+} + 3e^-$	-1.66

In electronic systems, galvanic corrosion occurs often in connectors and switches, as they are commonly made of multi-layer metallic coatings [2], [10], with different electrochemical properties. A typical example is the ENIG layers on top of copper metallization on PCBs, where the nickel layer plays a barrier role against copper-gold inter-diffusion. As long as the golden top layer is without defects or porosities, the underlying layers of nickel or copper do not undergo any galvanic corrosion. Otherwise the large difference in electrochemical potential between Ni and Au cause the corrosion of the former one, while the Au acts as a powerful cathode. As the corrosion proceeds, the pitting of the Ni layer exposes Cu at deep pit areas, damaging the device.

3.5 Anodic corrosion and electrochemical migration

When the applied potential of the anode is raised above the equilibrium potential of the metal is a specific environment, the anode material becomes thermodynamically unstable. The metal can either form a metal-oxide layer on the surface of the anode by reacting with the H_2O of the electrolyte, or dissolves as metal ion M^{n+} according to Eq.1. These ions or their salts can migrate through the electrolyte and be reduced at the cathode[10], [40]. This deposition of metals or their salts is termed electrolytic migration and can cause short-circuiting and malfunctioning in the system. The electrolytic migration it is thus an electrochemical phenomenon which involves the dissolution of the anode and deposition at the cathode. However, only some metals can cause electrochemical migration and whether a metal shows ECM or not depends on the thermodynamic stability of the metal ions in solution as a function of pH and relative deposition potential in comparison with hydrogen overvoltage. Therefore, only metals like Sn, Pb, Cu, Ag, and Au shows ECM on PCBAs, while other metals for eg. Al, Fe, Ni etc. shows simple anodic dissolution. The mechanism of ECM is controlled by the chemistry of the solution, the pH and the electric potential. An adsorbed surface layer of water on the component provides the necessary electrolyte, whose formation can be enhanced by charged particles and hygroscopic contaminants[11].

The whole process involves dissolution of the metal at the anode migration of its ions through the electrolyte and deposition at the cathode (Figure 16).

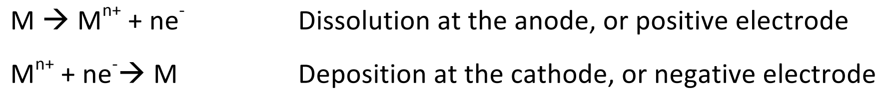

$M \rightarrow M^{n+} + ne^-$ Dissolution at the anode, or positive electrode

$M^{n+} + ne^- \rightarrow M$ Deposition at the cathode, or negative electrode

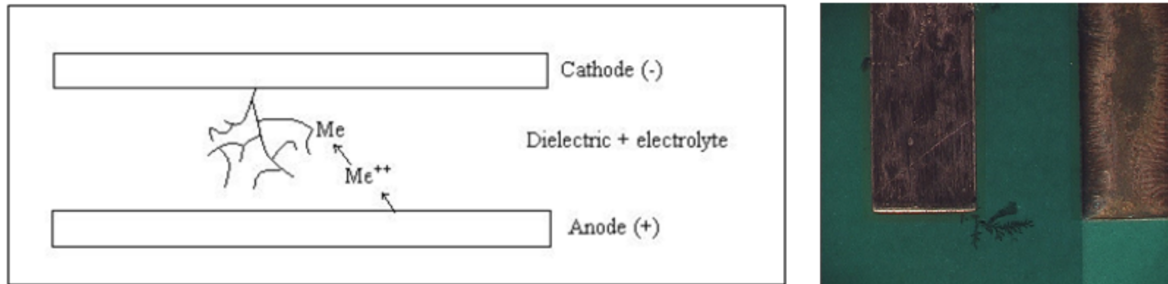

Figure 16Schematic representation of ECM (on the left) and a field case (on the right)[10]

Due to the resistance within the thin solution layer, a significant current localization occurs at the electrode surface: the metal ions deposition will thus not be uniformed but preferential, and dendrites will grow from cathode towards anode. When the electrode gap is filled a sudden rise in the leakage current is observed, lowering the SIR by several decades. When few dendrites are growing, the large current passing through them burns off the dendrites very fast, giving a temporary short-cut, until several dendrites make contact simultaneously and divides the short-circuiting current within them, allowing the dendrites to persist[9], [10], [40].

3.5.1 Factors influencing ECM

The possibility of ECM for a specific metal depends on the stability of the ions in aqueous solution and deposition potential relative to the hydrogen overpotential; therefore, only few metals like Cu, Ag, Sn and Pb are susceptible to electrolytic migration at least over a range of potentials and pH predicted by the Pourbaix diagram where particular ions are stable. If the potential for hydrogen evolution (ie. hydrogen overpotential) is lower than the deposition potential for the metal ions, most of the current will be used for hydrogen evolution rather than for metal deposition. Therefore metals like aluminum will not show electrochemical migration, instead the aluminium ion dissolution lead to precipitation of the hydroxide. .

Apart from the metal/alloys related factors, four other main factors which have a significant impact on ECM:

- Presence of halides which break down the oxide layer and facilitate anodic dissolution
- The pH value of the solution
- The applied potential
- The solubility of the species formed at the anode

As it is possible to notice from the Pourbaix diagrams (Figure 17), the change in pH dramatically modifies the nature of the formed species, due to its strong effect on anodic reactions. Additionally, due to electrolysis, the pH varies along the solution, influencing the region of stability for certain species, which may be stable close to the anode and unstable in the bulk solution.

The reduced distance between conductors on a PCB has further decreased the migration path of metal-ions, thus reducing the time to failure for a device.

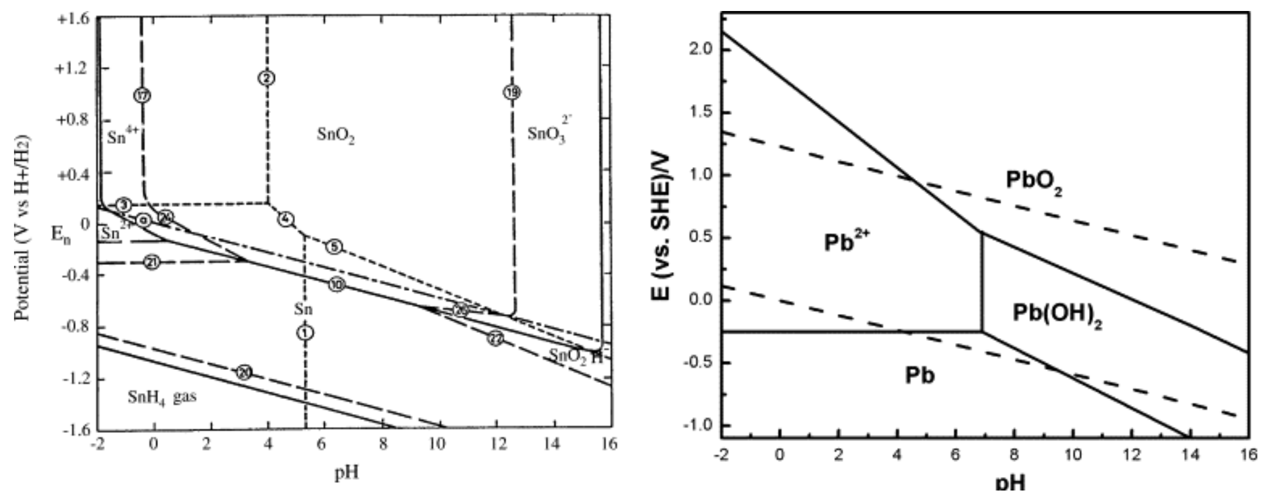

Figure 17 Pourbaix diagram for tin (on the left) and lead (on the right)

4 Critical factors for the reliability of electronic devices

Although the corrosion mechanisms which lead to the degradation of electronic materials and devices occur following the ones of most metals and structures, they differ due to the presence of these factors:

- The presence of an applied voltage
- The submicrometer dimensions
- The extremely small amount of corrosion products

In this chapter the environmental factors together with the main mechanisms will be introduced and explained.

4.1 Environmental factors

Environmental factors like temperature and humidity can, to some extent, be controlled due to the fact that electronic equipments are often housed in enclosures. Additionally, contaminants must be taken into consideration; within these the most important are gases, particles and a variety of organic and non-sulfur containing compounds[4][32]. Through the following paragraphs and explanation of how these factors affect the reliability of electronic devices will be introduced.

4.1.1 Temperature and humidity

RH is the amount of moisture in the air compared to what the air can "hold" at that temperature and it is defined as the ratio of the actual vapor density to the saturated vapor pressure[1]:

$$RH = \frac{actualvapordensity}{saturatedvaporpressure} x\ 100\% \text{Eq.4}$$

In order to achieve condensation on a surface it is necessary to reach a particular RH value, namely critical RH (cRH). This value is influence by many factors, like the surface finishing, the typer of the material and the contaminants. The higher the temperature is, the higher the amount of water air can hold. The Mollier diagram (**Appendix V**) is very useful to understand the relationship between moisture content, enthalpy and temperature of the air.

When an electronic device is exposed to a temperature colder than the surrounding, condensation occurs at lower relative humidity compared to the condition at thermodynamic equilibrium.

From the Mollier diagramis possible to extrapolate the graph in Figure 18. This depicts the temperature difference required for condensation between a metal surface and the air on various relative humidities

and temperatures of the surrounding air. An undercooling ΔT=-6 °C is sufficient to have condensation at relative humidity of 80%. This difference increases with decreasing relative humidity.
Since corrosion accelerates considerably already at relative humidity exceeding 50% the surfaces of the insides of the device should be at least 10-20°C (or more) warmer than the environment.
Due to the intrinsic ionization of water into hydrogen and hydroxide ions, a condensed water film has some conductive properties. This may be further enhanced by adsorption of some gases which form ionic compounds with water, such as CO_2. Nevertheless, the impact of a pure water film on the surface resistivity does not normally pose a problem. It is the function of the water film as a medium for ionization of ionic compounds that renders adsorbed water films hazardous.

It is important to mention that due to the different thermal profile of a PCB local condensation can occurs. The architecture of the PCB is thus extremely important in order to ensure a thermal profile as much homogenous as possible, avoiding crevices and allowing air circulation.

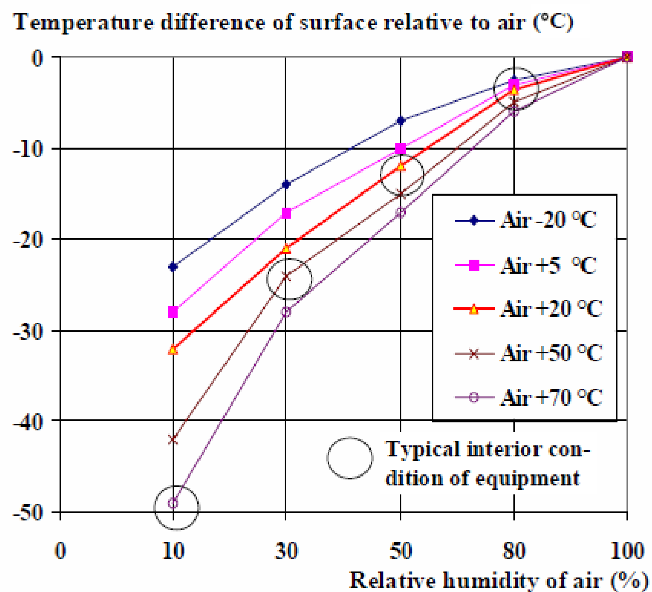

Figure 18temperature differences of the surface when the dew point is reached at various temperature and humidity values[1]

4.2 Sources of contamination

After describing which the main contaminants are, it is useful to explain where these contaminants come from. In this paragraph the sources will be divided into process and service related contamination.

4.2.1 Process related contamination

Many are the sources of contamination within the manufacturing of PCBAs: contaminants can be directly contained in the PCB substrate or can be released from various manufacturing processes, remaining this way on the surface. The submicrometer dimensions of the electronic devices trap these hazardous products into the small holes[1], [41].

Glass epoxy polymer and phenolic paper are the most common laminate material used for PCB manufacturing. The former one with woven glass cloth reinforcement has higher mechanical and electrical properties and it is therefore used for plated-through-hole and multilayer boards. The latter one, due to its poor temperature range and ability to absorb moisture, is mostly used for high volume domestic.

The PCB laminates contain flame retardants. Brominated flame retardants (BFR) have been widely used in industrial practices to improve the flame resistance on polymeric materials. Among the advantages of BFR are their efficiency, the high compatibility with many polymeric substrates and the limited influence on mechanical properties. The BFR that finds the wider industrial applications is tetrabromobisphenol A, namely TBBA. The main application of TBBA is in the production of brominated epoxy resins, commonly employed for printed circuit boards manufacturing. These can contain up to 20-25 wt.% bromine[42].

Decomposition of TBBA occurs between 150 and 270°C and the main products released from this process are HBr and methyl bromide. 150°C can be easily reached during the usage of the PCB, while 270 °C can be reached during the soldering process. These hazardous products accelerate the Au-Al bond failure[43], [44].

Surface finishing processes like Electroless Nickel Immersion Gold (ENIG) leave residue of sodium hypophosphite ($H_2PO_2^-$) and orthophosphate ($H_2PO_3^-$) which are strong reducing agents. They tend to remain the via-holes on PCB and can cause corrosion problems in presence of humidity and bias.

Among all the chemical processes used for PCB fabrication, the most contaminating one is application of solder. During solder the PCB is heated up to 240-260 °C, far above or close to the T_g of the polymer resins used for laminates[36]. This results in a softening of the laminates allowing flux residues to be absorbed into the resins and remained on the surface or in between the pins of components. This type of ionic contamination is the most common and harmful for the reliability of PCB assemblies. Field failures regularly occur due to not properly activated or fully removed flux residues. These flux residues can be corrosive themselves or absorb moisture at lower relative humidity than the one foreseen by the

Mollier diagram for the working conditions. By absorbing moisture they create a thin water layer on the surface of the electronic components, rendering the surfaces more conductive since there is a solution of ionasible material present. Hence a higher leakage current will be recorded and a greater probability of electrochemical migration will affect the devices.

Finally, a common source of contamination is due to impropriate human handling: human sweat contains, indeed, significant level of chloride and other inorganic ions and organic compounds which are really aggressive.

4.2.2 Service related contamination

Service related contamination is difficult to predict as it depends on the place of application of the device: field-environments near the sea or in tropic countries will deviate from those found in-land or in arctic areas. Significant differences will be found, as well, between highly industrials polluted locations and pristine nature or country side[1], [2]. The principal classes of contaminants that need to be considered are gases, particles with aggressive ions and hygroscopic compounds[45].

I. *Gaseous*.

Typical gaseous contaminants are of the type SO_2 NO_x or H_2S which are either corrosive in themselves or can react with moisture and increase the conductivity of the solution enhancing the corrosion process.. The most important pollutant in the form of a gas is SO_2, originating from combustion of oil, gas or coal containing some sulphur[46], [47]. Together with water it forms particularly aggressive sulphuric acid, H_2SO_4 very detrimental to silver coating alloys. H_2S is particularly dangerous for silver, as it forms silver sulphide crystals. The presence of halogenides like (HCl or HBr) is detrimental for the stability of the protective oxide-layers on the metals.

II. *Particles with aggressive ions*

The presence of aggressive ions like Cl^-, NH_4^-, SO_4^- , togheter with high humidity levels, tends to propagate electrochemical failure, such as leakage current, ECM and electrolytic corrosion

III. *Hygroscopic residues*

Dust and salts are the most important material components of the environment with respect to degradation of electronic devices. The higher the fraction of water-soluble ions with any particle, the higher is the corrosivity. Fine particles can absorb moisture; hence their cRH is a key factor concerning their corrosion behavior. When fine particles on surfaces absorb water, an

electrolyte film is formed: this is corrosive to many metals and can also lead to electrolytic corrosion when the circuit is biased[2][47].

Table 2 shows the cRH at 24 °C of some hygroscopic compounds

Table 2 cRH value for some hygroscopic compounds[47]

Salt	cRH (%)
NH_4HSO_4	40
$NH_4\ NO_3$	65
NaCl	76
NaBr	84
$CaCl_2$	29
Adipic acid	99,6
Glutaric acid	84
Malic acid	86
Succinic acid	98

5 Materials and theory behind experimental methods

In this chapter the materials, the setups and the techniques employed during this project will be introduced. Additionally the preparations of the solution to be investigated will be briefly explained.

5.1 Weak Organic Acids

Four weak organic acids have been investigated throughout this project, namely: adipic, malic, glutaric and succinic acid. Three different concentrations (1 $\mu g/cm^2$, 10 $\mu g/cm^2$ and 100 $\mu g/cm^2$) of the foretold WOAs have been preliminary prepared.

5.2 Tin

Pure tin has been employed for the polarization curves experiments, while the composition of the tin on the investigated components is the eutectic composition of 63% tin, 37% lead.

5.3 Solder Flux Systems

Commercial Cobar Solder Flux Systems were employed in this project. Their detailed characteristics can be found in Appendix III while in Table 3 Investigated *COBAR Solder Flux Systems*Table 3 the investigated systems are listed

Table 3 I*nvestigated COBAR Solder Flux Systems*

Flux Systems
327
380_R
390_RXT
396_DRM
327_Sel
94_Sel
385_Sel

5.4 Single Component Electrochemical Migration Setup

In order to test the effect of the WOA on the electrochemical migration on condensers a Single Component Electrochemical Migration setup was used. The component is held horizontally by two small adjustable probes, which act as connectors. Springs on both sides of the probes ensure the forces required to hold and maintain the component in position, while maintaining a good electrical contact between the tips of the probes and the terminals of the component. The SCEM setup used for the experiments consists of three separate pairs of metal probes (Figure 19). Four different WOAs and seven

solder flux systems were tested in this experiment at concentrations of 10 and 100 µg/cm^2 respectively. Three holders were used in order for simultaneous experiments using a Biologic VSP multichannel potentiostat. A numbers of 18 capacitors per concentration were tested in order to obtain replicable results.

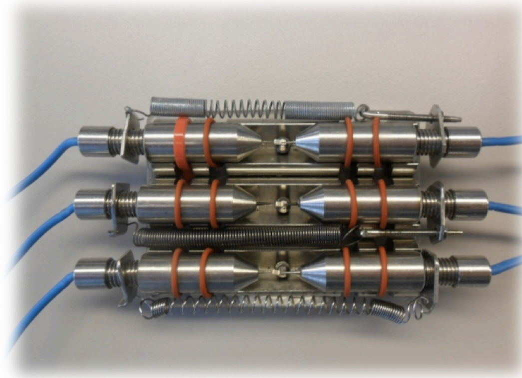

Figure 19 SCEM setup

The solutions were applied once the components were placed in SCEM setup. Through the use of a micropipette the desired amount of solution was placed in the form of a droplet on the surface of the SCM. The concentrations to be tested were 10 and 100 µg/cm^2. In order to achieve these concentrations the amount solution to be placed is selected with respect to the surface area of the component. By considering the assumption that 1 mm^2 of area is covered by 1 µl of solution, the 2,5 mm^2 top surface area of SMC will be covered by 2,5 µl of 10 ppm solution in order to get 1 µg/cm^2.

The power source and current measurement instrument for SCEM setup and data logging was carried out using a Biologic VSP potentiostat having a 0-20 V compliance voltage.

SCEM setup in this project was used to investigate ECM reliability on size 0805 10 nF multilayer ceramic capacitors. The SCMs were tested at ambient conditions: temperature 20-25 °C, relative humidity 25-40%.

5.5 Test PCB setup

In order to investigate the PCB level parameters on corrosion behavior the CELCORR test PCB was used (Figure 20). It consists of 18 circuits mounting surface mount components (SMCs) and 2 surface insulation resistance (SIR) patterns, for a total of 20 circuits. Each of the 18 circuit channels consists of

10 identical SM components soldered in parallel. Nine out of eighteen are resistors, while the remaining half are capacitors. The size and the electrical properties of the foretold components are summarized in Appendix IV. In total there are 90 capacitors, 90 resistors and 2 SIR patterns. One of the SIR patterns is covered by a soldermask, while the other has a reflow solder surface finish.

The SIR patterns on the test PCB are designed for surface insulation resistance testing which is performed to determine whether the materials used in an assembly are likely to produce unacceptable current leakage levels, or shorts due to metal migration between conductors. By measuring changes in current over time at different temperatures and humidity it is possible to evaluate the likelihood for possible failures due to environmental issues. The main parameters which affect the insulation resistance are the sheet resistance, the bulk conductivity and the electrolytic contamination.

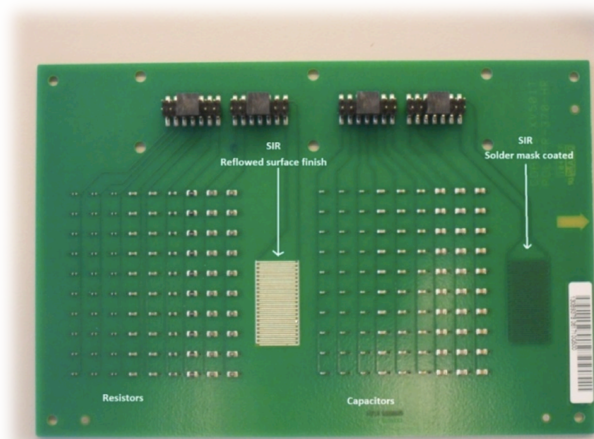

Figure 20 Test PCB setup

Each row consists of 10 capacitor or resistors connected in parallel: the leakage current measured on a single channel, is thus the sum of the currents of all the components in one row. This provides information on corrosion issues related to PCBA level. In order to measure the leakage currents an ammeter connected to the circuit via a double switch system is used. This enables to measure the current circulating without interrupting the potential bias. While one switch guarantees a constant potential bias, the other one switches on the ammeter to the circuit to read the current values. This is done really quickly for a short amount of time. Due to the very low internal resistance of the ammeter

the change of potential biased due to the switching of circuits can be neglected. This fast switching and its scarce influence on the total bias allow evaluating the electrochemical behavior of corrosion without interruptions or interferences. The sensitivity of the current measuring instrument is comprised within 1 μA and 100 mA and it is possible to obtain five measurements on each circuit per seconds. The possibility of choosing the sampling rate on each circuit and manually enabling/disabling a given channel is guaranteed by the software interface created with LabView. For each channel, the current value vs. time is displayed. In this way it is possible to monitor dendrite formations due to the fact that if a dendrite shorts two electrodes on a component a current spike is observed in the current-time signal.

5.6 RTD Sensors

Resistance Temperature Detectors (RTD, Figure 21) sensors enable to measure temperature changes by correlating them to changes in their resistance. The core element of a RTD sensor is made of a pure material which has a predictable change in resistance as the temperature changes. This material is shaped in a form of a coil wrapped around a ceramic glass core placed inside a sheathed probe to protect it.

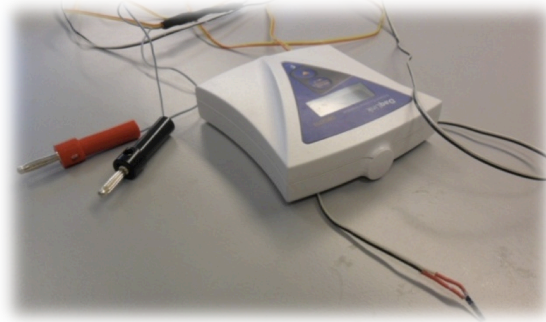

Figure 21 RTD sensor setup

The common materials used for this purpose are platinum, copper or nickel. These have a repeatable and predictable resistance versus temperature changes: The R vs T relationship is defined as the amount of resistance change of the sensor per degree of temperature change. The linear approximation of the R vs: T relationship between o and 100°C is referred as α, which is defined by the following equation

$$\propto = \frac{R_{100} - R_0}{100 R_0} \qquad \text{Eq.5}$$

Within these materials, Platinum is the one whose resistance to temperature relationships follows a well defined linear trend with and alpha of 0.00395. Additionally, this R vs. T relationship is highly repeatable over a temperature range from -275 °C to 961.78 °C. Its chemical inertness is a supplementary properties which makes Platinum the most suitable material for this purpose.

The RTD sensor used for the measurements in this project is a Thin Finite Elements type. A thin layer (10 to 100 Å) of resistive material, platinum in this case, is deposited on a ceramic substrate. This film is then protected by either an epoxy or a glass coating, which acts also as a strain relief for the external lead-wires.

Different wiring configurations are available to measure this change of electrical resistance due to variation in temperature: 2-wire, 3-wire and 4-wire circuits with increasing accuracy due to the possibility of reducing the effects of the lead resistance. With the 2-wire circuit the resistance of the connecting wires is added to that of the sensor, leading to errors of measurement. However, in the case where the lead wire resistance is much smaller than the change in resistance of RTD as a response to an increase of temperature per 1 °C, the 2-wire circuit gives quiet reliable results. The RTD used in this project is a 2-wire circuit and gives a 3.9 increase of resistance per 1°C increase of temperature and the resistance of the lead wires is much lower than 1 ohm. The total error will thus be less than 1 °C. These conditions made t a suitable RTD for this project. This circuit can be seen in Figure 22.

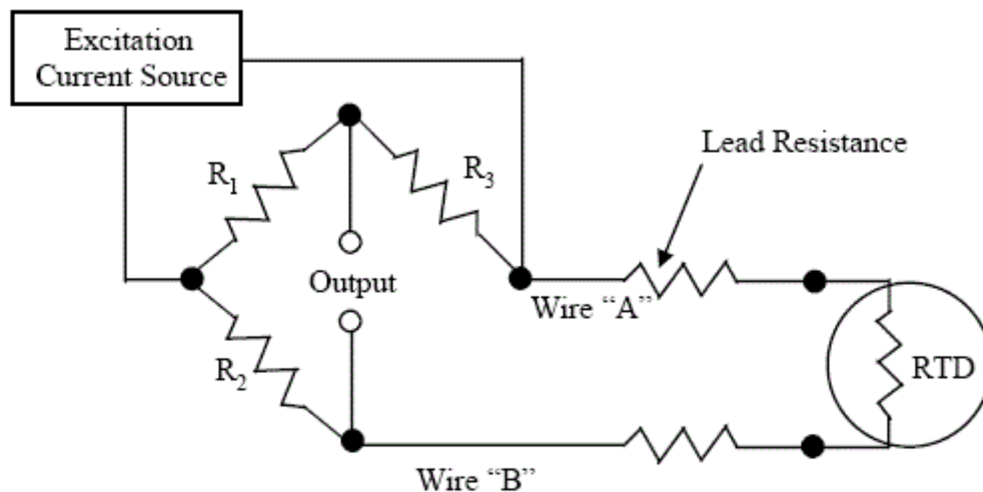

Figure 22 RTD connection into 2-wire circuit

Considering the nominal resistance of the circuit of 1000 ohm and by neglecting the resistance of the lead wire, the output voltage will, thus be

$$V_{out}=\left(\frac{R_{RTD}}{R_{RTD}+R_3}-\frac{R_1}{R_1+R_2}\right)V_S \qquad \text{Eq.6}$$

Where V_s is the applied voltage (1,5 V for this purpose).

The resistance change of platinum RTD in relation with temperature is given by

$$R_T = R_0[1 + AT + BT^2 + CT^3(T-100)](-200°C < T < 0°C) \quad \text{Eq.7}$$

$$R_T = R_0[1 + AT + BT^2](0°C \leq T < 850°C) \qquad \text{Eq.8}$$

Where

R_T is the resistance at temperature T

R_0 is the resistance at 0 °C

A=3.9083 x 10^{-3} C^{-1}

B=-5.775 x 10^{-7} C^{-2}

C=-4.183 x 10^{-12} $°C^{-4}$

5.7 Climatic conditions for investigations

For qualification of new materials and products with respect to corrosion resistance accelerated corrosion tests generally need to be adopted during product design work. The higher the degree of acceleration of a corrosion test the more favorable the accelerated corrosion test will be in keeping the required testing time short. On the other hand, the higher the acceleration of the corrosion process needs to be during testing the harder is to simulate properly the natural occurring corrosion processes. This is pointing at the main problem in designing meaningful accelerated corrosion tests for product qualification.

The main parameters which play a consistent role in accelerating the corrosion test for failures are environmental factors like temperature, humidity and contamination. In addition to this, the potential bias applied to the circuit, influences to a great extent the rate and the speed of the corrosion mechanisms. By increasing these factors is thus possible to reduce the time testing for failure. It is important to mention, though, that the choice of hazardous parameter to be increased in the experiments strongly depends on the failure mechanism to be investigated as well as on the conditions wherein the device is expected to be operating.

Different conditions were tested on the PCBs in this study. In this paragraph the environmental conditions applied are briefly described.

5.7.1 Climatic chamber

In order to simulate the humidity and the temperature of the surrounding an *ESPC PL-3KPH* climatic chamber (Figure 23) was used. In this chamber it is possible to place the specimen to be investigated, bias it, and stress it with both temperature and humidity changes. By contaminating the specimen is thus possible to investigate and evaluate the combined impact of environmental factors and contamination on susceptibility for corrosion failures. The same environmental conditions were guaranteed during each experiment.

Figure 23 ESPC PL-3KPH climatic chamber

Two main setups were simulated by using the foretold climatic chamber:

- Elevation of relative humidity at constant temperature: rH increasing from 40% to 98% in step of 5% every two hours at constant T=25°C
- Constant T= 25°C and constant rH= 60% while lowering the temperature of the PCB with a peltier sage in order to achieve condensation

5.7.2 Peltier stage set up for cooling

When a substrate is experiencing a lower temperature than the surrounding, the vapor density on the surface increases up to the point where condensation happens to be. This is well explained from the Mollier diagram and the temperature at which the condensation occurs is the so called dew point. Electronics devices experience this phenomenon to considerable extent. Outside electronics devices are subject to temperature changes due to night and day shifts with considerable variations in temperature and humidity. Even more common is the case of small electronics like mobile phone and mp3 readers: the environmental changes they experience when carried from an outside to an inside location might be sufficient to create a temporary water layer on the components of the PCB placed inside the device which promotes the corrosion process.

In order to simulate nearly dew point condition an aluminum stage with embedded Peltier elements was used. The Peltier elements are thermoelectric cooler which uses the Peltier effect to create a heat flux between the junctions of two different types of materials. When a current is flowing through the junction of dissimilar metals, heat is generated at the upper junction and adsorbed at the lower junction. This depends on the direction in which the electrical current flows: Heat generated by current flowing in one direction is absorbed if the current is reversed. When a DC current is applied heat is moved from one side of the device to the other - where it must be removed with a heat sink.

For this study two peltier elements were placed into an aluminum block. The PCB was placed on the top of the block where the cooling surface was situated. In order to guarantee the highest possible contact within the two surfaces, the PCB was screwed at each corner of the stage. This was done in order to ensure the most uniform temperature distribution on the PCB and its components (Figure 24).

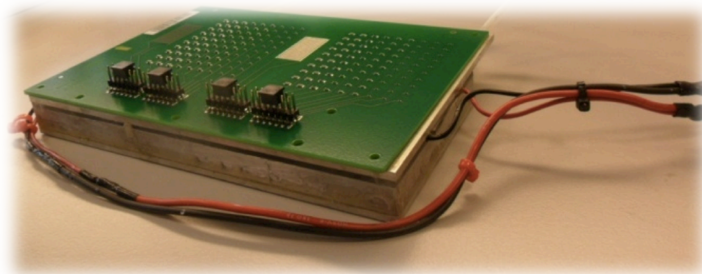

Figure 24 Test PCB setup mounted on an aluminum case containing two Peltier stages

The heat from the top side, where the PCB is placed,is thus transferred to the bottom side. However the total amount of heat generated by Peltier elements is rising in time, due to their low efficiency. In order to absorb this increasing heat, water circulating at constant temperature through the aluminum block, from the heating side of peltier elements has been used. This ensures a constant temperature on the surface of the PCB to be tested. An internal heating system maintains constant the temperature of the cooling water.

5.8 Double Pt electrode set up for leakage current measurements

A double platinum electrode set up shown in Figure xx is used for measuring the leakage current through a tiny drop-let of solution. In order to measure the leakage current of the foretold WOAs a 100 µl droplet of each solution was used. This droplet was placed on a polystyrene substrate, previously cleaned with ethanol to remove any possible trace of contamination which can interfere with the measurements. The leakage current measured is a function of various parameters related to the duel platinum electrode set up, and these are:

- The exposed area A of the electrodes
- The distance d between the electrodes

The testing tool designed at DTU provides the possibility of fixating the distance between the electrodes keeping this way the exposed area constant. Thus Platinum wires with a constant diameter of 0.5 mm have been used. The area which is not exposed has been coated with a polymer wiring insulation and the top parts are kept bare in order to connect them to a potentiostat. The wires are held by an acrylic aggregate with grooves and holes. Through the use of screws placed on the shaft of the tool it is possible to set the electrodes at a fixed distance of 3.55 mm. The length of the bare tip was regulated to 1 mm by using cyanoacrylate type superglue (Figure 25).

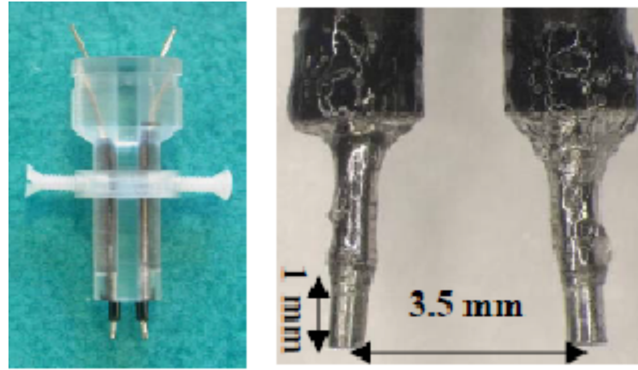

Figure 25 LRTD setup (on the left); close up of the platinum tips (on the right)

The wires are made out of platinum as it exhibits a very stable behavior even at large potentials end electrolyte concentrations. By looking at the Pourbaix diagram for platinum (Figure 26) is possible to notice that the dissolution of the material it is limited to a region of pH between 0 and 3 and potentials between 1 and 1.5. At higher potentials it will react to form a stable PtO_2 compound at the anode and remain as stable Pt at the cathode, which will not contribute to the measured leakage current.

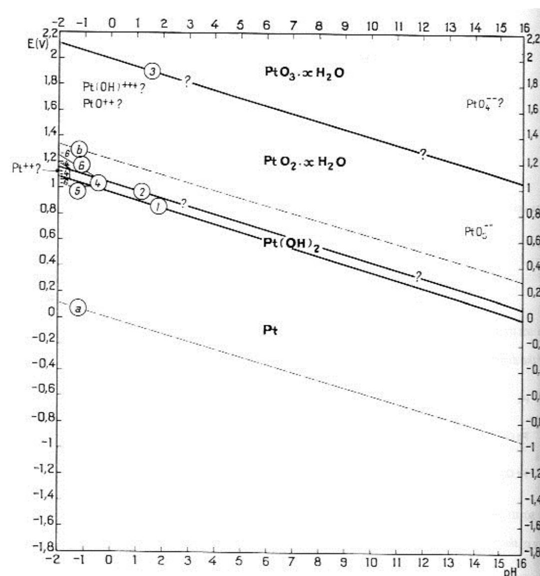

Figure 26Purbaix diagram for platinum

The LRTD was mounted on the carrousel of an optical microscope and the leakage current between the electrodes were measured with "BioLogic VSP" multichannel potentiostat. The terminals of the potentiostat were connected to the electrodes and the response of the leakage current through the electrolyte to applied potential was measuered.

5.9 Potentiostat

In order to measure the leakage currents in all the experiments of this project a BioLogic VSP multichannel potentiostat (Figure 27) was used. It has three independent potentiostat units with a current ranging from 1 nA up to 400 mA with a 760 pA resolution. The voltage is adjustable within a range from 0 and 20 V with a resolution of 300 µV and an acquisition time of 20 µS. The potentiostat is controlled from a PC by a USB connection. Measurements were conducted with the EC-Lab® software in the Chronoamperometry mode. Chronoamperometry is an electrochemical technique in which the potential of the working electrode is stepped and the resulting current from faradic processes occurring at the electrode (caused by the potential step) is monitored as a function of time.

Figure 27 BioLogic VSP multichannel potentiostat

The system consists of three electrodes, namely: the working electrode W (the specimen to be investigated); the counter electrode C and the reference electrode R. W and R are connected through a salt bridge as shown in Figure. The potentiostat functions by maintaining constant the potential of the WE with respect to the RE. This is done by delivering the necessary current between the cell consisting of the CE and the WE. For the WE this is experienced as an external current.

5.10 Conductivity measurement setup

In order to measure the conductivity of the solutions to be investigated in this work, a CDM201 conductivity meter has been employed. Each solution was placed in a 5 ml vial were the 4-electrode conductivity cell was dipped to perform the measurements (Figure 28). This tool uses an alternating current and it measures the conductivity within a range from 0.01 µS to 400 µS with an accuracy of ±

0,2% of reading ± 3 on least significant digit. Since the AC current is applied only on the outer electrodes there is no polarization effect on the inner electrodes, which measures the voltage.

Figure 28 CDM210 conductivity meter (on the left); 4-electrode conductivity cell

5.11 Reference Electrode

In order to draw the polarization curves on tin for the different WOAs a Silver/Silver Chloride electrode has been used as a reference electrode in the potentiostatic set-up. Due to its simplicity, stability and non toxicity it has been employed as a reference electrode in this project. It is made of a single silver wire coated with a thin layer of silver chloride by electroplating. The redox reactions which occur between the silver metal (Ag) and its salt (AgCl) are the following:

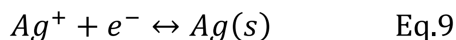

$$Ag^{+} + e^{-} \leftrightarrow Ag(s) \qquad \text{Eq.9}$$

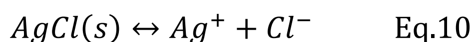

$$AgCl(s) \leftrightarrow Ag^{+} + Cl^{-} \qquad \text{Eq.10}$$

This can be written as an overall reaction:

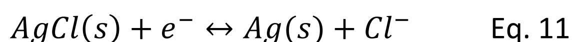

$$AgCl(s) + e^{-} \leftrightarrow Ag(s) + Cl^{-} \qquad \text{Eq. 11}$$

The redox reaction, which includes the dissolution of the metal or the cathodic deposition of the silver ions, has 100% efficiency due to the fast electrode kinetics. This ensures that sufficiently high current can be passed through the electrode without losses.

The potential developed by the Ag/AgCl electrode it is proportional to the activity of chloride ions as it is shown by the Nernst equation

$E_{Ag/AgCl} = E^0_{Ag/AgCl} - 0.059 log_{10} a_{Cl^-}$ Eq.12

When the electrode is placed in a saturated potassium chloride solution it develops a potential o 199 mV vs. SHE.

5.12 Techniques

In this paragraph the theory behind electrolyte conductivity and leakage current measurements and the polarization curves will be discussed. Conductivity and leakage current measurements are procedures employed to investigate the effect of contamination on the corrosion failures and mechanisms on PCBAs. Polarization curves were instead recorded in order to understand the behavior of tin, one of the main materials used in electronics, in contact with three different concentrations of the four WOAs.

5.12.1 Leakage Current and Conductivity

The corrosion reliability of an electronic circuit depends to a great extent on the possibility for a leakage current to flow between two conductors and its magnitude.

In order to measure leakage currents it is necessary to create an electrochemical cell by immersing two metal electrodes in a solution (electrolyte) and applying a bias potential (Figure 29 a)). The applied potential will be the driving force which moves the negatively charged ions (anions) to the positive electrode (anode) and the positively charged ions (cations) to the negative electrode (cathode). Charged species will be build up at the electrodes creating the so called Helmoltz double layer (Figure 29 b))[48]. The current it is thus carried by electrons in the electrodes and by charged ions in the solution. However the charge build-up and transfer across the electrode-electrolyte interface is responsible to introduce large non-ohmic contributions. Therefore it is possible to represent the electrodes in series with the electrolyte, as a parallel combination of a capacitor and a non linear resistance. The former stands for the capacitance of the double layer, whereas the latter for the electrolytic resistance. In order to avoid this polarization effect, an alternating voltage has to be applied[49].

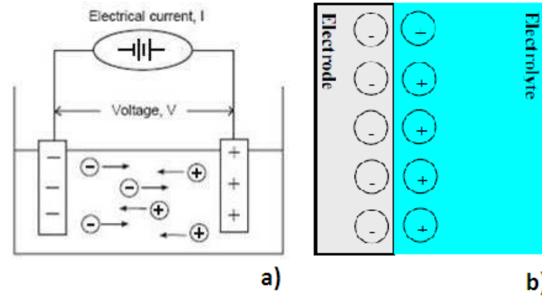

Figure 29 a) basic DC electrochemical cell; b) build up pf Helmoltz double layer

During this work a direct voltage has been used, sufficiently high to overcome the decomposition potential for electrolysis. Above this potential there is a direct proportionality between the applied potential and the current passing through the electrolyte. In this way, the measured current is a contribution of the ohmic current (related to ions migration) and faradaic current (due to charge transfer during the redox process occurring at the electrodes).

When the electrode are biased and placed in an electrolyte, the electrons produced at the cathode are consumed at the cathode. As a consequence, there will be a development of a negatively and positively charge could, respectively on the cathode and the anode. These charges are neutralized by the ions in the solution, enabling the electrons to keep flowing.

5.12.2 Conductivity measurements

The conductivity of a solution is defined as the ability o conducting electricity. In order to define the conductivity it is first necessary to know the resistance of the solution R which can be calculated using the Ohm's law[50]

$$R = V/I \qquad \text{Eq. 13}$$

Where V is the applied voltage and I is the current flowing through the solution.

What the conductivity meter measures is, however the conductance $G = 1/R$ (S) and it displays the reading converted into conductivity (S/cm)

$$\kappa = G \cdot K \qquad \text{Eq.14}$$

Where K is the cell constant (cm^{-1}), which is defined as the ratio of the distance d (cm) between the electrodes to the area a (cm^2) of the electrodes:

$$K = {}^{d}/_{a}$$

In order to measure the value of the cell constant k two different concentrations of KCl were taken, namely 1M and 0.1M. Their conductivity values were then adjusted to the standard ones at the measured temperature. From these test a cell constant $k=0.521\ cm^{-1}$ was determined.

A typical conductivity meter applies an alternating current at a certain frequency to two active electrodes and records the potential. These two are then converted into conductance G and then through the cell constant into conductivity κ. The value of the applied frequency has to limit the accumulation of ionic species near the electrode surfaces and the consequently chemical reaction at the surfaces. Otherwise a polarization resistance arises leading to erroneous results. This effect can be avoid by using a 4-cell conductivity cell, as it was done in this project.

5.12.3 Polarization Curves

Before describing the technique used to record polarization curves on Tin it is helpful to briefly introduce the theory behind the electrode kinetics with particular focus on the polarization and overvoltage effects.

If a basic Zn-H cell is taken into consideration, the reaction occurring at the electrodes are:

$Zn \rightarrow Zn^{2+} + 2e^{-}$ oxidation Eq.15

$2H^{+} + 2e^{-} \rightarrow H_2$ reduction Eq.16

These two electrode reaction are, usually moved away from equilibrium, *polarized*, as a result of the net electric current flowing through the interface between metal and liquid. When a corrosion process occurs on a surface the real measured potential it is measured to be at a value between the equilibrium potential of the cathodic and anodic reaction, as illustrated in Figure 30.

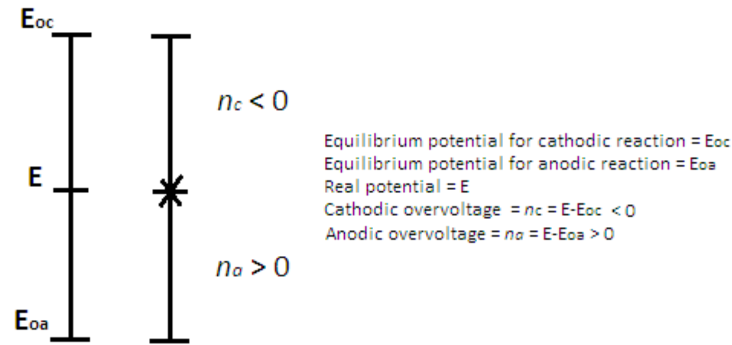

Figure 30 Equilibrium potentials, real potentials and overvoltages

The difference between the measured potential and the equilibrium potential is the *overvoltage*[34]. Thus, both a cathodic and an anodic overvoltage will be recorded. These are defined by the following equations

Cathodic overvoltage = $\eta_c = E - E_{oc} < 0$

Anodic overvoltage = $\eta_a = E - E_{oa} > 0$

Without entering into the details of activation and concentration polarization, it is worth to emphasize that in the anodic reaction, activation polarization is often dominating (except when passivation effects occur). For activation polarization the relationship between current density, i_a, and the anodic overvoltage η_a is given by the *Tafel equation*

$$\eta_a = b_a \cdot log\frac{i_a}{i_0} \qquad \text{Eq.17}$$

Where i_0 *is* the exchange current density, and b_a *is* the anodic Tafel constant defined as

$$b_a = \frac{2.3RT}{\alpha zF} \qquad \text{Eq.18}$$

With

R= 8.314 J K^{-1} mol^{-1}

T= temperature K

F= Faraday's constant = 96485 J

α= transfer coefficient; most frequently in the range 0.05-0.15 V/current density decade

In the reduction process (cathodic reaction) both type of polarization occur. Thus the relationship between overvoltage and current density will therefore be:

$$\eta_c = -b_c log\frac{i_c}{i_0} + 2.3\frac{RT}{zF}\log\left(1 - \frac{i}{i_L}\right) \qquad \text{Eq.19}$$

Where $i_L = DzF\frac{c_B}{\delta}$ is the *diffusion limiting current density* (where $c_b$is the concentration in mol cm^{-3} at a distance δ in cm from the electrode and *z* is the number of electrons per mole oxygen reacting).

The polarization curves determine the degree of potential change as a function of the current applied to the metal surface of the specimen to be investigated, establishing this way the corrosion rate. When the current is applied in a positive direction the potential of the metal surface is said to be anodically polarized; a negative direction signifies that it is cathodically polarized. Polarization curves allow investigating the effect of activation and concentration processes on the rate at which anodic or cathodic reaction scan give up or accept electrons, meaning the corrosion rate[51].

It is seen that the overvoltage curves (Tafel Lines) are asymptotes to the polarization curves. The cathodic and anodic linear portions of the polarization curves can, thus, be extrapolated to the corrosion potential "E_{corr}", where, under ideal conditions, they should intersect (Figure 31). The value of the current at their intersection will be the corrosion rate "i_{corr}" expressed in current density.

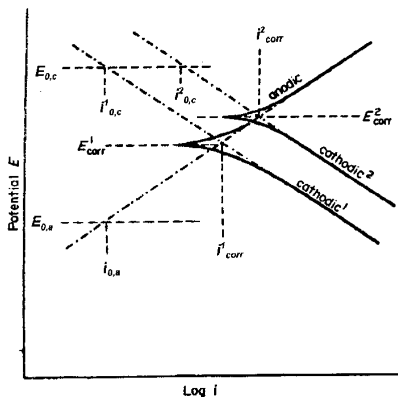

Figure 31 Extrapolation of Ecorr from polarization curves

5.13 Electrolyte preparation

Several electrolyte solutions were prepared during this project, with the purpose of investigating their effect both on leakage current and ECM. The solvent used for all the electrolytes was water purified with Sinergy MILLIPORE water purification system, which allow to purify water up to 18.2 MΩ·cm resistivity at room temperature. The first electrolyte was used as a reference and it contained sodium chloride which is a strong electrolyte. The second set of solutions contained the previously introduced

WOAs, which are the most common activators in solder fluxes. Due to partly disassociation of WOAs in water, these are considered as weak electrolyte. The third sets of electrolytes were commercial flux systems, from COBAR. The table below summarizes previous statements.

Table 4 WOAs and Flux systems tested in this project

Reference	WOAs	Flux Systems
NaCl	Glutaric acid	327
	Adipic acid	380_R
	Malic Acid	390_RXT
	Succinic acid	396_DRM
		327_Sel
		94_Sel
		385_Sel

This section reviews the electrolyte preparation procedures of all the electrolytes employed in this work.

5.13.1 Sodium chloride and WOAs

IPC J-STD-001D (*Requirements for Soldered Electrical and Electronic Assemblies)* standard and IPC-650 ROSE test method refer to the value of 1.56 μg/cm^2 as an upper allowable limit of ionic contamination to be present on PCBAs. Various concentrations in the rage of this limit had been previously investigated in the Master Thesis project of Vadimas Verdingovas, thus for this purpose a unique concentration of 1.56 μg/cm^2 has been taken as reference to compare the behavior of the others electrolyte systems to the standard one.

Three different concentrations of the four WOAs have been prepared for this project, namely 1, 10, 100 μg/cm^2. As the acidity of these acids is lower than NaCl, these solutions have been selected in order to test these acids on a range of value which may correspond to the standard one.

For the preparation of the foretold solutions at specific concentration the chemically purified NaCl, and the WOAs were weighted with electronic *Sartorius research. R160P.* semi-balance and then dissolved in Millipore water.

Since the standard refers to concentration values expressed in μg/cm^2 and the electrolyte has a concentration expressed in g/l a direct conversion is needed. In Verdingovas' project it was found that a surface area of 1 mm^2 can be covered with 1 μl of solution, thus to move from μg/cm^2 to g/l the following sequence has been employed:

1 µg/cm²→ 0.01 µg/mm²→ 0.01 µg/ µl →**0.01 g/l**

This conversion has been employed for all the electrolyte solutions used in this project.

5.13.2 Solder Flux residues

Cobar "No-clean" wave solder fluxes were used for investigation in this work. A single concentration of 100 µg/cm² per flux type was tested in order to study the effect on the ECM on capacitors. The datasheet regarding the properties of these solder flux can be found in **Appendix III**. The flux residues were separated from the solvent and then dissolved into Millipore water. The steps followed to prepare the solution are the same as in Verdingovas' project and can be read from there.

Each flux system had an average solid content of WOA around 2% in weight.in order to obtain a concentration of 100 µg/cm² it has been assumed that 1 ml of flux weights 1 g. This assumption is quiet realistic and it has been empirically verified. Thus, 5 ml of flux in 100 ml of Millipore water correspond to 5 g/100ml. If an average solid content of WOA of 2% has been considered, 5 g/100ml will correspond to 0.1 g/100ml, which becomes 1 g/l of acid content. By following in the reverse way the previous conversion sequence, the requested concentration of 100 µg/cm² is achieved. To briefly summarize 5 ml of flux dissolved into 100 ml of Millipore water give a solution with a concentration of 100 µg/cm².

6 Physical and chemical properties of the investigated WOAs

In this chapter the physical and chemical properties of the four WOAs investigated in this project will be introduced. These will be used throughout the report in order to understand and explained the obtained results.

6.1 Chemical Structure

Weak organic acids are often the main activating species in "No-clean"-fluxes, either alone or as a mixture of different acids. The most employed ones are especially short-chain carboxylic or dicarboxylic acids like adipic, glutaric, succinic and malic acids. As activators, these acids must react with the oxide layers on the PCB and evaporate after thermal exposure during soldering. Carboxylic and dicarboxylic acids have a similar structure consisting of an aliphatic backbone of hydrocarbons (CH2) with a carboxyl-group (-COOH) attached to the end of the molecule[9], [52]. The main difference between these two species consist in the number of carboxyl-group at the end of the molecule: carboxylic acids only have one carboxyl-group in one end and a CH3 group in the other end, whereas both the ends of dicarbooxylic acids terminate with a carboxyl-group. Figure 32below shows the chemical structure of the investigated WOAs.

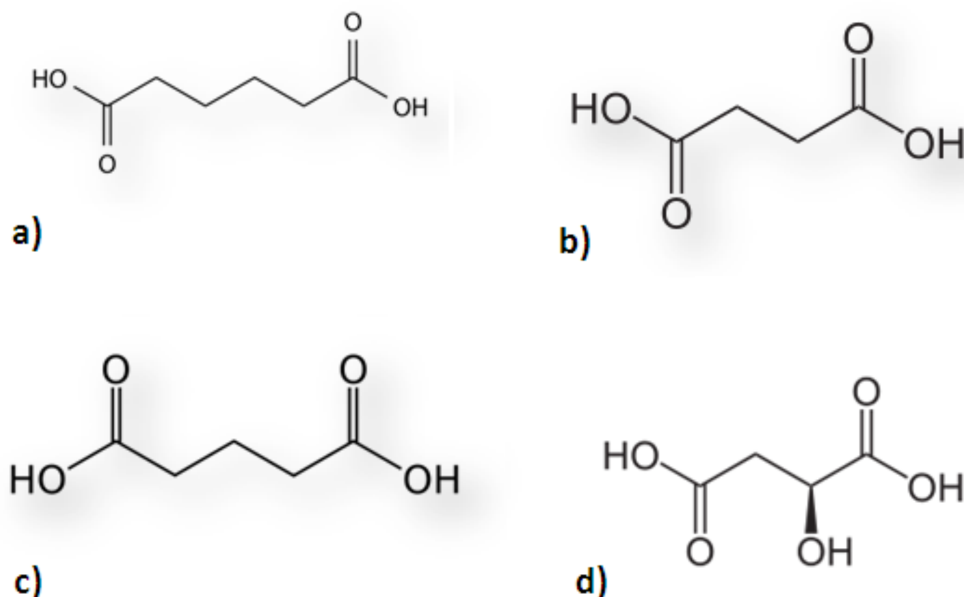

Figure 32 a) adipic acid b) succinic acid c) glutaric acid d) malic acid[53]

6.2 Physical Properties

Table5summarizes some physical and chemical properties of the foretold acids

Table5 Physical Properties of Weak Organic acids[54]

Acid	pK_{a1}	pK_{a2}	Solubility in water at 20 °C (g/l)
Adipic	4.4	5.4	14
Succinic	4.2	5.6	80
Gluaric	4.4	5.4	639
Malic	3.4	5.1	558

All four of the WOAs possess two acidic groups (COOH) per molecule, thus they are all dycarboxylic acids. By looking at the relative acidities, the malic acid is the most acidic of the four, having the lowest pK_a[1], whereas the acidity value of the remaining is quiet comparable[54].

Melting point and solubility in water are dependent on chemical structure. This is similar for the first three acids, which differ only in the number of methylene (CH2) groups between the carboxylic-acid groups. Malic acid has an additional hydroxyl group (OH) attached to the backbone of the hydrocarbons chain. Although the glutaric acid has a number of methylene that is intermediate between adipic acid and succinic acid, its melting point in considerably lower and solubility considerably higher than both adipic acid or succinic acid. This is due to the bulk structures of adipic acid and succinic, which involves association of carboxylic acid groups, thus giving a "harder" structure (Figure 33). Glutaric acid, on the other hand, arranges itself with less interaction leading to a lower melting point and greater solubility in water. Malic has a comparable solubility in water to glutaric acid, as a result of the hydroxyl group.

[1] pK_a = pH of a solution of WOA if $[RCOO^-]$ = [RCOOH]

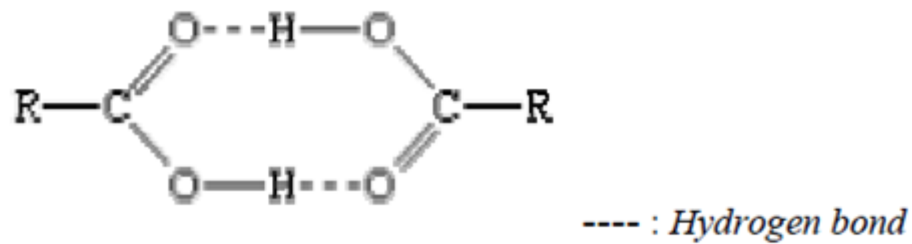

Figure 33 Dymeric form of carboxylic acid

The chemical reactions involving the organic acid functional groups and the metal-oxide explain the reduction effect of these acids. The hydrogen atoms from the carboxyl groups in the organic acid molecules react with oxygen from the oxide to form water, while the metal will attach to the remaining organic molecule. The reaction is the following:

7 Results and discussion

The results of the investigation on the effect of weak organic acids as activator in Solder Flux on the climatic reliability of PCBAs are introduced. In addition to this, the results from Solder Flux Systems employed in PCB manufacturing will be presented. Short conclusions for each chapter, briefly summarize the outcomes. The results from each chapter will be used and related with each other. An overall summary at the end of this chapter provides an overview of the findings, linking the results from a broader point of view.

The first topic of study is the effect on the corrosion rate of pure tin under WOA contamination. From this experiment polarization curves are drawn which allow to understand how the different metal-WOA interact with each other. Additionally, from these curves, it will be possible to determine which solution of the WOAs is more aggressive towards pure tin.

The electrolytic properties of the four WOAs are investigated with the purpose of obtaining the concentrations of acids which give the same conductivity as 1.56 $\mu g/cm^2$ of NaCl (contamination limit referred in IPC J-STD-001D standard). The results of these experiments provide an understanding of the aggressiveness of the investigated acids together with the determination of the concentrations to be analyzed in the other experiments.

The tendency of WOAs and Solder Flux System to induce ECM has been investigated at full condensation conditions. Test in the climatic chamber enabled to study the effect of temperature and relative humidity on LC of the SIR pattern and capacitor on test PCB. These tests were carried out at near and full condensing condition. LOM, SEM/EDX analyses help to understand the corrosion failures and products.

The results of each experiment are compared with physical and chemical properties of the investigated WOAs found in literature and previous experimental results.

7.1 Electrochemical studies on pure Tin in WOA

This chapter described the results of the investigation on the electrochemical behaviour of Tin in various weak organic acid solutions (Adipic, Succinic, Glutaric, and Malic) using potentiodynamic polarization experiments.

A potentidynamic approach has been employed to recorder the polarization curves.The potential (E) of the corroding metal is varied systematically at a scan rate and recording the current response as the potential changes. The current (I) needed to maintain the metal (working electrode WE) at each applied potential (E_w) is ascertained and the potential/current data is plotted to give the experimental polarization curve. The curves are displayed with the independent variable (in this case the potential) as ordinate. The $\log_{10}$ of the current density (log *i*) is plotted in the positive x direction. Value of Ew represents the surface potential of the corroding metal, which could be compared with the various potentials the metal can experience on a PCBA surface. The resulting current then will represent the magnitude of electrode reactions (such as metal dissolution or any other possible electrochemical reactions), part of of it is related to the metal dissolution in the corroding environment. Depending on the corrosion system under study it follows that from the shape of the polarization curve it is possible to obtain information on the kinetics of the corrosion reactions, protective film formation as a function of potential (passivity), ability of a compound (for eg. WOA) to act as a corrosion inhibitor, and corrosion rate of the material.

7.1.1 Effect of different concentrations of WOAs on the polarization curves

Overlay of the polarisation curves for tin in increasing WOAs concentrations is shown in Figure 34. The potential value (intersection of the anodic and cathodic reaction) where the current changes from negative to positive (or the potential value at which the cathodic current is equal to the anodic current), is called the steady state corrosion potential, E_{corr}. This can be seen as a "notch" at potentials between -500 mV and -600 mV in all the curves. At potential less than this values, the current is negative, and the surface is in cathodic domain. At potentials larger than E_{corr}, the current is positive, and anodic dissolution of tin is observed. The Ecorr values did not show significant change with increase in WOA concentrations irrespective of the acid types. However, cathodic part of the curves showed an increase in current density at all potentials

with increase in concentration of acids. The magnitude of increase was approximatively one decade. A similar behaviour could be seen for the anodic part of the curves except that the malic and succinic acid shows higher anodic current values compared to adipic and glutaric acid. This indicate that the dissolution of tin in malic and succinic acid at anodic potential can be in general higher than that for adipic and glutaric acids.

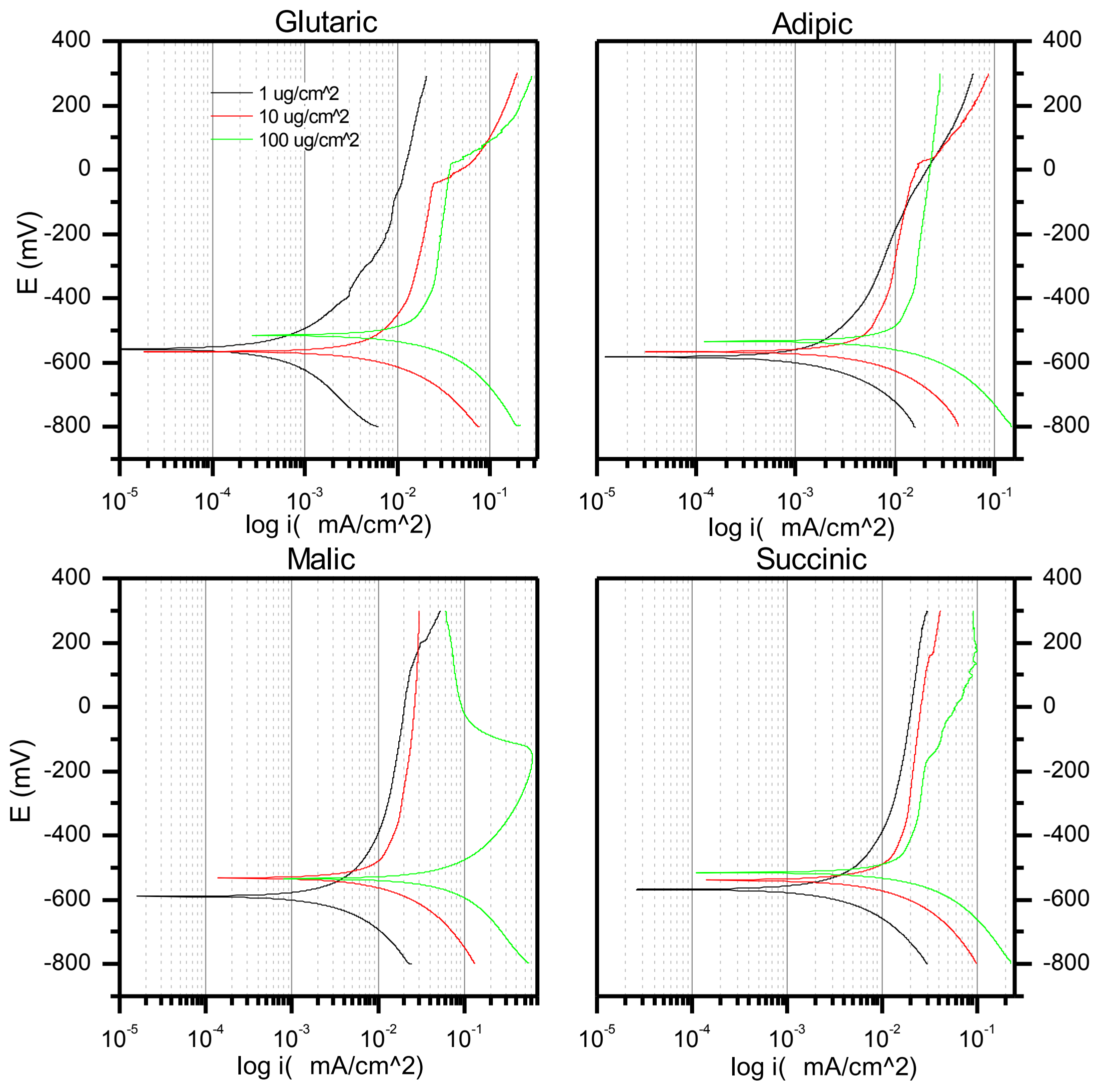

Figure 34 Polarization curves on pure tin in WOA

7.1.1.1 Discussion

From the curves it is possible to notice that the dissolution rate of the tin is seen to increase with the acid concentration for all the couples WOA-metal. The adipic-Sn system is the one which shows the lowest current increase values within the same range of 10^3 mA/cm^2. Both malic-Sn and succinic-Sn couples have a decade increase of current observed when the concentration is increased from 1 µg/cm^2 to 10 µg/cm^2, while it remains in the same order of magnitude for the highest concentration. Almost a decade increase in current was observed, instead, for the glutaric-Sn system with 10 times increase in WOA concentration.

7.1.2 Comparisons

In Table 6, the value of the i_{corr} for each system and concentration are collected. It is possible to notice how the diverse couples behave differently with respect to the concentration.

Table 6 i_{corr} values recorded for each metal-woa system

	i (mA/cm^2)		
	1 (ug/cm^2)	10 (ug/cm^2)	100 (ug/cm^2)
Adipic	2,13E-03	5,95E-03	9,66E-03
Glutaric	5,79E-04	9,56E-03	2,71E-02
Malic	3,75E-03	1,45E-02	6,95E-02
Succinic	5,18E-03	1,56E-02	2,88E-02

The succinic-Sn sytem shows the highest current density for the first two concentrations, while for the highest one the malic-Sn system has a steep increase of the i_{corr} value which represents the highest corrosion rate. The glutaric one has the lowest i_{corr} for the 1 µg/cm^{2}concentration which reaches values similar to the succinic one at the highest concentration. As it is possible to notice the succinic-Sn system has a similar behaviour to the malic one, with a close corrosion rate at the intermediate concentration, whereas at the highest concentration the behaviour becomes comparable to the glutaric-Sn system. Figure 35 shows a graphical representation of the values inserted in Table 6.

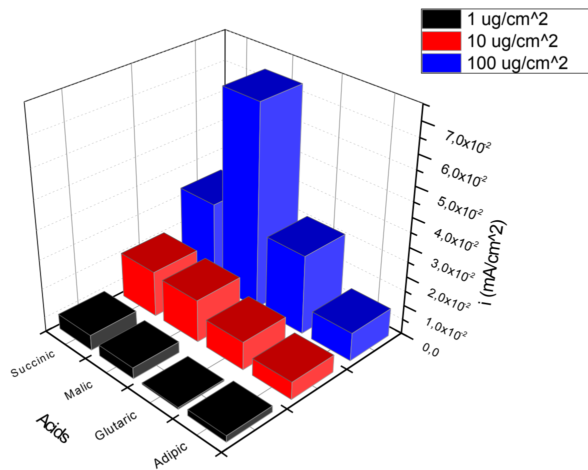

Figure 35 Graphical representation of icorr values for different acids at various concentrations

7.1.3 Comparision between acids (behaviour at 100 μg/cm²)

In order to better visualize the behavior of the different systems, explained before, Figure 36becomes helpful. It plots for a fix concentration of 100 μg/cm^2 the polarization curves for the WOA-Sn couples, and it is useful to compare the results previolsy obtained. It shows indeed the higher corrosion rate which occurs when the malic solution is employed. From the graph it is also possible to notice the similar trend of tin towards the succinic and glutaric solution, with a comparable i_{corr}, and the lower dissolution rate which takes place with the adipic one.

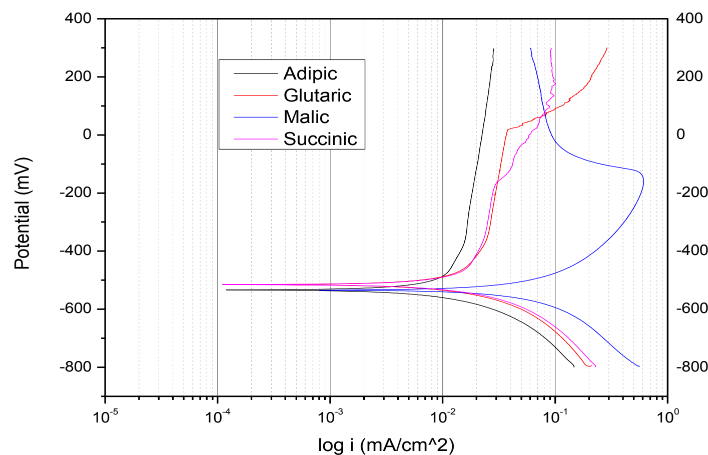

Figure 36 Polarization curves for different WOAs at 100 μg/cm^2

7.1.4 Chemical structure and physical properties

In Chapter6the chemical structure and the physical properties of the aforementioned WOAs have been introduced. The molecular structure is basically the same for all four of the WOAs, as they are all dicarboxylic acids.

The dissociation constant pK_a can be used to compare the relatiive acidity. Malic acid is the most aggressive, as it shows the lowest value for the constant (3.4), it is then followed by the succinic acid (4.2) and glutaric and adipic acid with the same value (4.4). These different acidity values help to understand the behavior of the WOAs solution. The highest i_{corr} of the malic acids finds its correspondence in its higher acidity. The close values of the corrosion rate for the glutaric and succinic solution reflects the relative comparable acidity.

Additionally, many acid molecules can form complex with metal ions and dissolve. How easy it forms depends on the molecular structure of WOA. Although all the WOAs have in general the same structure, there are differences in terms of orientation of functional groups, which makes them different. As Figure 37shows the additional hydroxyl group of the malic acid might increase the activity of the acid. In addition, the oxygen of the two carboxyl-groups lay on opposite sides of the hydrocarbons chain. This increased activity and higher availability of space, might lead to the possibility of more interactions with metal ions. The remaining three acids have lower activity and their structure is less open than the malic, which might explain the lower aggressiveness.

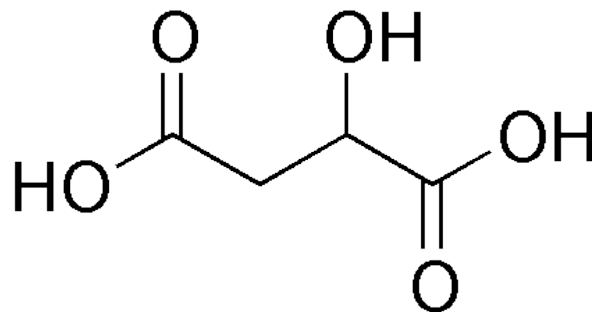

Figure 37 Malic acid

7.1.5 Conclusions

From the above results, it is possible to summarize the following:

- The corrosion potentials E_{corr} lay between -600 and – 500 mV for all the concentrations of WOAs
- The dissolution rate of tin increase with increase concentration
- The adipic-Sn system shows the lowest increase in corrosion rate
- Almost a decade increase in current was observed for the glutaric-Sn system with 10 times increase in WOA concentration
- Malic-Sn system shows the highest corrosion rate at 100 $\mu g/cm^2$
- The low pK_a value and the chemical structure of the malic acid might explain its higher aggressiveness compared to the other WOAs

7.2 Measurements for finding equivalent concentrations of WOAs to provide equivalent conducitivity to NaCl

The IPC standards set 1.56 μg/cm^2 of NaCl equivalent as the maximum level of ionic contamination left on PCB after manufacturing and post treatment process, thus the knowledge of the amount of contaminants which reach this equivalent value is of great help to the electronic industry. The purpose of this experiment is to determine the concentration of the four WOAs and $CaCl_2$ that has the same conductivity and leakage current values of 1.56 μg/cm^2 of NaCl. This was carried out with conductivity measurements and leakage current measurements using the setups described in section x of this project.

7.2.1 Conductivity measurements

Three concentrations of the four WOAs and $CaCl_2$ have been investigated, namely 1, 10 and 100 μg/cm^2. A number of three measurements for each WOAs and concentration have been done in order to obtain an average reliable value of the conductivity of the solution. The results of solution conductivity are listed in the following table.

	CaCl			Adipic			Glutaric			Malic			Succinic			NaCl
Concentration ug/cm^2	1	10	100	1	10	100	1	10	100	1	10	100	1	10	100	1.56
1	20,2	208	1930	9,05	50,6	169,5	3,73	62	222	9,99	136,1	582	25,7	146,8	256	37,6
2	21,2	207	1970	9,12	50,8	168,2	3,72	62,2	221	10,58	136,2	585	26,5	148,2	259	36,5
3	20,4	206	1999	9	50	168,7	3,72	63,4	224	10,58	136	584	26	148,2	258	37,2
Avg. κ,μS/cm	**20,6**	**207**	**1966,3**	**9,1**	**50,5**	**168,8**	**3,7**	**62,5**	**222,3**	**10,4**	**136,1**	**583,7**	**26,1**	**147,7**	**257,7**	**37,1**
St.Dev.	**0,53**	**1,00**	**34,65**	**0,06**	**0,42**	**0,66**	**0,01**	**0,76**	**1,53**	**0,34**	**0,10**	**1,53**	**0,40**	**0,81**	**1,53**	**0,56**

The value for the conductivity of NaCl at 1.56 μg/cm^2 was found to be 37.1 μS/cm which is comparable to 36.2 μS/cm found in Verdingovas's project for the same concentration.

7.2.2 Determination of the equivalent concentration

In order to find the concentration of these samples which has the same conductivity of 1.56 µg/cm^2 of NaCl, a graph showing the conductivity values vs. the concentration has been plotted (Figure 38). A straight horizontal line has been drawn on it, which starts from the point on the y axis which corresponds to the conductivity of sodium chloride equivalent, previously determined. This line crosses then the other curves. From the point of intersection with these, straight vertical lines intercept the x axis at specific concentration values. These will be the values for the WOAs and $CaCl_2$ that will have the same conductivity as 1.56 µg/cm^2 of sodium chloride. Figure 38 graphically summarizes what has been explained and the results can be read.

The equivalent concentration values, determined in this way, needed then to be approximated to the closest integer value, in order to ease the preparation of the respective solutions. Table 7 lists the determined values and the related approximation used for the purpose.

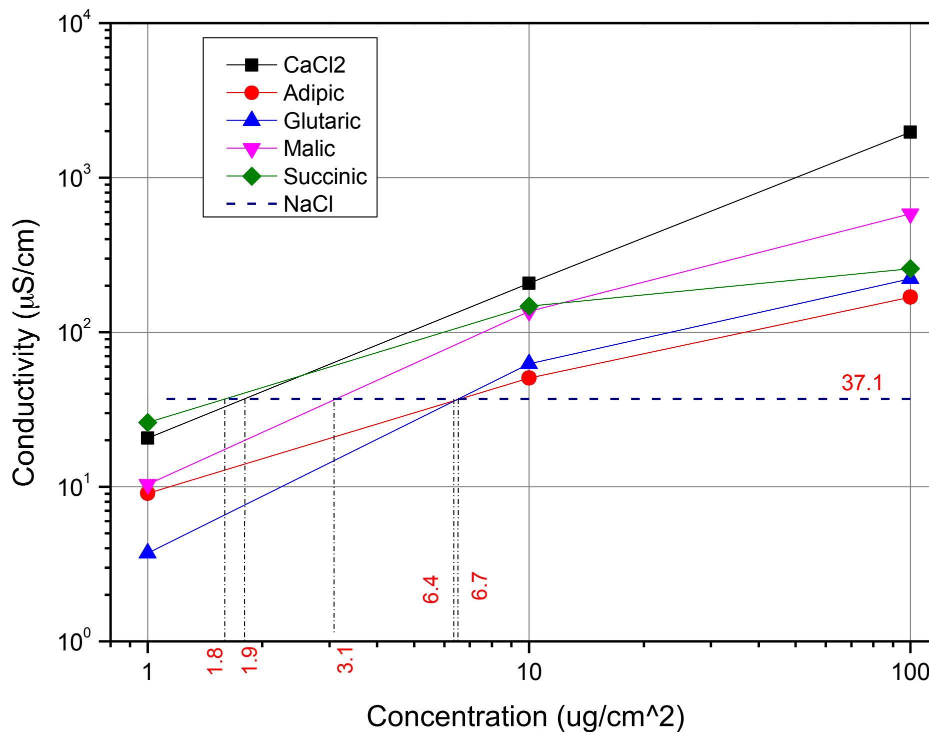

Figure 38 Equivalent concentration determination

Table 7 Determined and approximated concentration values

	$CaCl_2$	Adipic	Glutaric	Malic	Succinc
Determined	1,8	6,7	6,4	3,1	1,9
Approximated	2	7	6	3	2

7.2.3 Strong electrolytes vs. weak electrolytes

From the graph X is possible to notice the different behavior of the WOAs with $CaCl_2$ and with each other. The curve for calcium chloride solution is linear whereas the ones for the WOAs tend to flatten with the increase concentration. Calcium chloride is a strong electrolyte and completely dissociates in a solution, breaking apart into ions completely. The dissolution reaction occurs entirely in only one direction, as it is shown by the single reaction arrow in the following reaction path:

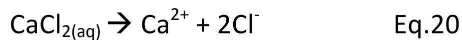

$CaCl_{2(aq)} \rightarrow Ca^{2+} + 2Cl^{-}$ Eq.20

Thereby the conductivity of $CaCl_2$ solution can be described by equation X which shows a simple linear relationship between conductivity κ and concentration *c* for strong electrolytes.

$$\kappa = v_{\pm} z_{\pm} c N_A e_0 (u^{+} + u^{-}) \qquad \text{Eq.21}$$

Where

- $v_{\pm}$ is the number of moles of cations and anions created from the dissociation of 1 mole of the dissolved electrolyte
- $z_{\pm}$is the valence number of the ions
- c is the concentration of the electrolyte in mol/m^3
- $N_a$is the Avogadro's number equal to 6.022 mol^{-1}
- e_0= 1,6 $\cdot 10^{-19}$ C is the electron charge
- $u^{\pm}$ is the ions mobility [$m^2V^{-1}s^{-1}$]

Equation X is valid only for concentrations below 3 $mol \cdot dm^{-3}$ since at higher concentrations, the inter-ionic interactions increase as the mean distance between ions decreases. The concentrations used for this experiment are, however, far below the limit for ionic interactions to be taken into account.

The WOAs are, instead, weak electrolytes and thus only partially disassociate in a solution. The relationship between the conductivity and the concentration will thus not be linear as the concentration of ions in the solution is less than the concentration of the electrolyte itself. The increment of the conductivity with respect to concentration decreases with the increased concentration.

7.2.4 Discussion

As previously seen in the polarization curves, the behavior of the four WOAs varies with the concentration. At the lowest concentration, the succinic acid shows the highest conductivity, followed by the malic acid, the adipic acid and the glutaric. By increasing the concentration of one order the conductivity of the glutaric solution becomes higher than the adipic one and the values for the remaining solution get closer, with the succinic solution having still a higher value than the malic one. At the highest concentration of 100 µg/cm^2 the malic solution shows a steep increase of the conductivity, which doubles the values or the other ones. The increment of the conductivity of the succinic solution decreases but the value is still higher than the glutaric one, although the respective values become much closer. The adipc solution keeps showing the lowest conductivity.

7.2.5 Aggressiveness of the WOA solutions: the pK_a value

Going back to the results obtained with the polarization curves leads to notice a trend in the behavior of the different solutions of WOAs. If the obtained values of the corrosion rate and the conductivity can be taken as indicators of the aggressiveness of the solutions, the exact same behavior is recorded for increased concentration (Table 8). The succinic solution shows the highest aggressiveness at the concentrations of 1 µg/cm^2 and 10 µg/cm^2 and it is overtaken by the malic solution at 100 µg/cm^2.

Table 8 Aggressiveness of the investigated WOAs

Concentration ug/cm^2	1		10		100	
Aggressiveness	icorr	κ	icorr	κ	icorr	κ
	Succinic	Succinic	Succinic	Succinic	Malic	Malic
	Malic	Malic	Malic	Malic	Succinic	Succinic
	Adipic	Adipic	Glutaric	Glutaric	Glutaric	Glutaric
	Glutaric	Glutaric	Adipic	Adipic	Adipic	Adipic

In the same way behaves the glutaric solution which shows the lowest aggressiveness for the least concentrated solution, which, then, surpass the adipc solution at 10 µg/cm^2 and further. Table 8 lists the translation.

The order of aggressiveness obtained with these experiments, finds its reason in the physical properties of the four WOAs explained in Chapter6. The malic acid shows the lowest value of the logarithmic of the acid dissociation constant, pK_a, followed by the succinic acid. The lower the value is, the stronger the acid is, meaning that the acid dissociates to a greater extent, leading to a higher conductivity and aggressiveness. The other two acids have the same value, which is comparable to the one of the succinic. This reflects the obtained results as the values of the conductivity of these three acids are close to each other at the concentration of 100 µg/cm^2.

7.2.6 Leakage current measurements

The leakage currents of the four WOAs solutions previously employed have been recorded using the LRTD setup described in Section 5.8. The test records the changes in the leakage current of the solution, biased with a potential of 5V, over a period of 130 seconds. The value of the current recorded after 120 seconds has been chosen as the LC value of the solution. This has been chosen due to the fact that, after an initial increase of the current measured by the system, its trend tends to develop asymptotically to a constant value. Thus the data recorded at 120 second is a good approximation of the leakage current value of the solution. Figure 39 shows the LC measurements of the adipic acid solution at three different concentrations. A green vertical line has been drawn at 120 seconds in order to intersect the corresponding value of the leakage current. The same modality has been employed for all the other solutions.

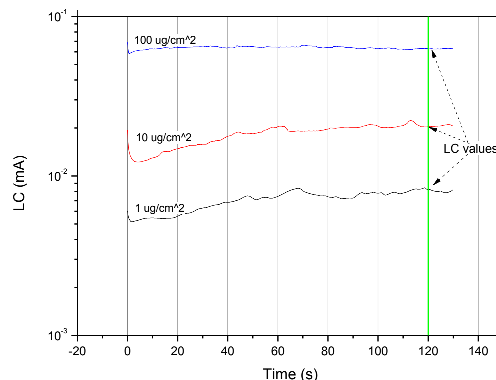

Figure 39 Leakage current measurements

7.2.7 Determination of the LC

The results obtained for all the solutions are listed in Table 9.

Table 9 Leakage current values for different acids and concentrations

Concentration ug/cm^2	1	10	100
Adipic	8,25E-03	2,04E-02	6,33E-02
Glutaric	8,05E-03	2,22E-02	5,67E-02
Malic	2,44E-03	3,01E-02	1,36E-01
Succinic	5,87E-03	2,31E-02	6,72E-02

These values were then plotted on a log (LC) vs. concentration graph (Figure 40) and the same modality, previously followed,has been employed in order to find the concentrations of the WOAs which give the same value of LC as 1.56 ug/cm^2 NaCl equivalent. As it is possible to notice the trend of the different solutions is not linear at all and the lines tend to flatten with the increased concentration.

The values of the LC and conductivity are physically different, and different is the applied current: DC for the former test, AC for the latter. The equivalent value of NaCl will thus be different as well. From Verdingovas' project, this value has been measured to be $8 \cdot 10^{-2}$ mA. This same value has been used throughout this experiment.

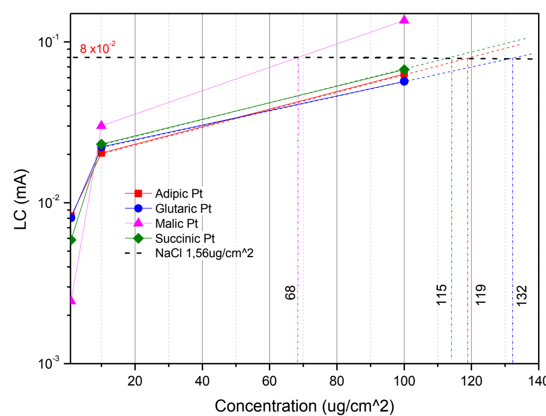

Figure 40Determination on equivalent concentrations through leakage current

The values obtained are listed in the Table 10 below. These values were not used for further investigation on PCB, as this experiment was carried out after the equivalent concentrations of WOAs,

found with the conductivity measurements, had been tested on the PCBs. These will be explained in chapter X but it has been recorded that the effect of the equivalent solutions was quiet comparable to the effect of 1,56 ug/cm^2 NaCl.

Table 10 Equivalent concentrations determined through LC

	Adipic	**Glutaric**	**Malic**	**Succinc**
Concentration ug/cm^2	119	132	68	115

7.2.8 Discussion

As it is possible to notice inFigure 41, the equivalent concentrations found with the LCs measurement are much higher than the tested ones: empirical tests of these solutions would have led to misleading results. It was, thus, not considered convenient to prepare and investigated the equivalent solutions found with these method.

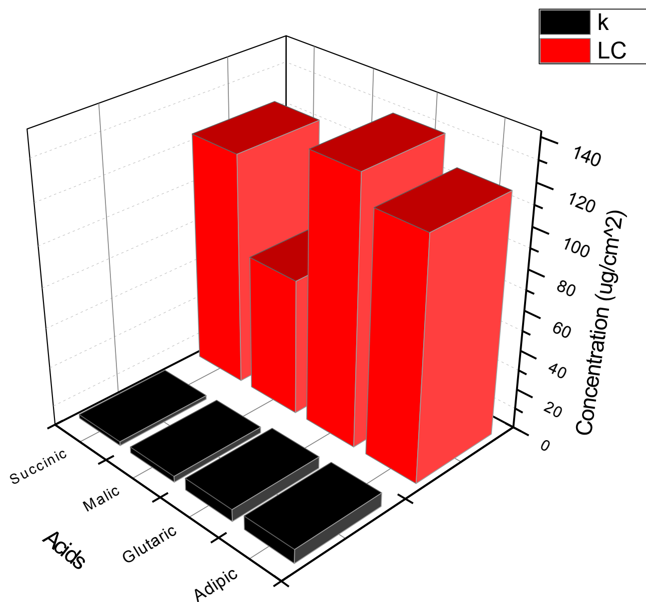

Figure 41 Comparison between equivalent concentrations found thorugh conductivity and leakage current measurements

However, they were compared to the one found with the conductivity measurements to better understand how the different WOAs behave with respect to the type of potential applied. This will be better explained in the next chapter.

7.2.9 Different behavior in AC and DC voltage

It is worth to mention how the solutions of the WOAs behave differently when biased with direct and alternate voltage. In Figure 42 values of the leakage current, measured in DC, and the valuse of the conductivity, measured in AC are plotted for the different acids and concentrations. If a straight line is drawn at an angle of 45°, two domains are identified: the AC domain, in light grey, and the DC domain, in white. For both the domains there is an increase trend with increase electrolyte concentration, as expected, but, almost all the curves lay in the DC domain, as the rate of growth is higher. From this graph it is possible to notice that the WOAs solutions are more sensitive to a DC bias than to an AC one, displaying a faster increase in this domain.

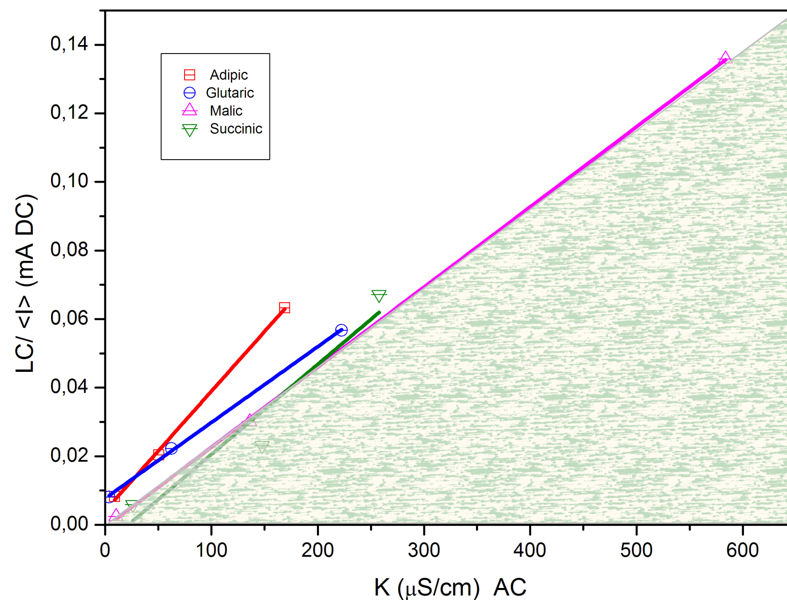

Figure 42 Behavior of the different WOAs under DC and AC current

7.2.10 Conclusions

From the previous results is possible to summarize the following conclusion

- Both the graphs show an increase trend with increase electrolyte concentration
- For $CaCl_2$ the conductivity dependence of concentration is linear as it is a strong electrolyte and completely dissociates in water. WOAs electrolytes only partially dissolve in water and the dependence of concentration is not linear. As a result, the WOAs electrolytes show lower conductivity values at the same concentrations compared with $CaCl_2$
- From the conductivity measurements is possible to define a degree of aggressiveness for the different WOAs at different concentrations. This degree reflects the results previously obtained with the polarization curves.
- This degree of aggressiveness finds an additional confirmation in the value of the pK_a recorded by Sohn et al. The malic acid is the more acidic since its pK_a is the lowest; the other three have comparable values of $pK_{a.}$
- From these graphs the values of the WOAs concentrations which give the same conductivity and leakage current as 1.56 ug/cm^2 of sodium chloride equivalent have been determined
- The values of the equivalent concentrations obtained with the LC measurements are much higher than the one obtained with the other method. The concentrations obtained with the conductivity measurements were employed for further investigations on PCBs
- The equivalent concentrations obtained with both the methods are higher than the concentration of NaCl specified by IPC standard. The WOAs are thus less dangerous to be present on the PCB compared to NaCl. This reflects even more in the much higher equivalent concentrations obtained with the LC measurements
- The WOAs solutions show a greater sensitiveness to an alternate voltage compared to a direct one, displaying a higher rate of growth

7.3 Effect of WOAs and flux types on Electrolytic migration

This chapter describes results of the investigation on the effect of various WOAs and wave solder flux types on the electrochemical migration using drop-let experiments on a chip capacitor under potential bias. The component used for the testing was 0805 10 nF capacitors. The SCEM setup has been employed for these investigations and each WOA (glutaric, malic, adipic, and succinic) and is tested for at 10 μg/cm^2. In addition to this the seven flux systems previously introduced (see 5.13.2) have been tested at 100 μg/cm^2. Table 11 lists the solder fluxes employed; their specifications are collected in **Appendix III**. The area of one capacitor was measured to be 2.5 mm^2, thus a 2.5 μl droplet would ensure the requested concentration on the components according to the relation explained in Chapter5.13.1. In this way, full condensation condition was established on the component surface with needed contamination. The capacitors were biased under a 5 V potential and data were recorded for 15 minutes. SCEM set up allow testing of 3 components at a time, and a total of 18 capacitors were tested in each case for providing better statistics with 98% confidence level on the probability for migration.

Table 11 WOAs and Flux Systems investigated in this project

WOAs	Flux Systems
Glutaric acid	327
Adipic acid	380_R
Malic Acid	390_RXT
Succinic acid	396_DRM
	327_Sel
	94_Sel
	385_Sel

The variation of leakage current through the drop-let was measured as a function of time, and various parts of the curves were then analyzed for leakage current levels and migration probability. In the following sections the effect of the WOAs and flux residues solutions on ECM probability will be introduced and compared. Pictures of the capacitors were taken using optical and SEM microscopes.

7.3.1 Results and discussion

After a general description of the ECM phenomenon the effect of the WOAs and flux systems residues will be introduced. The behavior of the flux systems will be related to the type of WOA which is the activator of the flux. The results are then compared with optical pictures and SEM and EDX analysis

7.3.1.1 *Leakage current vs. time*

ECM involves metal dissolution from the anode (positively charged electrode) and ions migration through the electrolyte toward the cathode (negatively charged) where they deposit. This deposition implies the growth of dendrites which leads to component failure or malfunctioning when they bridge the two oppositely biased terminals. The effect of dendrite growth and bridging is recorded with LC vs. time curves: spikes on the behavior of the current mean that the dendrites have bridged the two terminals. This short can be permanent or temporary. For the latter case, the sudden increase in LC is followed by an equivalent drop of the LC down to initial values: the dendrites burned off.

7.3.1.2 *Migration as a function of time*

A typical leakage current vs time curve resulting from the SCECM experiment is shown in Figure 43. The graphs shows the base leakage current level followed by intermittent peaks at various times corresponding to the dendrite formation and breakdown. Vertical dotted lines shown in the graphs correspond to the migration events shown below in the optical pictures.

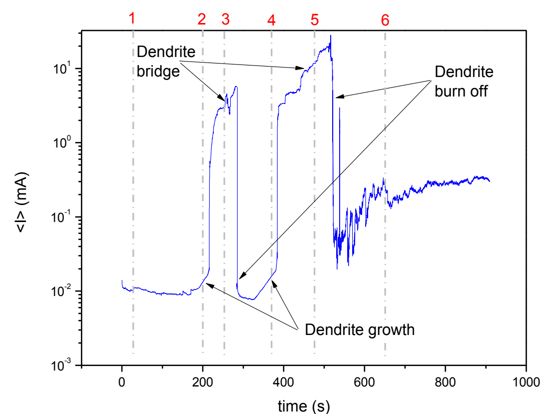

Figure 43 Typical LC vs. t curve for a 0805 capacitor during SCEM experiment

Point number 1 inFigure 44 corresponds at the initial condition when the potential has been applied. During the first three minutes no visible dendrite nucleation was recorded and little corrosion is

observed at the anode and some corrosion products are seen in the solution, most likely tin hydroxides. Afterwards the dendrite starts to nucleate and grows for approximately 40 seconds (2) until it reaches the anode, short circuiting the system (3). Due to the bridging the current increases almost three orders, until the dendrite bridge degrades (burns off) at approx. 285 seconds when the current drops back to base level. After two minutes a new dendrite bridge is formed, giving a even higher LC peak, which is again degraded (4, 5). The higher current recorded after the second burn off is both due to dendrite branches which keep growing from the backbone and touching each other increasing the current passing through, and drying of the dendrite due to evaporation of water (6).

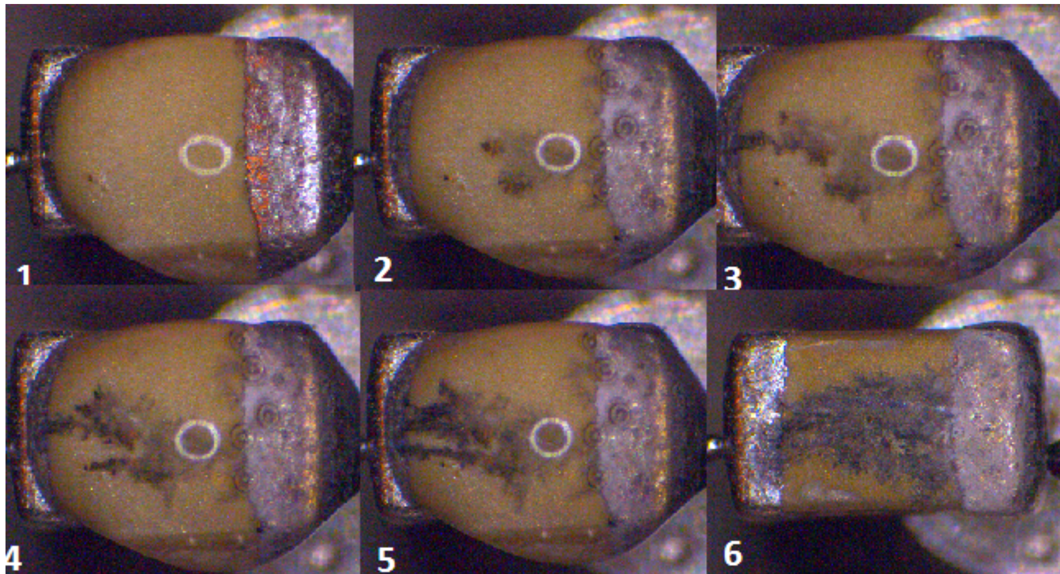

Figure 44Dendtric growth on 0805 capacitor

7.3.1.3 *Analysis of leakage current vs time curves for WOA residues*

The effect of the four WOAs on the ECM probability can be seen in the graphs in Figure 45. Percentage of failed capacitors vs. the time to first dendrite bridge was plotted for each WOA (Figure 45a)) . Figure 45(b) shows instead the percentage of survived capacitors and its dependence on time.

It is possible to notice how the cumulative percent failure increases with time for all the WOAs, with succinic acid showing the fastest increase in cumulative percent followed by the malic and the glutaric. Adipic acid did not induce any migration on all the specimens at concentrations investigated in this

study. The first migration is recorded after 126 seconds for succinic acid, 190 s and 400 s for malic and glutaric acid respectively.

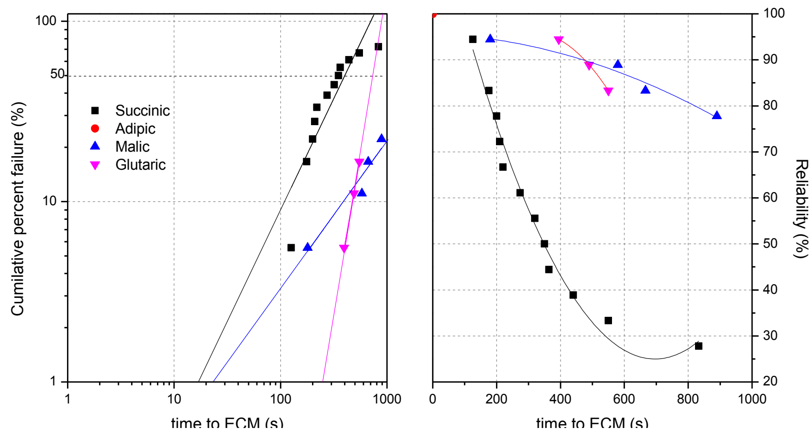

Figure 45 WOAs contamination: a) Percentage of failed capacitors vs. the time to first dendrite bridge; (b) percentage of survived capacitors vs. time

7.3.1.4 *ECM probability vs. WOA type*

The percentage probability for ECM corresponding to the various WOAs is shown in Figure 46. The data represents the percentage of capacitors which shown ECM during testing out of 18 components in each case.

Nearly 72 % of the capacitors showed migration when contaminated with succinic acid, which has the highest failure rate within the WOAs system, followed by the malic acid with ~22% and glutaric acid with ~16%. As said, the adipic solution did not give any migration. This is in accord with the obtained results regarding the aggressiveness of the WOA solution at 10 μg/cm^2 (Chapter7.2.5) and the data listed in Sohn et al. concerning the pK_a values. The aggressiveness of various acids is different, therefore it can dissolve different amount of metal ions. At this concentration the succinic acid is the most aggressive, showing both the highest i_{corr} and conductivity, followed by the malic acid and the glutaric acid. Succinic acid seems, therefore, to assist deposition and dendrite formation by adsorbing on to the cathode.

The low pK_a value for the malic might suggest that the solution is so aggressive that it inhibits the dissolution of metal ions from the anode, reducing the probability of ECM. The behavior of the glutaric acids is in accord with its mild aggressiveness and its intermediate value of pK_a (4.4). Due to the low aggressiveness of the adipic acid (low i_{corr} and conductivity combined with the same pK_a value of the glutaric acid), the dissolution of metal might be too low to induce ECM

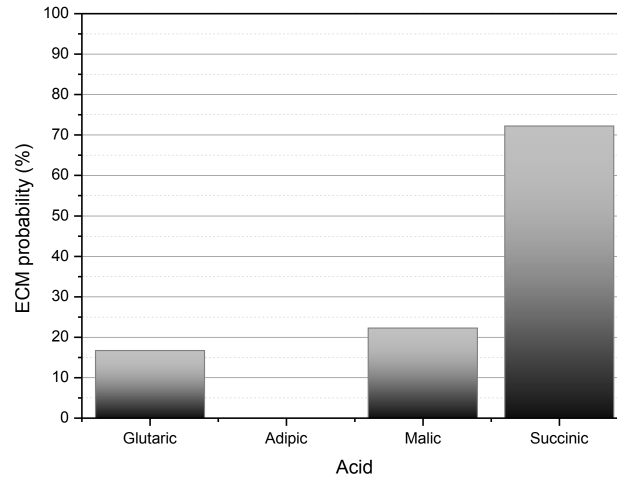

Figure 46ECM probability (%) plotted for each WOA

7.3.1.5 *Surface morphology vs. WOA type*

Before describing in details the surface morphology after ECM, it is necessary to explain the electrochemical behavior of tin, which leads to the formation of different compounds. These compounds due to pH changes along the capacitor will deposit differently, originating different morphologies.

7.3.1.5.1 Electrochemical behavior of tin

Tin has two valence states: Sn^{2+} (stannous) and Sn^{4+} (stannic), equally stable and readily convertible. Figure 47 shows the Pourbaix diagram for Tin. From this diagram it is possible to underline the amphoteric behavior of Tin which is soluble both in acid and alkali[40].

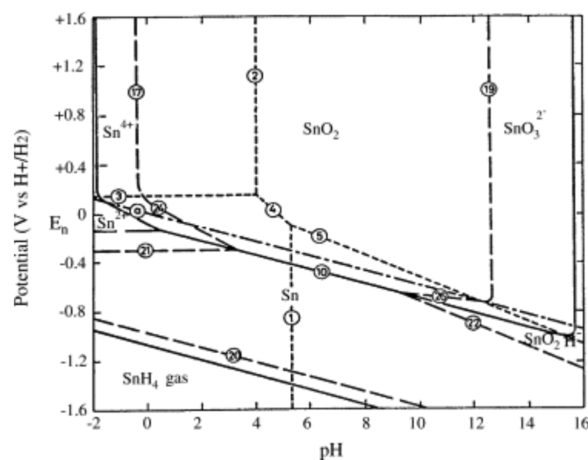

Figure 47 Purbaix diagram for tin[55]

Important electrode reactions of tin in the presence of water are:

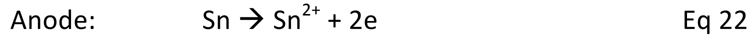
Anode: $Sn \rightarrow Sn^{2+} + 2e$ Eq 22

$Sn^{2+} \rightarrow Sn^{4+} + 2e^{-}$ Eq 43

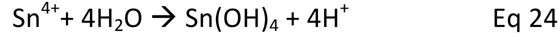
$Sn^{4+} + 4H_2O \rightarrow Sn(OH)_4 + 4H^{+}$ Eq 24

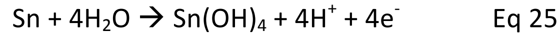
$Sn + 4H_2O \rightarrow Sn(OH)_4 + 4H^{+} + 4e^{-}$ Eq 25

$2H_2O \rightarrow 0_2 + 4H^{+} + 4e^{-}$ Eq 26

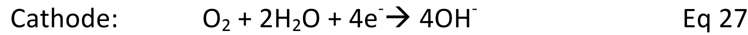
Cathode: $O_2 + 2H_2O + 4e^{-} \rightarrow 4OH^{-}$ Eq 27

$H_2O + 2e^{-} \rightarrow H_2 \uparrow + 2OH^{-}$ Eq 28

7.3.1.5.2 Stability of tin species in solution and connection to ECM

Due to reaction explained in Equations 24, 25 and 26, the generation of H^{+} ions will make the environment more acidic, while at the cathode and increase in pH will be experienced due to oxygen reduction (Equation 27) and hydrogen evolution from water dissociation (Equation 28). This pH changes along the surface will lead to different tin-compounds precipitation. The stannous and stannic ions from the anode (low pH) dissolve and migrate towards the cathode (high pH); during their path due to the increasing pH they will first hydrolyze into many intermediate species, mainly stannic hydroxide $Sn(OH)_4$. This will then convert into stannate $Sn(OH)_6^{2-}$ under an alkaline pH at the cathode. Figure 48 shows a schematic representation of the pH gradient formation inside the droplet on the capacitor; it illustrates, additionally, the areas of stability for various species with local chemistry changes.

This phenomenon will result in a different surface morphology as the tin hydroxides will produce whiter deposits whereas the tin darker ones. This will be shown in the following chapter.

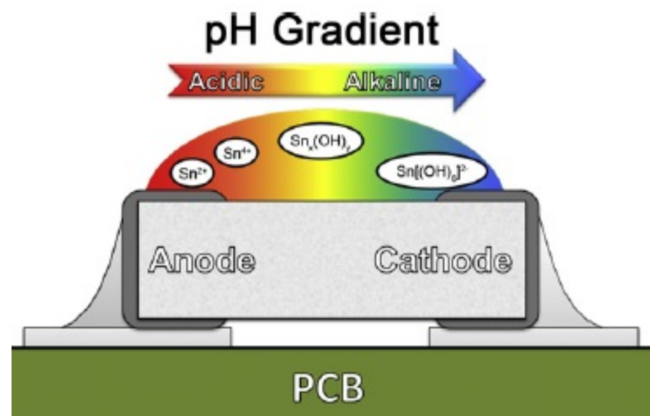

Figure 48 pH gradient formation in the droplet on a capacitor

7.3.1.5.3 Visual appearance of the dendrites after WOA contamination

Figure 49 shows optical pictures of the capacitors, taken at the end of the test. The adipic acid (picture 1) did not create sufficient condition to induce ECM: degradation of the anode can be noticed but the pH and the reaction rate were not maintained to the levels required to ensure Sn deposition at the cathode. On the other capacitors it is possible to notice the dendrite formation which led to leakage current spikes. The malic solution (picture 2) created a more acidic environment as can be noticed by the presence of a dark dendrite due to mainly deposition of tin. The less acidic environment generated by the remaining glutaric and succinic solutions (picture 3 and 4 respectively) is seen on the wither dendrites due to deposition of tin hydroxides. The dendrites formed by the succinic solution are also wider and more branched as it facilitates deposition at different places.

From Figure 49 is possible to notice that the black dendrite grows under the tin hydroxides until the pH for their deposition is favorable. When it gets closer to the anode to lower pH, the black dendrite becomes more visible as hydroxides deposition does not take place.

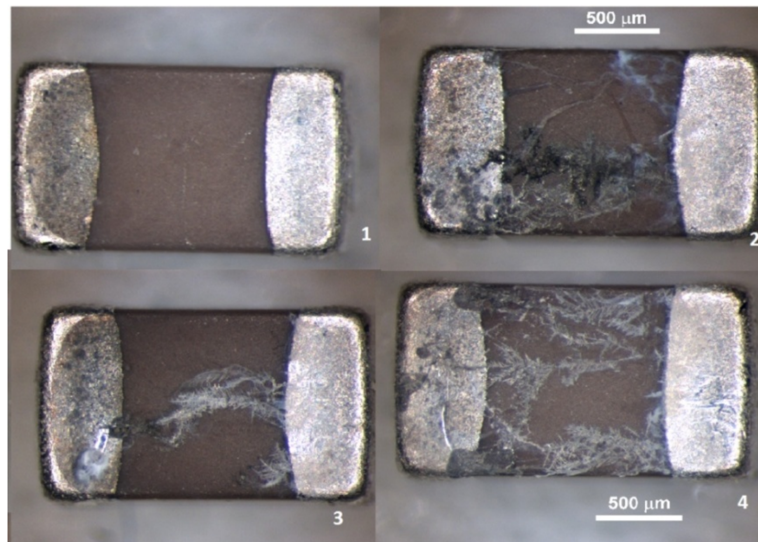

Figure 49 Visual appearance of the surface of the capacitors after SCEM experiments at 10 µg/cm^2: 1) adipic; 2)malic; 3)glutaric; 4) succinic

7.3.1.6 *Analysis of leakage current vs time curves for Solder Flux Residues type*

Figure 50 shows the cumulative percent failure (picture a)) and reliability (picture b)) plots for various wave solder flux systems residues at 100 µg/cm^2. All the flux systems showed migration after 100 seconds and the reliability decreases with time as more capacitors failed with increasing time.

As for the WOA case, the cumulative percent failure increase with time for all solder flux residues, with the 327 solder flux showing the fastest increase in cumulative percent, followed by the 380_R and 390_RXHT. 385_Sel did not induce any migration on all the specimens at concentrations investigated in this study.

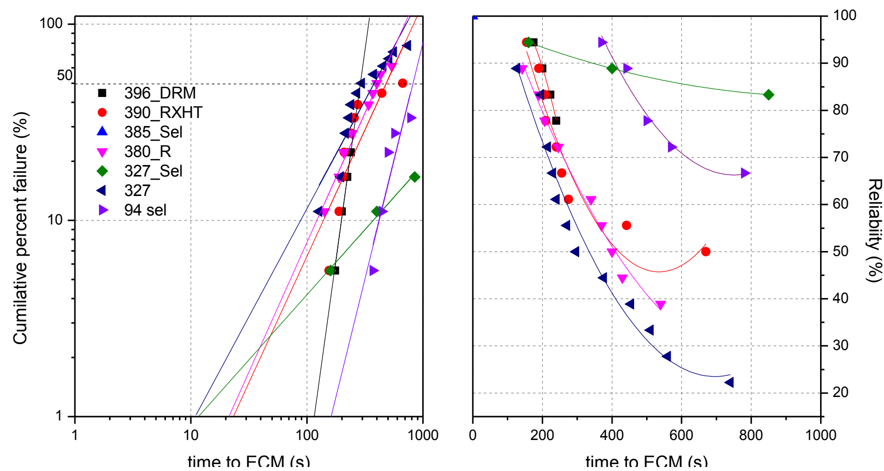

Figure 50 Solder Flux Sysems contamination: a) Percentage of failed capacitors vs. the time to first dendrite bridge; (b) percentage of survived capacitors vs. time

7.3.1.6.1 ECM probability vs. Solder Flux Residues type

The percentage probability for ECM corresponding to the various solder flux residues is shown in Figure 51 The data represents the percentage of capacitors which shown ECM during testing out of 18 components in each case.

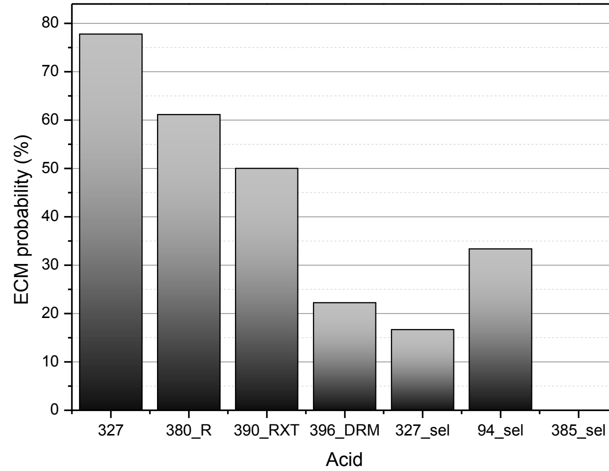

Figure 51 ECM probability (%) plotted for each Solder Flux System

Solder flux residues from 327 show the higher percentage of failures, ~77 %, followed by the 380_R flux residues with ~61%. 385_sel flux residues did not produce any migration. In order to understand and compare the behavior of the flux systems it is necessary to explain some properties of these fluxes like the acid number and the type of WOA which constitutes the activator for each flux. This will be explained in the following paragraph.

7.3.1.6.2 Solder flux analysis

Table 11 shows the solid content and acid number for various flux systems for comparison. The acid number of the flux can be directly compared with the level of leakage current and ECM susceptibility, although the effect is also a function of the type of acid in each flux systems.

Table 12 Solid content and acid number

Product (Flux Type)	Solid content	Acid no
380R	4.15	30.69
390 RX HT	2.2	15.8
396 DRM	4	36.85
94 SEL	2.57	13.85
327	4.94	29.00
327 SEL	4.94	19.7
385 SEL	1.91	18.75

Comparing Figure 51 with Table 12, although in general migration probability increases with acid number (eg. higher ECM probability for 327 and 380 R), some higher acid number fluxes shows lower probability while low acid number fluxes shows higher probability. Overall the results indicates that the effect is a mixture of higher acid content and acid type similar to that observed for the four acid types tested. Among the four acid types, succinic acid shows higher probability for ECM, while glutatric and malic acids shows much lower probabilities. Adipic acid on the other hand did not show any migration within the concentration level tested. This shows that a flux system with succinic acid in general has the capability to show higher ECM levels, while adipic show least. This provides an indication to the possible reasons why various flux systems showed contrasting effects on ECM when comparing with acid content. Table 13 shows the Ion chromatographic analysis of the flux types indicating the acid types and other ions present in the flux systems. It is difficult to separately identify the peaks for adipic/glutaric and malic/succinic, therefore comparison of the results with ECM probability needs some generalizations. Higher ECM capability for flux type 327 is understandable as it consists of aggressive acids and some level chloride. Similarly 380 R consists of higher levels of acids (expected to be glutaric as the ECM susceptibility was higher unlike observed for adipic acid) and some chlorides. Similarly 390-RXHT shows comparatively higher ECM levels, although less than 327 and 380 R. Therefore the acid type in this case might be glutaric, otherwise the expected effect should be less comparing the behaviour for adipic acid. On the other hand, 396-DRM showed only lower ECM probability although it consists of significantly higher levels acid, therefore expected to be made of adipic acid.

Table 13 IC analysis of the different Solder Flux Systems

Flux type	Adipic/glutaric Ret. 7,35 [ppm]	Malic/succinic Ret. 7,85 [ppm]	Chloride [ppm]
94-SEL	-	-	-
327	-	14,7	0,5
327-SEL	-	9,7	-
390-RXHT	15,9	-	-
380-R	32,3	-	0,4
385-SEL	-	19,2 (difficult to determine)	-
396-DRM	50,3	-	-

Further investigation on the morphology of the tested capacitors under the effect of solder systems can be utterly helpful to understand the different behaviors. These results are explained in the following paragraph.

7.3.1.7 Visual appearance of the dendrites after Solder flux residues contamination

Figure 52 below displays the surface of the capacitors pre contaminated with 100 µg/cm^2 of solder flux residues. Picture 1,3,5 and 7 show the effect of 94_Sel, 327_Sel, 385_Sel and 396 DRM solder flux residues respectively. For all these cases the anode, on the left, changed color displaying a combination of grey, green and yellow: the electroplated layer of tin has been severely corroded exposing the underlying layer of copper to the solder flux solution which corroded it. High level of corrosion inhibits the ECM migration, which is the reason why lower ECM probability has been shown from this sample, regardless the relatively high acid number and acid concentration discussed before.

385_Sel and 396_DRM showed migration but the reaction rate and the condition were not sufficient to induce short circuits. It is indeed possible to notice from the related picture that the dendrite stopped at the very beginning for the former one, and closer to the anode for the latter one. Their dendrites appear to be thicker than the other and much less hydroxides deposition can be seen compared to the other cases. The pH of the solution remains probably too low along the whole distance between the two terminals, inhibiting the deposition of the hydroxides.

For the other solutions the morphology does not change so much from the ones previously described with the glutaric, malic and succinic acid.

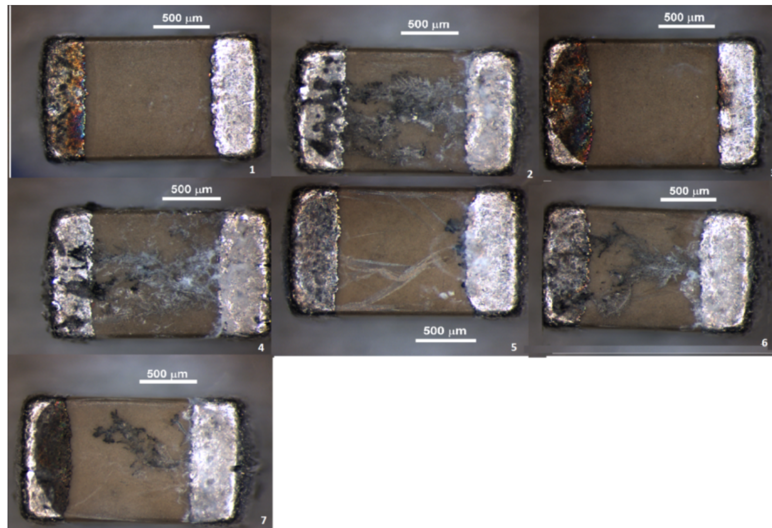

Figure 52Visual appearance of the surface of the capacitors pre-contaminated with Solder Flux: 1) 94_sel; 2) 327; 3) 327_Sel; 4) 380_R; 5) 385_Sel; 6) 390_RXHT; 7) 396_DRM

7.3.1.8 *SEM analysis*

Figure 53 shows a SEM analysis of the capacitor contaminated with 10 µg/cm^2 of glutaric acid. Two magnifications have been done: one of the wither dendrite the other of the darker one. As it is possible to notice the white one has more branches of thinner dendrites while the black one is less branched but the dendrites are thicker.

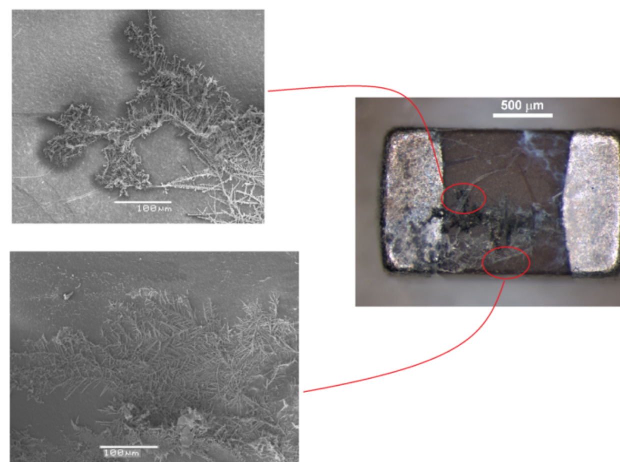

Figure 53 SEM analysis of a 0805 capacitor pre contaminated with 10 µg/cm^2 of glutaric acid

An EDX analysis of these spots (Figure 54 and Table 14) reveals that the dendrites are mainly formed on tin. Additional element like Ti, Ag, O, Nd and Bi (Spectrum 1) were identified in the body of multilayer chip capacitor as they are commonly employed for the production. A part from this it is not possible to draw significant conclusion on the composition of the backbones of the darker and wither dendrite. The formation of hydroxides is, however, very likely.

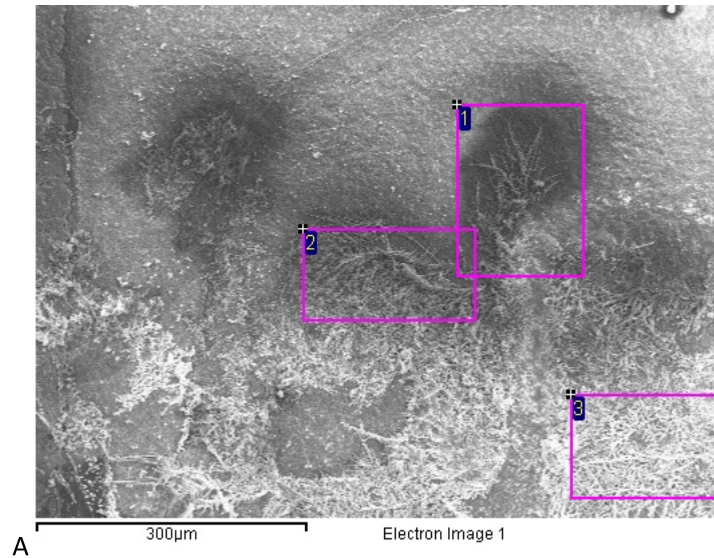

Figure 54 EDX analysis of dendrites on capacitor pre contaminated with glutaric acid

Table 14 EDX spectrum of capacitor pre contaminated with glutaric acid

Spectrum	In stats.	O	Ti	Ag	Sn	Nd	Bi	Total
1	Yes	14.0	22.4	3.0	31.6	23.4	5.6	100.0
2	Yes	9.7	12.4		65.4	12.4		100.0
3	Yes	10.2	5.5		78.9	5.4		100.0
Max.		14.0	22.4	3.0	78.9	23.4	5.6	
Min.		9.7	5.5	3.0	31.6	5.4	5.6	

Another EDX analysis has been carried out on the anode of the chip capacitor pre contaminated with 327_Sel Solder Flux. As previously observed the anode was degraded and the surface was not more metallic grey but colored. The results are presented in Table 15and Figure 55. The presence of oxygen and tin (spectrum 1) on the anode is an indicator that the terminal underwent severe corrosion which inhibit the ECM process, as no migration occurred. It is, indeed, known that tin can precipitate as an

oxide (casserite SnO_2), preventing the electrochemical migration to happen. The EDX analysis of this component was expected to show traces of Cu as it is the metal layer under Sn,instead no traces of this element were found.

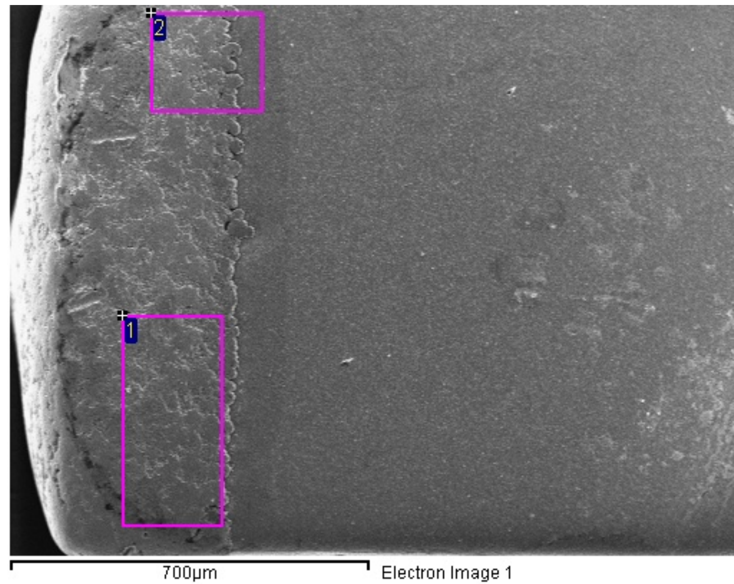

Figure 55 EDX analysis of the tin terminal of the capacitor pre contaminated with 327_Sel

Table 15 EDX spectrum of the tin terminal of the capacitor pre contaminated with 327_Sel

Spectrum	In stats.	O	Ti	Sn	Total
1	Yes	12.4		87.6	100.0
2	Yes	13.4	9.9	76.7	100.0
Max.		13.4	9.9	87.6	
Min.		12.4	9.9	76.7	

7.3.2 Possible implications on PCBA manufacturing

The type of acid which plays the activator in a solder flux system has a great impact on the climatic reliability of a PCBA. As seen, the succinic acid itself, under humid condition eases the deposition and thus the electrochemical migration, compromising the functioning of electronic devices. Therefore solder flux systems containing succinic acid as activator might be more hazardous to the climatic reliability, especially under full-condensing conditions. As seen the ECM under the effect of this acid

could happen within 100s and, although full condensation condition in a real life situation may not be the most frequent, can lead to malfunctioning in a short period of time.

7.3.3 Conclusion

From the previous results the following conclusion can be drawn:

- The succinic acid is the one which showed the highest percentage (72.2 %) of ECM probability between the WOAs. 327 solder flux system induced more component failures (77.8 %) compared to all the tested solutions.
- No migration was recorded for adipic acid and 385_sel flux residues.
- The presence of chloride in 327 and 380-R greatly enhances ECM. Its presence is much more relevant than the kind of acid contained in the solder flux. The reasons for ECM promotion have been previously explained.
- An acid number around 29 together with an acid content around 15 ppm seem to enhance ECM. Lower values have less influence on the process, whereas higher values lead to a high rate of corrosion of the anode which prevails against electrochemical migration
- Solder fluxes 94_sel and 327_sel enhance anode corrosion but not ECM
- SEM analysis revealed a higher thickness of the black dendrites close to the anode compared to the whiter one along the body. Through EDX analysis was, however, not possible to have a clear comprehension of the possible different composition of the dendrites.
- Traces of oxygen have been recorded on the anode of the component pre contaminated with 327_sel solder flux. The anode has been severely corroded and no migration was noticed.

7.4 Effect of WOAs residues on SIR pattern under non-condensing conditions

In this section the results of the investigation on the effect of WOA residues on the leakage current using an SIR pattern is presented. Leakage current measurements have been carried out on reflow soldered SIR pattern on the CELCORR test PCB setup biased at 5 V potential and pre contaminated with four different concentrations of the previously introduced (Chapter 5.1) weak organic acids. The whole setup was placed inside the climatic chamber described in Chapter 5.7.1 and the leakage current flowing through the SIR pattern pre contaminated with different concentrations of WOAs has been recorded with "BioLogic VSP" potentiostat.

The temperature inside the chamber was kept constant at T=25 °C and the RH humidity were increased from 40 % to 98 % with step increase of 5 % every two hours. The experiment was left running for 26 hours.

7.4.1 Results and discussion

7.4.1.1 *Leakage current from SIR pattern: effect of RH and contamination*

It was discussed in Chapter 4 how the synergistic influence of ionic contamination together with the effect of RH exerts a significant impact on the reliability of PCBA. Different concentrations, starting from the ones which give the same conductivity as 1.56 $\mu g/cm^2$ of sodium chloride (Chapter7.2.2), were tested at increasing humidity level. These were then doubled and tripled in order to achieve electrochemical migration; an additional concentration of 100 $\mu g/cm^2$ was investigated as the high level concentration. The results of these experiments are presented in Figure 56.

Glutaric acid and malic acid showed no significant increase in LC current for relative humidity below 65 %, above which the leakage current start to rise for all concentrations. Similar behavior is recorded for the succinic acid below 80 % RH and adipic acid below 90 % RH. Glutaric and malic acid show a more consistent increase above 65% with almost one decade increase every 10 % increment of RH, whereas succinic and adipic acid are less sensitive to these changes. Below these critical values, the base current for all the acids and concentrations has a similar value and it is only above them that the behavior of the different concentrations starts to differentiate: the higher the concentration is, the steeper the curve becomes. Thus the leakage current recorded at a specific RH level is higher the more concentrated the solution is, and greater is the rate of raise.

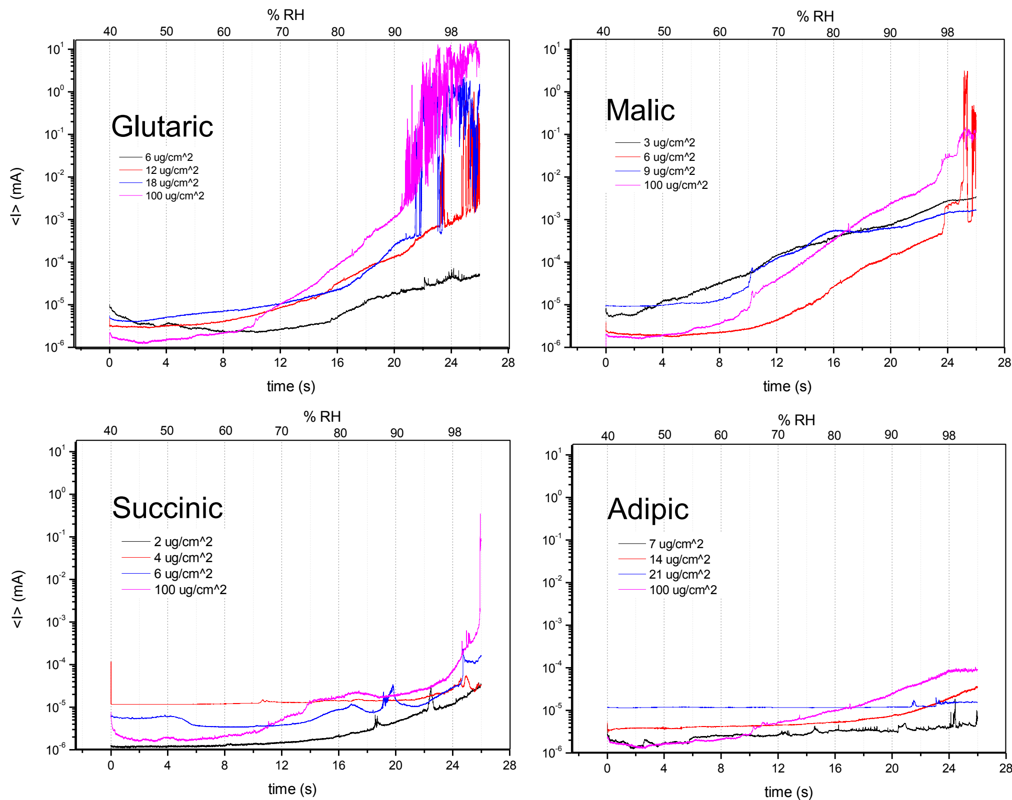

Figure 56 Effect of RH on the leakage current from SIR pattern pre-contaminated with different concentration of WOAs

Electrochemical migration is recorded for glutaric acid at 12, 18 and 100 µg/cm^2 above 90 % RH. Malic acid showed migration at concentrations of 6 and 100 µg/cm^2 while succinic acid only at 100 µg/cm^2. ECM occurred for malic and succinic acid after the RH of the chamber reached 98% RH. This can be noticed on the graph by sudden peaks on the curves which refer to abrupt current leakages through the dendrites. Adipic acid did not show any migration for all the concentrations.

7.4.1.2 *Surface morphology of the SIR pattern after migration*

Figure 57shows the ECM appearance on SIR pattern for glutaric, malic and succinic solutions at 100 µg/cm^2.

From the pictures, it is possible to notice the differences between the morphology of the dendrites, grown under the effect of glutaric and malic acids (pictures 1 and 2) and succinic acid (picture 3). For the first two WOAs, the dendrites look darker and thicker compared to the third one, where the dendrites are thinner and branched. When the dendrite grows thicker, more current can flow through it. This can be noticed in the higher current level reached for the glutaric and malic solution at 100 µg/cm^2 compared to the succinic solution at the same concentration.

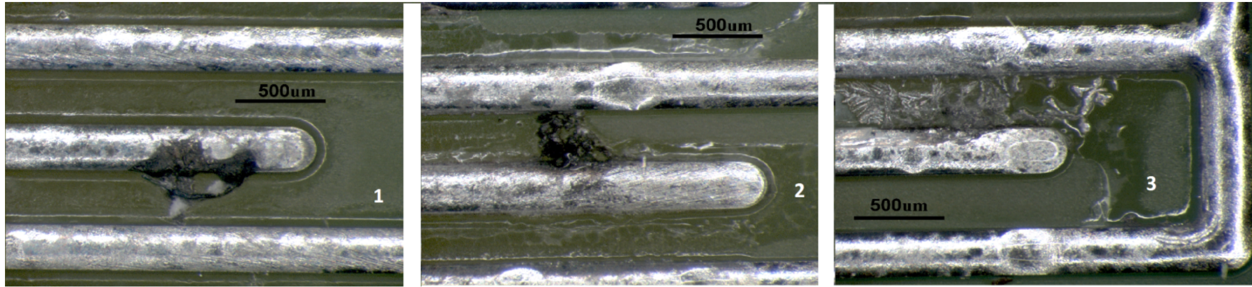

Figure 57 Surface morphology of the SIR pattern; 1) glutaric acid 100 μg/cm^2; 2) malic acid 100 μg/cm^2; 3) succinic acid 100 μg/cm^2

A common feature of the dendrite formation was that it always formed at the edges of the Sir pattern. This is due to the fact that the current density is higher at the edges and tips due to different ohmic voltage drops between different points[56]. This greater current density will attracts more metal ions, increasing their deposition on those points.

7.4.1.3 *Different behavior of the various WOAs at fix concentrations*

Figure 58 shows the effect of WOA on leakage current on SIR pattern with various curves plotted together for various acids with similar concentrations providing same conductivity. For example in Figure 58 (a), the conductivity of 1.56 μg/cm2 NaCl is similar to 7 μg/cm^2 of adipic acid, 6 μg/cm^{2}of glutaric, 3 μg/cm^{2}of malic, and to 2 μg/cm^{2}of succinic. In picture (b) and (c), the equivalent WOA concentrations are doubled and tripled. And Figure XX (d) shows the curves for all acids with a concentration of 100 μg/cm^2. Using equivalent concentrations will allow comparison of acid contaminations having same NaCl equivalent, while studying the effect of leakage current.

Focusing on the equivalent concentration curves it is possible to notice that the leakage current has a similar value for all the acids in general below 75% RH. When the humidity level overtakes ≈75%, NaCl starts to absorb moisture from the environment, as it reaches its cRH. This is followed by an increase of the leakage current on the SIR pattern pre-contaminated with sodium chloride.

The LC of the SIR pattern contaminated with glutaric and the succinic acid starts to rise above ≈ 65% and ≈80 % RH respectively. Their current increases reaching values approx. the same order as NaCl.

Only the malic acid shows an almost constant increase of LC from the starting point of the experiment, always displaying a higher current value. The adipic acid at 7 μg/cm^2, on the other side, does not show relevant increment of the LC during the whole experiment.

By doubling and tripling the concentration of WOA, the behavior of the WOA to leakage current becomes clearer, with the glutaric and malic, giving migration as soon as the concentration is doubled.

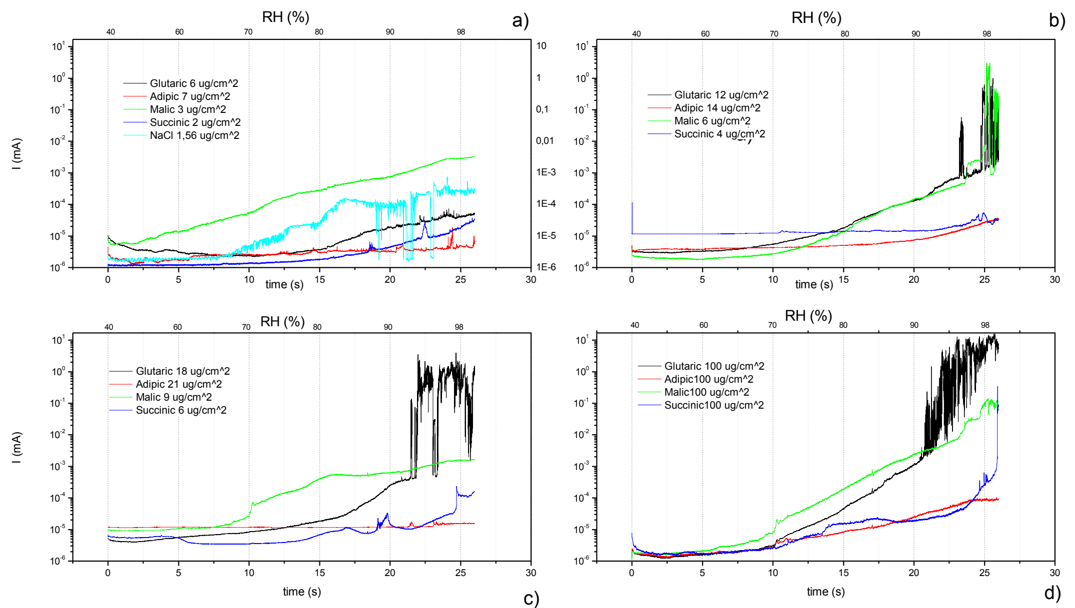

Figure 58 Comparison of the effect of different WOAs at fix concentrations

7.4.1.4 *Influence of the hygroscopic properties of the WOAs*

The different behavior of the WOAs towards relative humidity might be explained by the diverse hydroscopic properties of the acids, investigated by *Sohn et al.* and introduced in Chapter 6.

As evidenced by the relatively higher solubility of the glutaric and malic acid (639 and 558 g/l respectively) in water compared to the adipic and succinic acid (14 and 80 g/l respectively), the acid residues from the first two acids should be more hydrophilic.

The absorption of water will thus be higher with glutaric and malic acid residues, making the surface more conductive, leading to a higher leakage current and greater propensity for dendritic growth, as observed from the graphs. The different physical and chemical properties of the WOA residues result in significantly different surface conductivity when they are exposed to climatic changes.

However, their effects on ECM might be more complicated than just the solubility. Structure of the acids might also play a role as the conductivity of these acids is different for similar concentrations.

7.4.1.5 *Equivalent concentration of NaCl*

Figure 59 shows the LC vs. concentration trend for the four WOAs. The data were extracted from the results obtained before. These were taken at two different values of relative humidity, namely 70% (below critical RH) and 98% (Above critical RH). Additionally, on the top, the equivalent concentration of NaCl which would give the same conductivity has been considered. These have been calculating from

the LC measured at a certain concentration multiplied by a factor of 19.5. This constant is the ratio between the IPC concentration limit for NaCl equivalent and its value of leakage current. Namely:

$$Concentration\ NaCl\ equivalent\ \left[\frac{\mu g}{cm^2}\right] = \frac{I\ [mA]\ of\ the\ tested\ solution}{I\ [mA] of\ 1.56\mu g/cm^2\ NaCl} * IPC\ concentration\ limit\ \left[\frac{\mu g}{cm^2}\right] = \frac{I}{0.08} * 1.56 = I * 19.5$$

NaCl is a stronger electrolyte, compared to the various WOAs; therefore, in order to obtain the same value of LC, a lower concentration of NaCl will thus be necessary.

From these graphs it is possible to notice the general increase of LC with increased concentration and the higher sensitivity of the glutaric acid and the malic acid to the rise of humidity. This can be seen from the resulting higher current values at 98% RH for glutaric and malic acids compared to the adipic and succinic acid with respect to the current values at 70% RH.

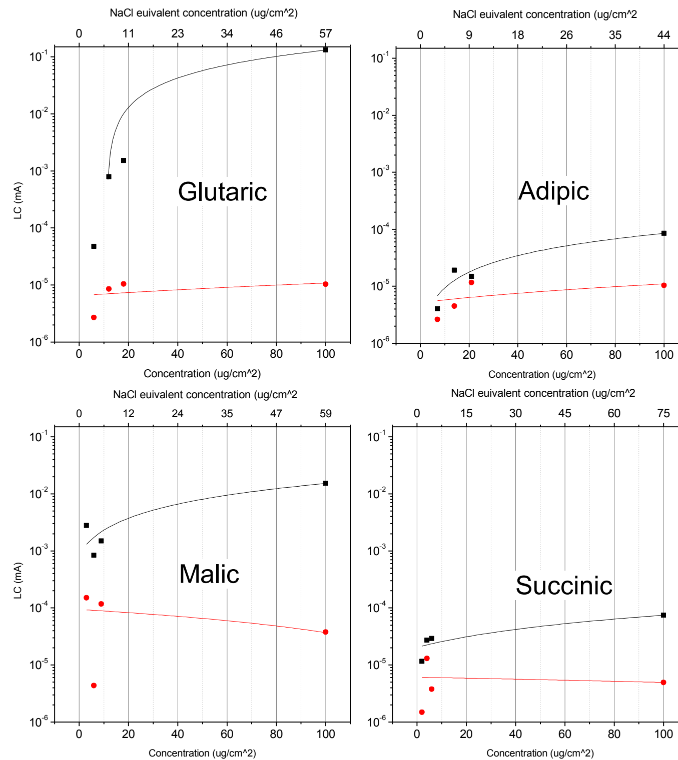

Figure 59LC vs. concentration trend for the four WOAs. On top is the Equivalent concentration of NaCl

7.4.2 Hydrophilic behavior of the various WOA residues

From these experiment is possible to notice how the acids start to have a different behavior from the one described in the preceding Chapter7.3. Especially the glutaric acid becomes, together with the malic, the most aggressive. This is due to the fact that the previous experiments were done under

condensation condition, directly using the solution in form of a droplet. In this experiment the residues is solid and is its hydrophilic behavior that exerts a great influence, as the more hydrophilic the residues are the more moisture at lower relative humidity can capture. The malic and the glutaric acid can attract more moisture creating the condensing humidity layer which allows the transfer of ions, enhancing this way the corrosion process. Therefore the type of WOA as an activator in a flux system plays an important role in the climatic reliability of an electronic device: the differences in physical and chemical properties of the WOA residues, when exposed to temperature and humidity, result in significantly different surface conductivity.

7.4.3 Possible implications in PCBA manufacturing

From these results it is possible to understand how the hygroscopic behavior of the WOA residues exerts a great influence on the climatic reliability of the PCBA. The presence of glutaric and malic acids as activators in a flux system is deleterious. Due to their high hygroscopic tendency they absorb humidity at lower RH, they render the surface more conductive and increase the leakage current. The propensity for dendritic growth istherefore much higher if these acids are present in solder fluxes as activators.

7.4.4 Conclusions

From the above results, it is possible to summarize the following:

- No significant increase in LC current was revealed for relative humidity below 60 % for 1.56 μg/cm^2 of NaCl, below 65 % for glutaric and malic acid, 80% for succinic and 90 % for adipic. Above these levels the leakage current start to rise for all the solutions and concentrations.
- Glutaric and malic acid showed a more consistent increase in leakage current above 65% with almost one decade increase for every 10 % increment of RH, whereas succinic and adipic acid are less sensitive to these changes
- The resulting leakage current levels were dependent on the acid concentrations with higher acid concentrations resulting in more leakage current.
- ECM was seen for glutaric, malic, and succinic acid at higher humidity levels, while no ECM was observed for adipic acid even at higher humidity levels.
- The higher aggressiveness of the malic and glutaric solution is due to their higher solubility in water which makes them more hygroscopic. This makes the water layer formation easy, and therefore enhances the corrosion process.
- Conductivity of various acids is different, which shows an influence of molecular structure on the dissociation of the acids.

- Results presented in this section has implications on the solder flux usage during soldering process indicating that the effect of flux types on climatic reliability depends on the acid types in the flux residue.

7.5 Effect of contamination on corrosion under condensing conditions

This chapter provides results on investigations related to water layer formation on the PCBA surface and corrosion reliability issues under differential temperature conditions between PCBA and outside atmosphere such as cooling effect. This leads to condensation on PCBA and relatively high water layer thickness.

7.5.1 PCB level tests using Peltier stage for continuous cooling

The purpose of this experiment was to investigate the effect of WOA residues on the leakage current of electronic components under condensing conditions. CELCORR test PCB has been employed and all the 9 rows of surface mounted capacitors have been tested, together with the reflow surface finish SIR pattern on the test PCB. In order to obtain nearly condensing condition, a peltier stage previously described has been used. The samples were placed inside the climatic chamber at constant condition of 25 °C temperature and 60 % relative humidity. The first experiment involves a concentration of 1.56 $\mu g/cm^2$ of NaCl on the SIR pattern and SMCs biased at 5 V. This test has been carried out in order to obtain a reference with respect to the IPC standards where to compare the succeeding results from the equivalent concentrations of WOA residues. This first test has been additionally used as a pilot test to verify and set the conditions for the following experiments with WOAs. Some parameters have been, indeed, changed after the test with sodium chloride: the voltage was increased to 10 V and the cooling conditions have also been modified. These changes will be better explained in the related paragraphs.

The temperature of the PCB has then been cooled down from ambient temperature down to the dew point when the condensation occurs. This has been achieved by increasing the voltage on the peltier stage through a programmable power source. RTD sensor has been used to monitor the temperature of the substrate and a video microscope has been employed to record the condensation on SMCs. All the experiments were carried out for 24 hours.

7.5.1.1 *Reference experiment using NaCl contamination*

SMCs component and the SIR pattern on the CELCORR test PCB setup have been pre contaminated with 1.56 $\mu g/cm^2$ of sodium chloride and tested under a 5V bias and condensing conditions. The PCB setup has then been mounted on the peltier stage, tightening it properly in order to ensure a good surface contact and heat transfer. The specimen has then been placed inside the climatic chamber and connected to the programmable power source. The voltage supply for the peltier stage has been programmed in order to rise from 0 to 5 V in 24 hours to ensure a constant cooling of the PCB.

The leakage current of the SIR pattern has been measured by means of a BioLogic potentiostat and the LC of the capacitors by means of the CELCORR PCB test setup, as it allows a greater number of channel to be recorded. The results from these measurements are displayed in Figure 60.

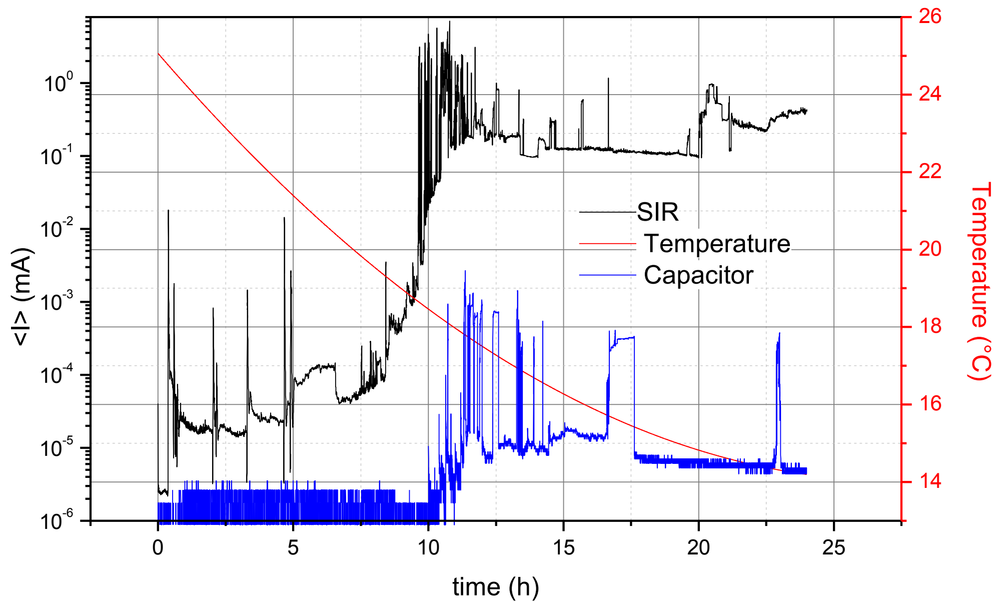

Figure 60 current leaking from the SIR pattern (black curves) and capacitors (blue curves). The red line represents the temperature of the PCB

On the same graph the LC vs. time and the temperature vs. time have been plotted. The LC can be read on the left y-axis while the temperature on the right y-axis. It is thus possible to read three curves from this graph: the black and the blue one represents the current leaking from the SIR pattern and one row of capacitors, respectively. The red line shows the temperature changes on the PCB due to cooling. The row of capacitors has been randomly chosen as the behavior is similar for all the rows. The current leaking from all the row of capacitor is shown in Appendix II

7.5.1.2 *Leakage current from the SIR pattern*

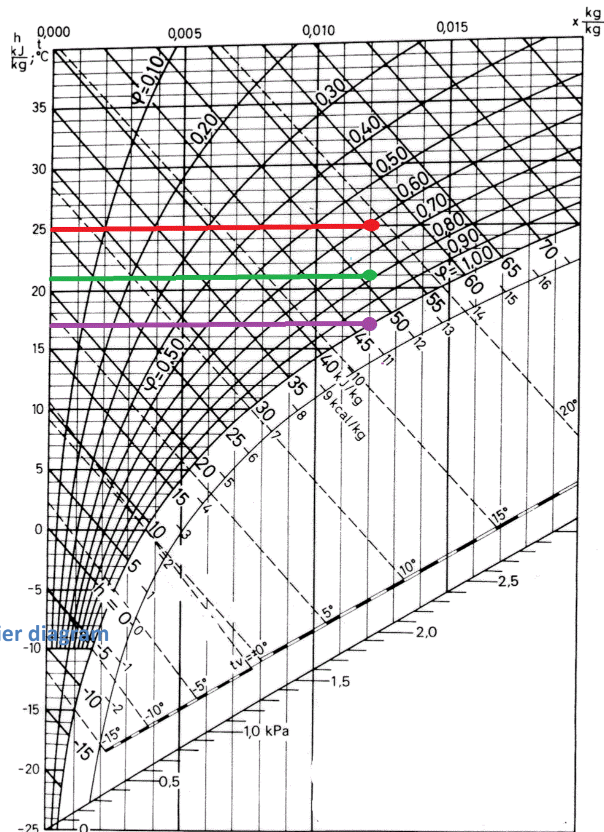

Figure 61 Mollier diagram

Focusing on the current leaking from the SIR pattern it is possible to notice that it starts to increase after around 6-7 hours when the temperature of the PCB is around 21 °C. At this temperature the first condensation droplets start to form: the dew point has been reached and the corrosion process is triggered. From this point the LC increases rapidly reaching its maximum after more or less ten hours at a temperature approx. of 18 °C. By looking at the Mollier diagram (Figure 61) it is possible to notice that at the experimental condition (T=25 °C and RH=60 %, red dot on the graph) the dew point is reached at T=17 °C (purple dot), meaning a ΔT=-8 °C. However, in this experiment a ΔT=-4 °C (green dot) is sufficient to reach the dew point. This is due to the hydrophilic properties of NaCl which reduce by 4 degrees the under cooling necessary to reach the dew point for these conditions. At this T=21 °C corresponds a value of relative humidity between 75 % and 80 %, which reflects the critical RH for NaCl (75 %) found in literature [47].

7.5.1.3 *Effect of condensation on the leakage current*

Condensation exerts a remarkable effect on the leakage current. The base current level at the beginning of the experiment is in the order of 10^{-5} mA; near condensing condition (21 °C < T < 20 °C) lead to an increase of approx. 2 orders, rising the current up to 10^{-3} mA. When full condensation occurs on the PCB (T≈ 18 °C), the current is increased again up to 10^{-1}.

In addition to this, it is possible to observe that the rate of increase is faster on the SIR patterns than on the capacitors. This greater sensitivity is due to the higher exposure area of the SIR than to the one of the SMCs.

7.5.1.4 *Leakage current on capacitors*

Focusing now on the current leaking from the capacitors row (blue curve in Figure 60) two differences can be immediately noticed. Before getting into their details it is worth to mention that the current presented in the graph is comprised from the currents leaking through 10 capacitors connected in parallel.

As it is possible to notice the magnitude of the LC measured on the row of capacitors is around two and more orders lower than the one recorded on the SIR. This is due to the fact that the exposure area of the SIR is higher compared to the SMCs, leading to a higher sensitivity of current measurements using SIR pattern than the current measurements from SMCs .In addition to this the condensation process for the SMCs is delayed by approx. one hour due to the fact that condensation happens first on the tin terminals and then along the ceramic body of the capacitors. When the two terminals are bridged the corrosion process takes place and the current increases.

The highest LC measured on the SMCs is comprised within 10^{-3} and 10^{-2} mA. Electrochemical migration for this size of capacitor induces, usually, a leakage current above 1 mA (experimental result), thus on the SMCs the current level is not high enough. Visual examination of the surfaces revealed indeed no sign of migration on the capacitors and the increase in current is due to corrosion products.

As it is possible to notice from the pictures collected in Figure 62 condensation occurs first on the tin terminals at around 19 °C (≈85 % RH) and becomes clearly apparent on the body of the capacitor when the surface of the PCB reaches 17 °C.

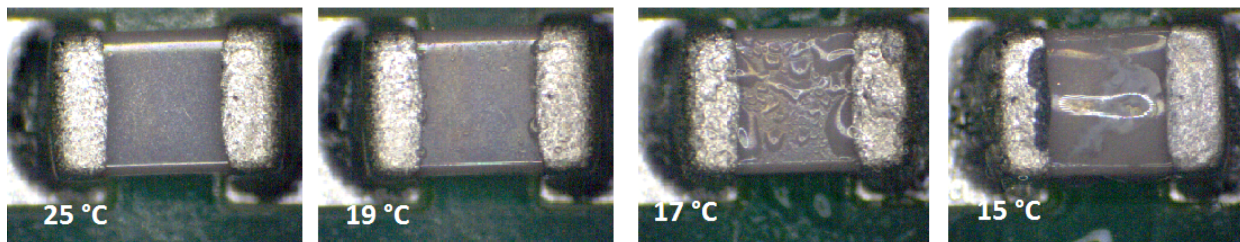

Figure 62 Temperature effect on condensation on a 0805 capacitor pre contaminated with 1.56 μg/cm^2 of NaCl

7.5.1.5 *Remarks*

From the results of this experiment it has been decide to modify some of the parameters like the applied voltage and the cooling profile. The voltage has been increased to 10 V, in order to compare the results with literature results and IPC standard testing. Additionally, the condensation reached with the NaCl experiments was too intensive and thus unrealistic for real life situation, therefore the cooling curves has been differently programmed. From the previous results the condensation obtained around

10 hours, which corresponds to an applied potential to the peltier stage of 3 V, has been considered realistic. Thus the temperature profile for the WOAs experiments foresees an increased voltage from 0 to 3 V in 10 hours and then a constant potential of 3 V will be maintained for the next 14 hours.
The results will be illustrated in the next paragraph.

7.5.2 Experiments under condensing conditions using WOAs residues

Experiments described above has been repeated with the test PCB pre-contaminated with the equivalent concentrations of WOAs previously found, which provides leakage current levels similar to 1.56 µg/cm2 NaCl levels. These concentrations are listed in Table 16below.

Table 16Concentration of WOAs equivalent to 1.56 µg/cm^2 of NaCl

	Adipic	Glutaric	Malic	Succinc
Concentration (µg/cm^2)	7	6	3	2

The potential applied to the SMCs has been increased to 10 V while the potential applied to the Peltier stage has been programmed to increase from 0 to 3 V within 10 hours and then remain constant at 3 V for the remaining 14 hours. This will result in a constant cooling, corresponding to the increasing potential, followed by a stationary temperature till the experiment terminates.

7.5.2.1 *Leakage current from the SIR pattern with WOA residues*

Focusing on the SIR patterns of Figure 63the comparable trends for all the solutions can be noticed with condensation starting between 18 and 19 °C for all the WOAs. The malic and the glutaric acid begin to rise at a temperature between 18.5 and 19 °C, while the other at a lower T≈18 °C, in accord to the hydrophilic properties of the solutions summarized in Table 17.

The hydrophilic behavior of the malic acid, underlined by the solubility in water is comparable to the one of the glutaric acid: their solid residues start to absorb humidity at a lower RH≈90 % (taken from the Mollier diagram(Appendix V).The adipic and succinic acids form in the bulk a more compact structure, which is harder to break by dissolution, therefore condensation occurs at a lower temperature and higher RH≈95 %.

The current level, after the migration has occurred (~7 hours), is comparable with all the solutions as their conductivity should be approximately the same.

.

Table 17 Hydrophilic properties of the investigated WOAs

Acid	Solubility in water g/l
Adipic	14
Succini	80
Glutaric	639
Malic	558

The lower hydroscopic behavior of the WOAs reflects also in the lower rate of LC increase compared to the one recorded for NaCl. When sodium chloride residues reach the dew point (RH≈75 %) the current suddenly increases. This rapid raise is, indeed, not recorded for the WOA residues, which show a smoother and more gradual increase when the dew point is reached.

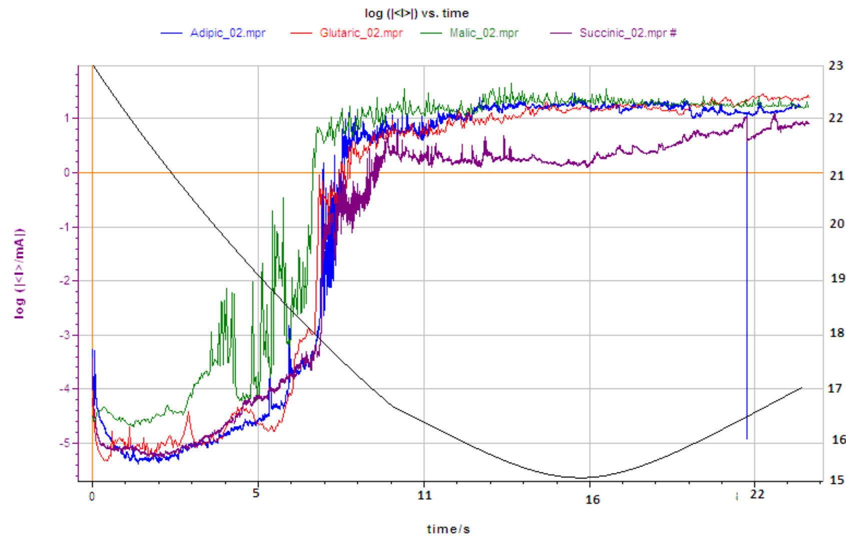

Figure 63 LC from SIR pattern pre-contaminated with the equivalent concentration of WOAs

7.5.2.2 *Comparison with literature and previous experimental results*

The critical RH of these WOAs has been previously investigated by *Adams et al.*[57] and through former experimentsin CELCORR lab by mean of Quartz Crystal Microbalance (QCM). These results (listed in Table 18) show the propensity of the glutaric and malic acid to absorb water at lower relative humidity compared to the adipic and succinic acid. From the previous paragraph the glutaric and malic acid were found to have a cRH≈90 % while for the remaining two acids the cRH≈95 %. Both these values match with the previous experimental and literature results reflecting the more hydrophilic behavior of the glutaric and malic acid.

Table 18 Critical RH value collected from literature and previous experiments

Compound	$c.RH_{ref}$, %	$c.RH_{QCM}$, %
Adipic	99.6	-
Succinic	98	92-96
Glutaric	84	84-94
Malic	86	75-82

7.5.2.3 *Leakage current from capacitors with WOA contamination*

Figure 64illustrates the behavior of one row of capacitors pre-contaminated with one type of WOA. The results from the different contaminants have been displayed together to be compared. As it is possible to see the temperature after 10 hours is not stationary, as foreseen by the setup. This is due to the functioning of the power supply and not to a wrong setup. However the variation of temperature during the last 14 hours is of approx 1 °C which can be considered acceptable.

The LC of the capacitors contaminated with glutaric and malic acids starts to increase before the one contaminated with the remaining WOAs. It begins to rise after 8-9 hours at a temperature of approx. 18 °C, whereas for the other solutions it increases one hour later. This reflects the higher hydrophilic behavior of the malic and glutaric acids compared to the succinic and adipic acids. This higher hydrophilic behavior of these two WOAs is, however, still lower than the one of NaCl as observed in the previous experiment. Remarks concerning the cRH for the different WOAs will be elaborated in the following paragraph.

The row of capacitors pre-contaminated with malic acid shows the higher leakage current, at least for the first peak, which is around one order greater than the other cases. After the first peak the behavior becomes similar to the other solutions which show comparable values of leakage current $\approx 10^{-3}$ mA.

As for the NaCl case the LC is not high enough to be caused by electrochemical migration, therefore the increased of its value it is mainly due to corrosion products.

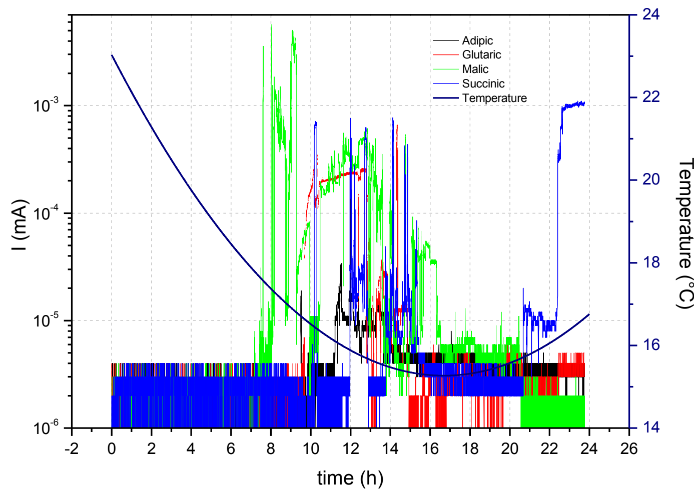

Figure 64 LC current from capacitors row pre-contaminated with different WOAs

Table 19 summarizes the approximate temperatures at which the dew point has been reached for the different solutions spread on the capacitors, together with the corresponding value of cRH extrapolated from the Mollier diagram.

Table 19Temperature and corresponding cRH values

	Adipic	**Glutaric**	**Malic**	**Succinc**
Temperature (°C)	17	18	18	17
cRH (%)	≈98	≈95	≈95	≈98

These values show, again, the higher hygroscopic behavior of the glutaric and malic solutions compared to the remaining ones. These values are higher than the ones obtained both from the SIR pattern and the one listed in Table 18. Condensation on the capacitors occurs first on the tin terminals and afterwards on the ceramic body of the components. It is only when the two terminals are bridged that a significant increase of the LC is recorded, which occurs with a certain delayed from the SIR. This delayed is followed by a decrease of temperature and increase of RH. This might explain the differences in the values obtained from the SIR pattern.

7.5.3 Comparison of leakage current for various contaminations and condensing conditions

Figure 65collects the values of the leakage current density from the SIR pattern for all the equivalent concentrations of WOAs and the solution of 1.56 μg/cm^2 of sodium chloride. LC density has been calculated considering the ratio of the LC (in mA) over the surface area of the SIR pattern (in cm^2). The values of LC are recorded at different humidity level, starting from the initial value at 60 %RH, where no cooling has been undertaken, to near and full condensation conditions. The area of the SIR pattern was measured to be 3.5 cm^2.

At 60 %RH when the dew point has not been reached yet the behavior of the glutaric, adipic and succinic acid is quiet comparable, with all the solution showing current values within the same order of 10^{-6} mA. At near condensing condition (approx. after 7/8 hours) the malic and glutaric solutions show values of LC density approx. one decade greater than the succinic and adipic. As the glutaric and malic acid start to absorb moisture before the remaining two acids, displaying a higher current density by time it was recorded At full condensation condition all the solution tend to get close to the same LC value $\approx 10^0$ mA. This is in accord to the results from the effect of increasing humidity obtained in Chapter X, where the equivalent solution had comparable value of leakage current at different humidity levels

NaCl contamination, although at equivalent concentration and strong electrolyte shows lower current than the WOAs values due to the lower potential bias used ie, 5 V. If the potential bias is higher (ie. 10 V), a current level higher than WOAs is expected for NaCl.

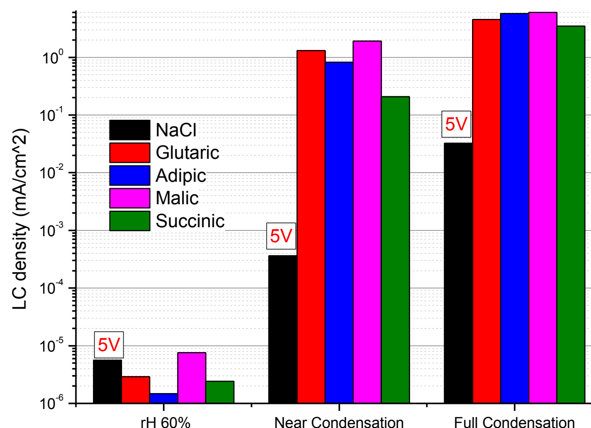

Figure 65 LC values from the SIR pattern at different condensation levels

7.5.4 Possible implication in PCBA manufacturing

Due to the higher hydrophilic behavior of the glutaric and malic acids which start to absorb humidity at lower RH value, compared to the adipic and succinic acids, their presence as activators in solder fluxes may have a more negative effect on the climatic reliability of the PCBAs. The conductivity of the condensed layer may, indeed, increase the leakage currents and promote electrochemical migration.

7.5.5 Conclusions

From the previous results is possible to summarize the following conclusion:

- NaCl has been tested under a potential of 5 V and the current leaking from the SIR pattern starts to increase after around 6-7 hours when the temperature of the PCB is around 21 °C
- NaCl reduces by 4 degrees the under cooling necessary to reach the dew point for the experimental conditions.Its critical RH was recorded to be ≈ 75 % RH, in accord with literature and previous experimental results
- The magnitude of the LC recorded from the capacitors contaminated with NaCl is approx. two orders lower than the one recorded for the SIR pattern. In addition to this it is delayed of approx. one hour
- The WOA residues have been tested under a 10 V bias. The higher hygroscopic behavior of the glutaric and malic acids is reflected in the LC rise which takes place before the other two acids at RH values ≈ 90%. The succinic and adipic residues start to absorb moisture ≈ 95 %. This critical RH values match the ones found in literature and through previous experimental results
- The hygroscopic properties, like the solubility in water, of the investigated WOAs might explain the different behaviors of the acids towards relative humidity.
- No migration has been recorded for the capacitors contaminated with WOA and NaCl residues

8 Conclusions

1. The corrosion rate of the WOA-metal system increases with increasing concentration. Different behaviors are recorded regarding the type of acid employed. Malic-Snsystem showed the highest corrosion rate ($6.95e^{-2}$ mA/cm^2) at 100 µg/cm^2, followed by succinic-Sn ($2.88e^{-2}$ mA/cm^2) and glutaric-Sn systems ($2.71e^{-2}$ mA/cm^2). Physical and chemical properties like the low pK_a value (3.4) and the presence of an additional hydroxyl (-OH) group in the structure of the malic acid, might explain its higher aggressiveness compared to the other WOAs
2. WOAs are weak electrolyte and only partially dissociate in water, thus the conductivity will not be linearly proportional to the concentration, as seen for strong electrolyte. The aggressiveness of the malic solution finds its explanation in the lowest pK_a value (3.4), while the other solutions have comparable value of pK_a (4.2 for succinic acid and 4.4 for glutaric and adipic acid)
3. Large differences in the equivalent concentrations were observed depending whether the values were measured using the conductivity meter (AC) or the LRDT setup (DC). DC measurements showed much higher results of equivalent concentration, due to the higher sensitiveness of the investigated solution to the direct current
4. Approximately 0.07 g/l of adipic acid, 0.06 g/l of glutaric acid, 0.03 g/l of malic acid and 0.02 g/l of succinc acid give the same conductivity values as 0.0156 g/l of NaCl. This value is equivalent to 1.56µg/cm^2 referred in IPC J-STD-001D standard if the assumption that area of 1 mm^2 is covered by 1µl of solution is fulfilled. In order to achieve the equivalent conductivity of 1.56 µg/cm^{2}NaCl, higher concentrations of WOAs are necessary. This is caused by dissociation rates of electrolytes. NaCl is a strong electrolyte and the conductivity dependence on concentration is linear, whereas WOAs show non-linear conductivity dependency on concentration.
5. Succinic acid at 10 µg/cm^2 showed the highest propensity of ECM (≈ 72%) within the WOAs. Succinic acid seems to assist deposition and dendrite formation, while malic acid, due to its low pK_a value seems to inhibit the dissolution of metal ions, reducing the probability of ECM. Adipic acid did not induce any migration due to its low aggressiveness.
6. Residues from Solder Flux 327 at 100 µg/cm^2 showed the highest propensity of ECM (≈ 77 %) within the Solder Flux systems. Overall results indicates that the tendency to induce ECM is a mixture of high acid content and acid type similar for the four WOAs tested. A flux system with succinic acid in general has the capability to show higher ECM levels, whereas adipic shows least.

7. The increase of LC over the SIR pattern with increase of WOA concentration has been observed. Glutaric and Malic showed ECM when the equivalent concentration has been doubled. No ECM was recorded for the adipic acid at any concentration
8. Presence of NaCl reduces the critical RH for water layer formation and increases LC. NaCl reduces the critical relative humidity down to ≈ 75%
9. The higher hygroscopic properties of the glutaric and malic acid reduce the critical RH for water layer formation down to ≈ 90 % RH. Succinic and adipic acid start to absorb moisture at a higher RH ≈ 95 %. Glutaric and malic acid might increase the concentration of water on the surface, rendering it more conductive since there is a solution of ionisable material present. This leads to higher LC and greater propensity for dendritic growth. The higher leakage current with malic acid compared with glutaric acid, may rise from the greater acidity of malic acid
10. The behavior of the investigated WOAs is strongly influenced by the condensing conditions in which they are investigated. At full condensing condition (when they are applied in form of a droplet or the water layer has already been formed) the acidity, given by the pK_a value, is determinant. The higher the acidity the more aggressive the acid is. Therefore the malic and the succinic acid are the most hazardous in these conditions. When the acids are present as solid residues it is their hygroscopic properties, like the solubility in water, which play the main effect. The ability of glutaric and malic acid to absorb moisture at lower RH makesthem dangerous for the climatic reliability of electronic products

9 Future perspectives

The subject of climatic reliability of electronic devices is a broad and highly complex research field. Due to the multidisciplinary knowledge it involves, the full overview and understanding of the related problems is very hard to gain. The aim of this project is to understand which of the four WOAs, which are present as activators in Solder Flux Systems, are significantly hazardous for the reliability of PCBAs. This has been done from a specific point of view, which focuses only on the residues of solder fluxes and WOAs.

Future research topics that came out from the present study and that would give a broader knowledge on the process are listed below:

1. Study of the effect of the WOAs as activators in Solder Flux Systems: understanding their influence on the quality of the solder in terms of mechanical, metallurgical, physical and chemical properties
2. Comparison between the quality of the solder and the effect of the WOA and solder flux residues obtained in this project
3. Investigation on long-term practical field applications

10 List of references

[1] R. Hienonen and R. Lahtinen, "Corrosion and climatic effects in electronics," *VTT PUBLICATIONS*, 2000.

[2] R. Ambat and P. Møller, "A review of Corrosion and environmental effects on electronics," *The Technical University of Denmark, DMS …*, 2006.

[3] M. Ohring, "An Overview of Electronic Devices and Their Reliability," in *Reliability and failure of electronic materials and devices*, London: Academic Pess, 1998.

[4] P. Virmani, "CORROSION COSTS AND PREVENTIVE STRATEGIES," *HRDI*, no. 202, pp. 493–3052, 1998.

[5] W. Brad and M. Stanley, "CORROSION ISSUES ASSOCIATED WITH ROHS CAN BE FATAL TO ELECTRONIC CONTROL EQUIPMENT," *CORROSION 2010*, no. 14941, pp. 1–7, 2010.

[6] M. Yunovich, "Appendix Z– Electronics."

[7] D. Mikkelsen, "Corrosion susceptibility of electronic components in offshore wind turbine nacelle," no. December, 2012.

[8] D. Minzari, "Investigation of Electronic Corrosion Mechanisms." Technichal University of Denmark, Lyngby, 2010.

[9] P. Westermann, "Investigation of process related residues during PCB manufacturing," no. September, 2008.

[10] R. Ambat, S. Jensen, and P. Møller, "Corrosion Reliability of Electronic Systems," *ECS Meeting: Corrosion (General) …*, vol. 6, no. May 2012, pp. 17–28, 2007.

[11] M. S. Jellesen, D. Minzari, U. Rathinavelu, P. Møller, and R. Ambat, "Corrosion failure due to flux residues in an electronic add-on device," *Engineering Failure Analysis*, vol. 17, no. 6, pp. 1263–1272, Sep. 2010.

[12] J. LaDou, "Printed circuit board industry.," *International journal of hygiene and environmental health*, vol. 209, no. 3, pp. 211–9, May 2006.

[13] C. . Coombs, "PCB Design," in *Pritned circuits handbook*, McGraw-Hill Professional, 2007, pp. 123–176.

[14] C. Young, V. Illingworth, and J. Young, *The penguin dictionary of electronics*. Penguin Books, 1988.

[15] J. Bird, *Electrical and Electronic Principles and Technology*. Elsevier Limited, 2010, pp. 63–76.

[16] "No Title." [Online]. Available: www.kpcomponents.ca.

[17] "Possible impact on corrosion reliability of capacitors." [Online]. Available: www.database.crecon.dk.

[18] S. Gibilisco, *Teach yourself electricity and electronics*. McGraw-Hill, 2002.

[19] "No Title." [Online]. Available: http://laserdiy.com/.

[20] R. P. Prased, *Surface mount technology*. Springer, 1997.

[21] "Passive components."

[22] G. K. Rao, *Multilevel interconnect technology*. McGraw-Hill, 1993.

[23] "No Title."

[24] M. Judde and K. Brindley, "Soldering process," in *Soldering in electronics assembly*, Elsevier Ltd, 1999, pp. 1–22.

[25] K. H. et al. Buschov, "Electronic packaging: Solder Mounting Technologies," in *Encyclopedia of Materials: Science and Technology*, Elsevier, 2001, pp. 2708–2709.

[26] M. Ohring, *Reliability and Failure of Electronic Materials and Devices (Google eBook)*. 1998.

[27] M. Judde and K. Brindley, "Flux," in *Soldering in electronics assembly*, 1999, pp. 89–108.

[28] K. Hansen and M. Jellesen, "Effect of solder flux residues on corrosion of electronics," *… , 2009. RAMS 2009. …*, pp. 502–508, Jan. 2009.

[29] M. Zado, "Water soluble flux," U.S. Patent 4,478,6501984.

[30] F. Classon, *Surface mount technology for current engineering and manufacturing*. New York, USA: McGraw-Hill, 1993.

[31] R. Strauss, *Surface mount technology*. Oxford, UK: Butterworth-Heinemann, 1994.

[32] R. Todd and D. Allen, *Manufacturing processes reference guide*. New York, USA: Industrial Press Inc., 1994.

[33] M. Johnson, "Effect of Contamination on Electrochemical Migration," Technical University of Denmark, 2006.

[34] E. Bardal, *Corrosion and Protection*. USA: Springer, 2005.

[35] J. W. Osenbach, "Corrosion-induced degradation of microelectronic devices," *Technol., Semicond. Sci.*, vol. 11, pp. 155–162, 1996.

[36] V. Verdingovas, "Investigation on the effect of ionic contamination on the corrosion reliability of printed circuit board assemblies," Technical University of Denmark, 2011.

[37] C. Dominkovics and G. Harsanyi, "Effects of flux residues on surface insulation resistance and electrochemical migration," *Electronics Technology, 2006. …*, pp. 206–210, 2006.

[38] G. Sarkar and Y. F. Chong, "A study of the factors affecting surface insulation resistance measurements," *Science*, vol. 17, pp. 1963–1965, 1998.

[39] R. P. Frankenthal, "Passivity and corrosion of electronic materials and devices," *Corrosion Science*, vol. 31, pp. 59–68, 1990.

[40] D. Minzari, M. S. Jellesen, P. Møller, and R. Ambat, "On the electrochemical migration mechanism of tin in electronics," *Corrosion Science*, vol. 53, no. 10, pp. 3366–3379, Oct. 2011.

[41] M. S. Jellesen, D. Minzari, U. Rathinavelu, P. Møller, and R. Ambat, "Investigation of Electronic Corrosion at Device Level," *The electrochemical society*, vol. 25, no. 30, pp. 1–14, 2010.

[42] et al. Lue, "Bromine- and- Chlorine-Induced Degradation of Gold-Aluminum Bonds," *Journal of Electronic Materials*, vol. 33, no. 10, pp. 1111–1117, 2004.

[43] K. Marsanich, S. Zanelli, F. Barontini, and V. Cozzani, "Evaporation and thermal degradation of tetrabromobisphenol A above the melting point," *Thermochimica Acta*, vol. 421, no. 1–2, pp. 95–103, Nov. 2004.

[44] F. Barontini, V. Cozzani, K. Marsanich, V. Raffa, and L. Petarca, "An experimental investigation of tetrabromobisphenol A decomposition pathways," *Journal of Analytical and Applied Pyrolysis*, vol. 72, no. 1, pp. 41–53, Aug. 2004.

[45] J. S. Vimala, M. Natesan, and S. Rajendran, "Corrosion and Protection of Electronic Components in Different Environmental Conditions - An Overview," *The Open Corrosion Journal*, vol. 2, no. 1, pp. 105–113, Apr. 2009.

[46] J. D. Sinclair, L. A. Psota-Kelty, G. A. Peins, and A. O. Ibidunni, "Indoor/outdoor relationships of airborbe ionic substances: comparison of electronic equipment room and factory environments," *Atmospheric Environment*, vol. 26, no. 5, pp. 871–882, 1992.

[47] P. Tegehall and B. Dunn, *Evaluation of Cleanliness Test Methods for Spacecraft PCB Assemblies*, no. October. 2006.

[48] C. H. Hamman, A. Hamnett, and W. Vielsitch, *Electrochemistry - theory and practice*. Wiley-VCH, 1998.

[49] Q. N. Xiao, F. Grundwald, and K. Carlson, "Surface Leakage Current (SLC) Methodology for Electrochemical Migration Evaluation," *Circuit World*, vol. 23, no. 4, pp. 6–10, 1997.

[50] R. Analytical, "Conductivity-theory and practice," pp. 1–50, 2004.

[51] H. J. Flitt and D. P. Schweinsberg, "A guide to polarisation curve interpretation: deconstruction of experimental curves typical of the Fe/H2O/H+/O2 corrosion system," *Corrosion Science*, vol. 47, no. 9, pp. 2125–2156, Sep. 2005.

[52] B. A. Smith and L. Turbini, "Characterizing the Weak Organic Acids Used in Low Solids Fluxes," *Journal of Electronics Materials*, vol. 28, no. 11, 1999.

[53] "No Title." [Online]. Available: http://www.chemicalland21.com/.

[54] J. E. Sohn and U. Ray, "Weak Organic Acids and Surface Insulation Resistance *," *Circuit World*, vol. 21, pp. 21–26, 1994.

[55] "No Title." [Online]. Available: http://www.doitpoms.ac.uk/.

[56] K. I. Popov, M. G. Pavlovic, and P. M. Zivkovic, "Electrochemistry Encyclopedia." [Online]. Available: http://electrochem.cwru.edu/encycl/.

[57] K. M. Adams, J. E. Anderson, and Y. B. Graves, "lonograph Sensitivity to Chemical Residues from ' No Clean ' Soldering Fluxes : Comparison of Solvent Extract Conductivity and Surface Conductivity," *Circuit World*, vol. 29, no. 2, pp. 41–44, 1994.

Appendix I: Materials and design used for electronic components

Component	Design	Materials
Printed Circuit Board	Metallic conductor separated by insulating materials	Copper, copper alloys, epoxy resins, ceramics, woven glass fiber, solder, tin, lead
Contacts	Electrical contacts maintained by mechanical forces	Base Metal - copper, stainless steels Contact Surface – gold, palladium, silver, tin
Connectors	Electrical connections between systems or boards	Spring Material – beryllium, copper, stainless steels Contact Surface – Contact Surface – gold, palladium, silver, tin
Switches and Relays	Cyclic electrical connection	Copper alloys, steels, stainless steels
Grounding contacts	For shielding	Copper, steels, aluminum, nickel, tin, tin-lead
Thermal contacts	Heat sinks Small dimension	Gold, silver, aluminum, Kovar, Solder,
Integrated circuits	Complex systems	Glass, silicon, tungsten

Appendix II: current leaking from capacitors

NaCl

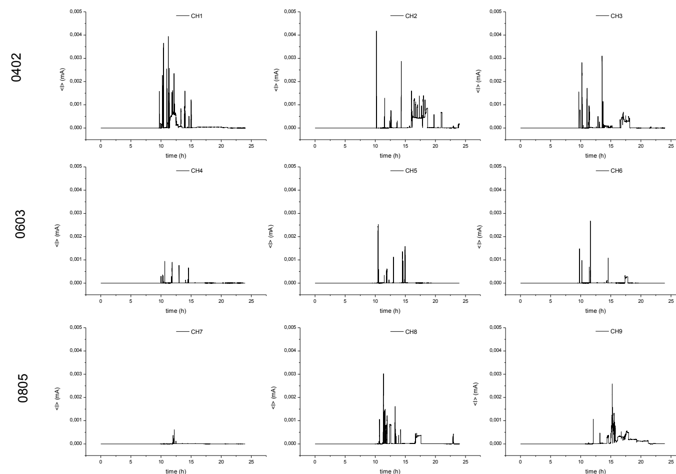

Adipic acid

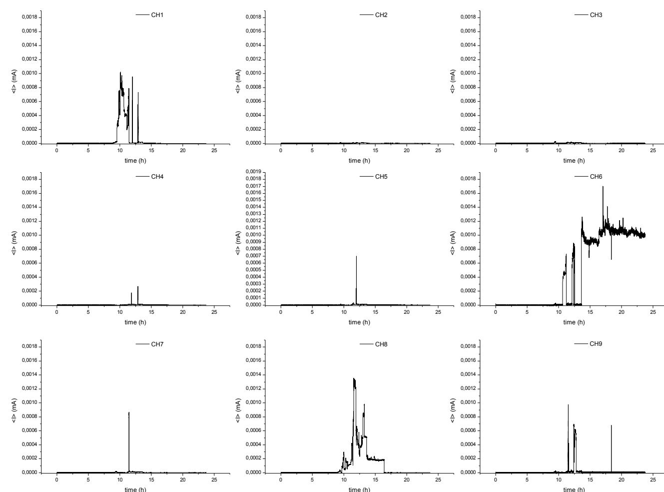

Glutaric acid

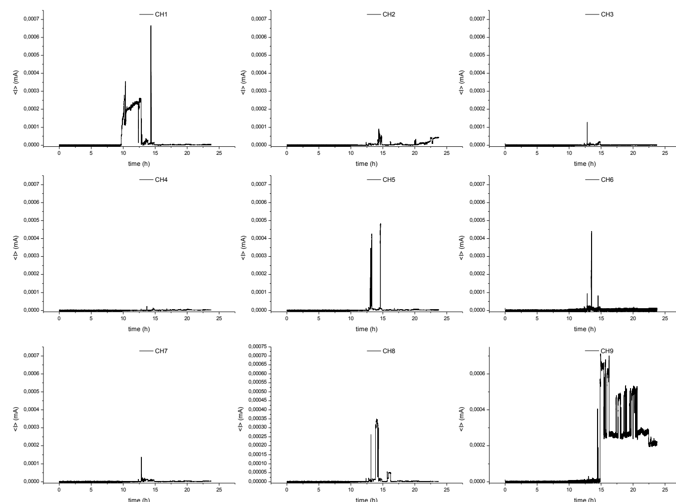

Malic acid

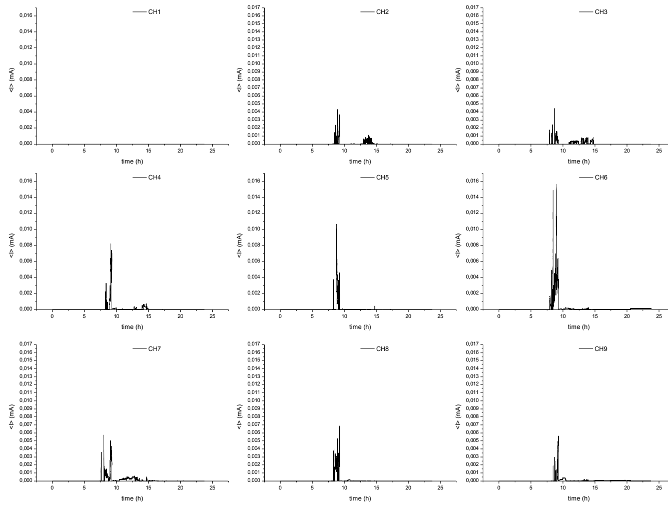

Succinic acid

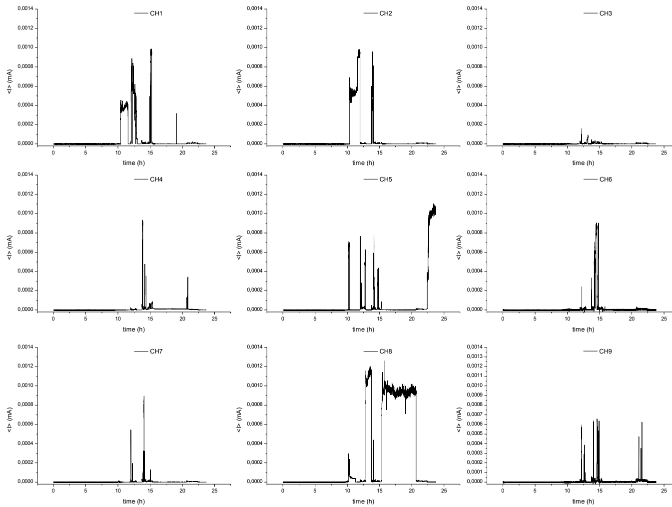

Appendix III:Product datasheet for Solder Flux Systems

COBAR®

Cobar Europe BV
PO Box 3251
4800 DG Breda

Tel +31 (0) 76 544 55 66
Fax +31 (0) 76 544 55 77
Internet http://www.cobar.com

Product Data Sheet

Product	**327**
Productgroup	General Wave Solder Flux
Date	13-08-2007
Release	6.2

5	Especially made for this purpose
4	Generally qualified for this purpose
3	Generally usable, but not the best choice
2	Generally not usable for this purpose
1	Wrong choice

ISO 9454-1	1.1.2.A
IPC-ANSI-J-STD-004	ROL1
JIS Z 3197	1.2.3.N_II
No-Clean process	5
Post-solder cleaning	3
Selective Soldering	3
Pb-Free process - Ambient	5
Pb-Free process - N2	5
N2 Process - Full Tunnel	2
N2 Process - Wave Only	5
Consumer electronics	5
Med-Rel electronics	4
Hi-Rel electronics	4
1-layer, video/tv boards	5
2-layer boards	5
Multi-layer boards	5
OSP compatible	5
Ni/Au compatibel	5
Ni/Pd compatible	5
Ag compatible	5
Sn compatible	5
Foam fluxing	5
Nozzle-spray fluxing	5
Moderate preheat	5
Short contact time with solder	5
Reduces skipped joints	5
Reduces solder balling	5
Reduces bridging	5
Promotes wicking	5
Cosmetic cleanliness	2
Cosmetic cleanliness N2	3
Dull/frosty joints	2
ICCT compatible	5
Conformal coating	1

SG @ 20 °C [kg/dm3] (+/- 0.5%)	0.840
Solids content [% w/w]	4.94
Halides [Silver-Chromate Test]	Pass
Halides [Potentiometric]	Detected
Acid number [mgKOH] (+/-2.5%)	29.00
Water content [% w/w]	5.
VOC-content [% w/w]**	90.00
Filmformer(s)	Resin
Flashpoint COC [°C]	13.5
Odor	Alcoholic
Color	Light amber
Telcordia/Bellcore TR-NWT-000078/3	-
Test report(s)	-
Certificate of Compliance	Available
SPC-data*	Auditable
Environmental Load Unit	6.00
RoHS-Compliance Certificate	Available
User's Guidelines	English
Thinner	425-00
Packaging	
Can (HDPE) [liter]	10
Drum (HDPE) [liter]	200
Shelf-life (Weeks)	
Storage 20 [°C]	52.
Storage 25 [°C]	40.
*Certain conditions apply.	
**Having a vapor pressure of >0.01 mm Hg @ 25 °C	
Industrial chemical product. Read MSDS before use.	

Cobar Europe BV
PO Box 3251
4800 DG Breda

Tel +31 (0) 76 544 55 66
Fax +31 (0) 76 544 55 77
Internet http://www.cobar.com

Product Data Sheet

Product	**327-SEL**
Productgroup	Selective Flux
Date	31-10-2011
Release	11.1

5	Especially made for this purpose
4	Generally qualified for this purpose
3	Generally usable, but not the best choice
2	Generally not usable for this purpose
1	Wrong choice

ISO 9454-1	1.2.3.A
IPC-ANSI-J-STD-004	REL0
JIS Z 3197	1.2.3.N_I
No-Clean process	5
Post-solder cleaning	3
General Wave Soldering	2
Pb-Free process - N2	5
Consumer electronics	3
Med-Rel electronics	4
Hi-Rel electronics	5
1-layer, video/tv boards	4
2-layer boards	5
Multi-layer boards	5
OSP compatible	5
Ni/Au compatibel	5
Ni/Pd compatible	4
Ag compatible	4
Sn compatible	5
Bubble jet fluxing	5
Nozzle-spray fluxing	5
Template/dip fluxing	4
Hot bar soldering	5
Static solder-nozzle	5
Flow solder-nozzle	5
Short contact time with solder	5
Moderate preheat	4
Reduces spread of flux	3
Reduces solder balling	5
Reduces bridging	4
Cosmetic cleanliness	3
Cosmetic cleanliness N2	4
ICCT compatible	4
Conformal coating	5

SG @ 20 °C [kg/dm3] (+/- 0.5%)	0.840
Solids content [% w/w]	4.94
Halides [Silver-Chromate Test]	Pass
Halides [Potentiometric]	Pass
Acid number [mgKOH] (+/-2.5%)	19.70
Water content [% w/w]	5.
VOC-content [% w/w]**	90.00
Filmformer(s)	Resin
Color	Colorless
Flashpoint COC [°C]	13.5
Telcordia/Bellcore TR-NWT-000078/3	Compliant
Test report(s)	Available
Certificate of Compliance	Available
SPC-data*	Auditable
Environmental Load Unit	6.00
RoHS-Compliance Certificate	Available
User's Guidelines	English
Packaging	
Bottle (HDPE) [liter]	1
Can (HDPE) [liter]	5, 10
Thinner	425-00
Shelf-life (Weeks)	
Storage 20 [°C]	52.
Storage 25 [°C]	40.

Cobar Europe BV
PO Box 3251
4800 DG Breda

Tel +31 (0) 76 544 55 66
Fax +31 (0) 76 544 55 77
Internet http://www.cobar.com

Product Data Sheet

Product	**380-R**
Productgroup	General Wave Solder Flux
Date	13-08-2007
Release	6.2

5	Especially made for this purpose
4	Generally qualified for this purpose
3	Generally usable, but not the best choice
2	Generally not usable for this purpose
1	Wrong choice

ISO 9454-1	2.2.3.A.
IPC-ANSI-J-STD-004	ORL0
JIS Z 3197	1.2.3.N_I
No-Clean process	5
Post-solder cleaning	3
Selective Soldering	3
Pb-Free process - Ambient	2
Pb-Free process - N2	2
N2 Process - Full Tunnel	2
N2 Process - Wave Only	2
Consumer electronics	5
Med-Rel electronics	4
Hi-Rel electronics	2
1-layer, video/tv boards	5
2-layer boards	5
Multi-layer boards	5
OSP compatible	5
Ni/Au compatibel	5
Ni/Pd compatible	5
Ag compatible	5
Sn compatible	5
Foam fluxing	1
Nozzle-spray fluxing	1
Moderate preheat	5
Short contact time with solder	5
Reduces skipped joints	5
Reduces solder balling	5
Reduces bridging	5
Promotes wicking	4
Cosmetic cleanliness	3
Cosmetic cleanliness N2	4
Dull/frosty joints	2
ICCT compatible	5
Conformal coating	1

SG @ 20 °C [kg/dm3] (+/- 0.5%)	0.821
Solids content [% w/w]	4.15
Halides [Silver-Chromate Test]	Pass
Halides [Potentiometric]	Pass
Acid number [mgKOH] (+/-2.5%)	30.69
Water content [% w/w]	3.
VOC-content [% w/w]**	92.00
Filmformer(s)	Synthetic
Flashpoint COC [°C]	11.8
Odor	Alcoholic
Color	Colorless
Telcordia/Bellcore TR-NWT-000078/3	Qualified
Test report(s)	-
Certificate of Compliance	Available
SPC-data*	Auditable
Environmental Load Unit	6.00
RoHS-Compliance Certificate	Available
User's Guidelines	English
Thinner	308-00
Packaging	
Can (HDPE) [liter]	10
Drum (HDPE) [liter]	200
Shelf-life (Weeks)	
Storage 20 [°C]	52.
Storage 25 [°C]	40.
*Certain conditions apply.	
**Having a vapor pressure of >0.01 mm Hg @ 25 °C	
Industrial chemical product. Read MSDS before use.	

Cobar Europe BV
PO Box 3251
4800 DG Breda

Tel +31 (0) 76 544 55 66
Fax +31 (0) 76 544 55 77
Internet http://www.cobar.com

Product Data Sheet

Product	**385-D**
Productgroup	General Wave Solder Flux
Date	19-09-2006
Release	6.1

5	Especially made for this purpose
4	Generally qualified for this purpose
3	Generally usable, but not the best choice
2	Generally not usable for this purpose
1	Wrong choice

ISO 9454-1	1.2.3.A
IPC-ANSI-J-STD-004	REL0
JIS Z 3197	1.2.3.N_I
No-Clean process	5
Post-solder cleaning	2
Selective Soldering	5
Pb-Free process - Ambient	4
Pb-Free process - N2	5
N2 Process - Full Tunnel	5
N2 Process - Wave Only	5
Consumer electronics	3
Med-Rel electronics	5
Hi-Rel electronics	5
1-layer, video/tv boards	2
2-layer boards	5
Multi-layer boards	5
OSP compatible	4
Ni/Au compatibel	5
Ni/Pd compatible	5
Ag compatible	4
Sn compatible	5
Foam fluxing	5
Nozzle-spray fluxing	5
Moderate preheat	5
Short contact time with solder	5
Reduces skipped joints	5
Reduces solder balling	4
Reduces bridging	4
Promotes wicking	4
Cosmetic cleanliness	4
Cosmetic cleanliness N2	5
Dull/frosty joints	2
ICCT compatible	5
Conformal coating	5

SG @ 20 °C [kg/dm3] (+/- 0.5%)	0.804
Solids content [% w/w]	1.91
Halides [Silver-Chromate Test]	Pass
Halides [Potentiometric]	Pass
Acid number [mgKOH] (+/-2.5%)	18.75
Water content [% w/w]	1.
VOC-content [% w/w]**	94.00
Filmformer(s)	Synthetic
Flashpoint COC [°C]	11.9
Odor	Alcoholic
Color	Colorless
Telcordia/Bellcore TR-NWT-000078/3	-
Test report(s)	-
Certificate of Compliance	Available
SPC-data*	Auditable
Environmental Load Unit	6.60
RoHS-Compliance Certificate	Available
User's Guidelines	English
Thinner	425-00
Packaging	
Can (HDPE) [liter]	10
Drum (HDPE) [liter]	200
Shelf-life (Weeks)	
Storage 20 [°C]	52.
Storage 25 [°C]	40.
*Certain conditions apply.	
**Having a vapor pressure of >0.01 mm Hg @ 25 °C	
Industrial chemical product. Read MSDS before use.	

Cobar Europe BV
PO Box 3251
4800 DG Breda

Tel +31 (0) 76 544 55 66
Fax +31 (0) 76 544 55 77
Internet http://www.cobar.com

Product Data Sheet

Product	**385-SEL**
Productgroup	Selective Flux
Date	31-10-2011
Release	11.1

5	Especially made for this purpose
4	Generally qualified for this purpose
3	Generally usable, but not the best choice
2	Generally not usable for this purpose
1	Wrong choice

ISO 9454-1	1.2.3.A
IPC-ANSI-J-STD-004	REL0
JIS Z 3197	1.2.3.N_I
No-Clean process	5
Post-solder cleaning	3
General Wave Soldering	3
Pb-Free process - N2	5
Consumer electronics	3
Med-Rel electronics	4
Hi-Rel electronics	5
1-layer, video/tv boards	3
2-layer boards	4
Multi-layer boards	5
OSP compatible	5
Ni/Au compatibel	5
Ni/Pd compatible	4
Ag compatible	4
Sn compatible	5
Bubble jet fluxing	5
Nozzle-spray fluxing	5
Template/dip fluxing	2
Hot bar soldering	5
Static solder-nozzle	5
Flow solder-nozzle	5
Short contact time with solder	3
Moderate preheat	4
Reduces spread of flux	3
Reduces solder balling	4
Reduces bridging	4
Cosmetic cleanliness	4
Cosmetic cleanliness N2	5
ICCT compatible	5
Conformal coating	5

SG @ 20 °C [kg/dm3] (+/- 0.5%)	0.804
Solids content [% w/w]	1.91
Halides [Silver-Chromate Test]	Pass
Halides [Potentiometric]	Pass
Acid number [mgKOH] (+/-2.5%)	18.75
Water content [% w/w]	1.
VOC-content [% w/w]**	94.00
Filmformer(s)	Resin
Color	Colorless
Flashpoint COC [°C]	11.9
Telcordia/Bellcore TR-NWT-000078/3	Compliant
Test report(s)	-
Certificate of Compliance	Available
SPC-data*	Auditable
Environmental Load Unit	6.66
RoHS-Compliance Certificate	Available
User's Guidelines	English
Packaging	
Bottle (HDPE) [liter]	1
Can (HDPE) [liter]	5, 10
Thinner	425-00
Shelf-life (Weeks)	
Storage 20 [°C]	52.
Storage 25 [°C]	40.

Cobar Europe BV
PO Box 3251
4800 DG Breda

Tel +31 (0) 76 544 55 66
Fax +31 (0) 76 544 55 77
Internet http://www.cobar.com

Product Data Sheet

Product	**390-RX-HT**
Productgroup	General Wave Solder Flux
Date	16-03-2010
Release	6.2

5	Especially made for this purpose
4	Generally qualified for this purpose
3	Generally usable, but not the best choice
2	Generally not usable for this purpose
1	Wrong choice

ISO 9454-1	1.2.3.A
IPC-ANSI-J-STD-004	REL0
JIS Z 3197	1.2.3.N_I
No-Clean process	5
Post-solder cleaning	2
Selective Soldering	4
Pb-Free process - Ambient	4
Pb-Free process - N2	5
N2 Process - Full Tunnel	5
N2 Process - Wave Only	5
Consumer electronics	3
Med-Rel electronics	5
Hi-Rel electronics	5
1-layer, video/tv boards	2
2-layer boards	5
Multi-layer boards	5
OSP compatible	4
Ni/Au compatibel	4
Ni/Pd compatible	4
Ag compatible	4
Sn compatible	5
Foam fluxing	5
Nozzle-spray fluxing	5
Moderate preheat	5
Short contact time with solder	5
Reduces skipped joints	5
Reduces solder balling	5
Reduces bridging	5
Promotes wicking	5
Cosmetic cleanliness	3
Cosmetic cleanliness N2	4
Dull/frosty joints	3
ICCT compatible	5
Conformal coating	5

SG @ 20 °C [kg/dm3] (+/- 0.5%)	0.813
Solids content [% w/w]	2.20
Halides [Silver-Chromate Test]	Pass
Halides [Potentiometric]	Pass
Acid number [mgKOH] (+/-2.5%)	15.80
Water content [% w/w]	5.
VOC-content [% w/w]**	92.00
Filmformer(s)	Synthetic
Flashpoint COC [°C]	12.4
Odor	Alcoholic
Color	Colorless
Telcordia/Bellcore TR-NWT-000078/3	Qualified
Test report(s)	Available
Certificate of Compliance	Available
SPC-data*	Auditable
Environmental Load Unit	6.00
RoHS-Compliance Certificate	Available
User's Guidelines	English
Thinner	425-00
Packaging	
Can (HDPE) [liter]	10
Drum (HDPE) [liter]	200
Shelf-life (Weeks)	
Storage 20 [°C]	78.
Storage 25 [°C]	52.
*Certain conditions apply.	
**Having a vapor pressure of >0.01 mm Hg @ 25 °C	
Industrial chemical product. Read MSDS before use.	

Appendix IV: CELCORR test PCB

Ch	Terminal	Dimensions (mm)	Resistance (Ω)	Power rating (W)	Ch	Terminal	Dimensions (mm)	Capacitance (F)
1 2 3	0402	1.0x0.5	1k 10k 100k	0.063 0.063 0.0625	11 12 13	0402	1.0x0.5	1000p 1000p 1000p
4 5 6	0603	1.5x0.8	100 0.1M 1M	0.1 0.063 0.063	14 15 16	0603	1.5x0.8	47p 1n 100n
7 8 9	0805	2.0x1.3	68 0.33M 1M	0.1 0.125 0.123	17 18 19	0805	2.0x1.3	22p 1n 100n
10	SIR	13x25	Reflow surface finish		20	SIR	13x25	Solder mask coated

Appendix IV: Mollier Diagram